UILU-ENG 84-3607

Report No. 107

SMALL CRACK GROWTH IN BIAXIAL FATIGUE

by

Dennis W. Worthem

Department of Mechanical and Industrial Engineering, UIUC

A Report of the

MATERIALS ENGINEERING - MECHANICAL BEHAVIOR

College of Engineering, University of Illinois at Urbana-Champaign

June 1984

ABSTRACT

Crack-growth rate studies were performed for thin-walled tubes of Inconel 718 under biaxial, strain-controlled fatigue loading at room temperature. Loading modes included axial, torsion, and combined tension-torsion where $\Delta\gamma/\Delta\varepsilon = \sqrt{3}$ for effective strain amplitudes of 1.0% and 0.5% at strain ratios of $R_\varepsilon = -1$, and $R_\varepsilon = 0$. From replicas of the surface, it was observed that from initiation through the "small crack" region (up to 1 mm) cracks initiated and propagated on or near planes of maximum shear amplitude. This indicated the presence of combined Mode-I and Mode-II loadings. On these replicas the cracks were measured tip to tip. The crack-growth rate was calculated from these measurements and plotted versus combined stress-intensity factor.

For nearly all loading cases the "small crack" effect is observed, i.e. a decrease or small increase in the crack growth rates versus combined stress intensity factor as compared to the "long crack" behavior where the rate increases much faster. Additionally an increasing Mode-I loading compared to Mode-II loading decreases the life of the specimen. Crack linking does not affect the overall crack growth behavior. The differences in life and behavior are probably explained by the different crack-growth micro-mechanisms. Possible crack-growth micro-mechanisms are described in the literature. The crack-growth data presented in this paper contains evidence for their presence. Recommendations for future study include tests to observe these mechanisms.

The results presented here are for a Mode-I loading that was at most 60% of the Mode-II loading.

ACKNOWLEDGMENTS

Professor Darrell F. Socie is gratefully acknowledged for his guidance and encouragement throughout the investigation. Jon Pollack is gratefully acknowledged for assisting in the tedious task of measuring the cracks on the replicas with the microscope.

Financial support was provided by the Air Force Materials Laboratory under contract F33615-81-C-5015.

TABLE OF CONTENTS

LIST OF TABLES

LIST OF FIGURES

1. INTRODUCTION

The design of modern engineering structures such as spacecraft, aircraft, automobiles, pressure vessels and printing machines has become increasingly complex. Increased load demands as well as strain rate and temperature combined with the pressure for cost effectiveness, requires the optimal design of every component in the structure. Designers must consider the low cycle fatigue region and frequently can not design for a stress level below the long life fatigue limit. This has created the need for increasingly more accurate and reliable design methods which would include the evaluation of the fatigue resistance of the component under dynamic loadings. Generally, the fatigue loadings are multiaxial states of stress (or strain). However, uniaxial test programs are typically used to generate data on the fatigue characteristics of materials. Few multiaxial fatigue tests have been done until recent years because of the complexity of multiaxial loading, the expense and unavailability of the test machines and the large number of tests required to develop the empirical data. In the past, research centered on developing an appropriate rule which converts the multiaxial loading to an "equivalent" uniaxial loading. The fatigue resistance of the components can then be estimated from uniaxial data.

A number of reviews of multiaxial fatigue have been published describing several theories for the low cycle fatigue region [1-3]*. Each one has its advantages and limitations. More recent approaches are based on the critical plane for crack initiation and growth. One of the

*Number in brackets refer to corresponding items in the list of references.

more popular theories was proposed by Brown and Miller [2] and modified by Socie and Shield to include mean stress effects [4]. Their theories postulate stress and strain parameters which quantify the shear strain on the critical plane and the normal stress and strain to that plane. A major advantage of this method is the characterization of the strains on the planes of crack initiation and propagation. Brown and Miller postulated that cracks initiate on maximum shear strain planes with crack propagation assisted by the normal strain on these planes. This parameter provided good correlation of the data for Inconel 718 under biaxial loading using uniaxial material properties [5]. However, to improve the life prediction of components with pre-existing cracks, detailed crack growth studies are required to understand the mechanisms of crack growth.

Most fatigue crack growth studies have been conducted for precracked (long crack) specimens under uniaxial loading. However, not only are many engineering components loaded multiaxially, but they also experience initiation and propagation of cracks through the region of "small crack" sizes (i.e. 2c less than 1 mm). For many materials, most of the component life is spent in this region. For example, Socie, et al. [5], has shown that for Inconel 718, 75 to 95 percent of the component life in axial and combined tension-torsion fatigue loading, and 50 to 70 percent in torsional fatigue loading is spent initiating and growing cracks to a length of 1 mm. At crack lengths greater than 1 mm, growth occurs at a much greater rate. Since a large percentage of the component life is frequently spent growing cracks to 1 mm, a good understanding of their growth characteristics is important.

1. INTRODUCTION

The design of modern engineering structures such as spacecraft, aircraft, automobiles, pressure vessels and printing machines has become increasingly complex. Increased load demands as well as strain rate and temperature combined with the pressure for cost effectiveness, requires the optimal design of every component in the structure. Designers must consider the low cycle fatigue region and frequently can not design for a stress level below the long life fatigue limit. This has created the need for increasingly more accurate and reliable design methods which would include the evaluation of the fatigue resistance of the component under dynamic loadings. Generally, the fatigue loadings are multiaxial states of stress (or strain). However, uniaxial test programs are typically used to generate data on the fatigue characteristics of materials. Few multiaxial fatigue tests have been done until recent years because of the complexity of multiaxial loading, the expense and unavailability of the test machines and the large number of tests required to develop the empirical data. In the past, research centered on developing an appropriate rule which converts the multiaxial loading to an "equivalent" uniaxial loading. The fatigue resistance of the components can then be estimated from uniaxial data.

A number of reviews of multiaxial fatigue have been published describing several theories for the low cycle fatigue region [1-3]*. Each one has its advantages and limitations. More recent approaches are based on the critical plane for crack initiation and growth. One of the

*Number in brackets refer to corresponding items in the list of references.

more popular theories was proposed by Brown and Miller [2] and modified by Socie and Shield to include mean stress effects [4]. Their theories postulate stress and strain parameters which quantify the shear strain on the critical plane and the normal stress and strain to that plane. A major advantage of this method is the characterization of the strains on the planes of crack initiation and propagation. Brown and Miller postulated that cracks initiate on maximum shear strain planes with crack propagation assisted by the normal strain on these planes. This parameter provided good correlation of the data for Inconel 718 under biaxial loading using uniaxial material properties [5]. However, to improve the life prediction of components with pre-existing cracks, detailed crack growth studies are required to understand the mechanisms of crack growth.

Most fatigue crack growth studies have been conducted for precracked (long crack) specimens under uniaxial loading. However, not only are many engineering components loaded multiaxially, but they also experience initiation and propagation of cracks through the region of "small crack" sizes (i.e. 2c less than 1 mm). For many materials, most of the component life is spent in this region. For example, Socie, et al. [5], has shown that for Inconel 718, 75 to 95 percent of the component life in axial and combined tension-torsion fatigue loading, and 50 to 70 percent in torsional fatigue loading is spent initiating and growing cracks to a length of 1 mm. At crack lengths greater than 1 mm, growth occurs at a much greater rate. Since a large percentage of the component life is frequently spent growing cracks to 1 mm, a good understanding of their growth characteristics is important.

There have been some investigations of "small crack" growth with an extensive review of the literature on the subject available [6]. Researchers like Dowling [7], Ritchie [8], Lankford [9], and El Haddad [10], have observed under uniaxial loading a "small crack" effect, i.e. a drop in the crack growth rate with an increase in the LEFM stress intensity factor at crack sizes on the order of the grain size. As the crack grows, the growth rate then increases and approaches the long crack behavior. This effect has been postulated on the basis of a "crack closure" effect plus the influence of metallurgical microstructural features [8]. Also Ritchie and Minakawa postulated a small crack effect for Mode II based on the mechanical interlocking of the crack surfaces [8,11]. Tschegg [12] has shown a drop in crack growth rate in Mode III based on microstructural mechanisms induced by the rubbing of the fracture surface. Extensive investigations are still required to observe and understand these mechanisms under multiaxial fatigue loadings.

The work described in this paper on crack growth rates is based on data obtained from the biaxial fatigue loading of smooth tubular specimens made of Inconel 718. Waill made observations of the surface behavior of the cracks [13]. She established that in all cases, the crack propagated along planes of maximum shearing stress (see Figs. 1 through 4). Only in the axial case, very late in the life, did the cracks turn to propagate along planes of maximum normal stress. This indicates that for the crack growth studies, both Mode I and Mode II loadings must be considered. Beer [14] made observations of the crack shapes and how the crack grew into the depth of the specimen. He found

that for these small cracks, the crack shape was part-through-the-thickness and semi-elliptical as shown in Figs. 5 and 6. These plots were obtained from a least squares fit of Beer's data for individual cracks. The aspect ratio was found to be independent of the type of loading, strain ratio, and size of crack (up to 1 mm) and was dependent only on the effective strain amplitude. Therefore, in analyzing the crack growth rates for this material, it is necessary to look at only the surface behavior of the crack to get the general nature of the crack growth.

In this paper, data is extracted from the specimens used for the work of Waill and Beer for crack growth rate analysis and observations are made on the small crack behavior under combined Mode I and Mode II loading. Some possible explanations for the observed behaviors are discussed with recommendations for future study.

2. EXPERIMENTAL PROGRAM

2.1 Material

The thin-walled tubular specimens were cut from a forged ring of Inconel 718, a high temperature nickel based superalloy. The dimensions of the specimens are shown in Fig. 7. A thin-walled tube was selected as the specimen configuration because its state of stress is easily determined and nearly constant through the wall thickness. After rough machining, the specimens were heat treated at 600°C for 12 hours to relieve residual stresses induced during forging. This prevented distortion of the specimen during final machining.

The microstructure is shown in Fig. 8. A mixture of grain sizes was observed in small clusters ranging from a typical diameter of 0.01 mm up to about 0.2 mm. For the largest grain sizes there were at least 10 grains though the specimen wall thickness. Material properties are given in Table 1.

2.2 Test Procedure

The specimens were tested under biaxial fatigue loading conditions in strain control. Tests were conducted for axial ($\lambda = 0$), torsional ($\lambda = \infty$), and combined tension-torsion ($\lambda=\sqrt{3}$) where λ is the ratio of torsional to tensile strain amplitude. In each case, one series of tests was conducted at an effective strain amplitude (Von Mises) of 1.0 percent and another series at 0.5 percent. The tests at each effective strain amplitude were conducted at two strain ratios, $R_\varepsilon = -1$ and 0 with the loadings proportional. The higher strain amplitude had equal elastic and plastic strains, while the lower

amplitude had about five times as much elastic as plastic strain after cyclic softening. Tests were stopped after a 10 percent drop in load was observed. Table 2 shows the test results for the 12 specimens that provided crack growth data. The crack growth data was obtained from replicas of the surfaces made at approximately every 5 to 10 percent of the estimated fatigue lives using cellulose tape moistened with methyl acetate solution which melted into the surface. After the solution dried, the tape was removed. In this way, the surface topography was imprinted and could then be examined under an optical microscope.

2.3 Data Reduction

Surface crack length versus cycles data was obtained from the replicas by measuring the crack from tip to tip under an optical microscope using a calibrated eyepiece. The cracks selected for measurement were the failure cracks plus 3 or 4 additional cracks selected on each specimen that were about 1 mm long on the last replica before failure. The surface crack growth rate (d(2c)/dn) was calculated using the Seven Point Incremental Polynomial Method described in ASTM Standard Test Method E647-81. Modifications to the computer program allowed the use of two of the three data points at each end of the data set for a crack for which a d(2c)/dn value is not calculated by the Seven Point Method. At each of these two points, respectively, the Three Point and Five Point Methods were used. Data is presented in terms of an effective stress intensity factor ΔK_{eff}, which is the combined loading stress intensity factor for combined Mode I and Mode II loadings. The model used for combining these modes was based on the addition of the Irwin energy release rate parameters [15]

$$G_{eff} = G_I + G_{II} \tag{1}$$

where the G's are related to the square of the linear elastic fracture mechanics stress intensity factors:

$$\Delta K_{eff} = (\Delta K_I^2 + \Delta K_{II})^{1/2} \ . \tag{2}$$

The models for ΔK_I and ΔK_{II} were [10]:

$$\Delta K_I = E \ \Delta\varepsilon \ \sqrt{\pi c} \qquad \text{E: modulus of elasticity} \tag{3}$$

$$\Delta K_{II} = G \ \Delta\gamma \ \sqrt{\pi c} \qquad \text{G: modulus of rigidity} \tag{4}$$

where $\Delta\varepsilon$ and $\Delta\gamma$ were the full normal and shear strain ranges, respectively, on the crack planes. These strain ranges included both the elastic and plastic strain ranges, and is known as a pseudo elastic stress method.

The raw and calculated data is presented in the APPENDIX. The data tables for each crack are presented in Tables A.1 through A.59. Figures A.1 through A.12 are linear plots of the surface crack length versus cycles for each loading condition which includes all the cracks analyzed on that specimen. Crack growth rate versus surface crack length linear plots are shown in Figs. A.13 through A.24.

3.3 General Results

The fatigue lives of the various loading conditions are given in Table 2. The shortest fatigue lives were for axial loading at $R_\varepsilon = 0$ and $\Delta\bar{\varepsilon}/2 = 1.0$ percent. There is an increase in the fatigue life as the loading goes from axial to combined to torsion. There is, of course, an increase with decreasing effective strain amplitude and, generally, an increase as one goes from $R_\varepsilon = 0$ to $R_\varepsilon = -1$, the exception being at combined and torsional loading at $\Delta\bar{\varepsilon}/2 = 1.0$ percent where they are about the same.

The crack density calculations by Waill [13] (Fig. 26) show that this density increases in going from axial to combined to torsional loading as well as increasing with increasing $\Delta\bar{\varepsilon}/2$. Generally, there is an increase in going from $R_\varepsilon = 0$ to $R_\varepsilon = -1$ except at combined and torsional loading at $\Delta\bar{\varepsilon}/2 = 1.0$ percent where this density is about the same for each of these loading cases at the two R_ε values.

In the case of axial loading, one crack generally clearly dominated and was larger that the others. Whereas in torsional loading at $R_\varepsilon = 0$, many large cracks developed and it was difficult to follow the dominant crack after about 70 percent of the fatigue life. For

combined loading, the behavior was intermediate between axial and torsional loading.

The crack growth results are discussed by the three loading modes.

3.4 Axial Tests

Figure 9 shows the crack growth rate plots for $R_\varepsilon = 0$. In this case, the "small crack" effect reported by others is observed, i.e. a drop in crack growth rate with an increase in the effective stress intensity factor which is seen for both effective strain amplitudes. This effect is observed in cracks other than the failure crack, however, the effect is at a longer surface crack length. It is useful to recall that the crack density is very low for this case and the other cracks are small in relation to the failure crack. In the more linear portions of the curves, there are slight drops in the slope of the curves, this is due to jumps in the crack sizes at crack linking followed by a slowing of the crack growth for which a reason will be postulated later.

The results for a strain ratio of $R_\varepsilon = -1$ are shown in Fig. 10. Here, the "small crack" effect is present, but not as pronounced, i.e. the crack growth rate is increasing at a much slower rate than the long crack rate. Crack density has increased and the effect of crack linking has increased. The cracks other than failure cracks have less crack linking and have a nearly linear growth rate, while the failure crack has a distinct slowing of the crack growth rate at about 70 percent of the fatigue life which is not a function of crack linking. This effect

becomes more noticeable with an increasing torsional loading component at $R_\varepsilon = 0$.

3.5 Combined Tests

Figure 11 is the plot for $R_\varepsilon = 0$. This case is similar to the axial loading at $R_\varepsilon = -1$ in that the "small crack" effect is not as pronounced compared to axial loading at $R_\varepsilon = 0$. The effect of crack linking is present. As seen in the data for $\Delta\bar{\varepsilon}/2 = 1.0$ percent, there is a marked slowing of the crack growth rate at about 70 percent of the fatigue life which was observed for the axial loading at $\Delta\bar{\varepsilon}/2 =$ 1.0 percent and $R_\varepsilon = -1$. This slowing was observed for both the failure crack and the "other" cracks, but was not observed at $\Delta\bar{\varepsilon}/2 =$ 0.5 percent.

The slowing observed at $R_\varepsilon = 0$ and $\Delta\bar{\varepsilon}/2 = 1.0\%$ is not observed at $R_\varepsilon = -1$ (Fig. 12). However, one crack at each strain amplitude did slow, but appear to be anomalous. Beyond the "very small crack" sizes (up to about two grains), the crack growth rate increased at nearly a constant rate. This distinction between the results at $R_\varepsilon = 0$, and $R_\varepsilon = -1$ becomes more obvious for torsional loading. Again, the "small crack" effect is present, but not pronounced as discussed for $R_\varepsilon = 0$ above. Also, the effect of crack linking is present.

3.6 Torsional Tests

Figure 13 shows the data for $R_\varepsilon = 0$. The most obvious result is the dramatic decrease in the growth rate for all the cracks at about 70 percent of the fatigue life or at the same stress intensity factors

for each of the two effective strain amplitudes. This is clearly distinguished from the $R_\varepsilon = -1$ data (Fig. 14) where the data is nearly linear beyond the very small crack sizes. This effect will be discussed more fully later. For both strain ratios, the small crack effect is present, but is a little more pronounced for $R_\varepsilon = -1$ than for $R_\varepsilon = 0$. The effect of crack linking is quite large which is expected since the crack density is highest for torsional loading plus these "other" cracks are large in relation to the dominant crack. In fact, the dominant cracks could not be followed beyond about 70 percent of the fatigue life because of the extensive crack linking beyond this point.

3.7 Comparison of Loadings

Figures 21 through 24 shows no distinct layering between axial, combined, and torsional loading. However, the following general observations can be made. There is more scatter in the data for $R_\varepsilon = 0$ than for $R_\varepsilon = -1$. In the case of $\Delta\bar{\varepsilon}/2 = 0.5$ percent and $R_\varepsilon = 0$, the combined loading curve was removed from the axial and torsional loading curves which are layered. This deviation cannot be explained. Also for $\overline{\Delta\varepsilon}/2 = 1.0$ percent and $R_\varepsilon = 0$, the torsional loading has a distinct slowing of the crack. Such effect is not observed or as distinct in the other loadings. Figure 25 clearly shows that the "small crack" effect is present for this material. This figure also shows an apparent joining up with the long crack behavior.

3.8 Discussion of Results

The observed "small crack" effect could be caused by at least two

main factors. In Mode I type loading, this could be the residual plastic stretch in the wake of the crack tip that increased in the small crack region up to a stabilized amount which leads to crack closure on the reversed part of the strain cycle [8]. This causes a reduced actual stress intensity factor with a lower crack growth resulting. A similar closure mechanism could be operative in Mode II. Correction for this could provide better predictions. This result has been obtained by others for uniaxial specimens [7,17].

Additionally, slowing of the crack growth rate may be due to the effect of the microstructure at these crack sizes. Cracks have been observed to slow after passing across grain boundaries or upon hitting a grain with slip bands offset [18]. Lankford [9] has postulated this effect on the basis of localized micro-plasticity within one grain which has decreasing influence as the crack grows across grain boundaries into grains of different orientation of favorable crystallographic structure for crack growth. Additionally, crack branching has been observed at very small crack sizes before one crack tip becomes dominant. Upon reaching a certain size, the crack mechanics are probably more adequately described by continuum mechanics models [8].

With Mode II loading, there is probably a rubbing of the surfaces plus mechanical interlocking of asperities on the crack surfaces. This was observed by others [8,12]. Waill [13] reported observing debris emanating from the cracks. It can be conjectured that the slowing of the cracks observed in torsional $R_\varepsilon = 0$ loading is caused by such mechanical interlocking. A discussion by Ritchie [8] postulates that when the crack is within one grain boundary, the crack has not become

faceted enough to provide this interlocking. However, as the crack grows, enough facets develop that interlocking starts. This effect may increase up to a maximum amount at which point the crack nearly stops growing. But damage could still be accumulated at the crack tip to where the crack may become of a size that the crack is wedged open by the asperities instead of locked. However, $R_\varepsilon = -1$ torsional loading does not display this behavior since the d(2c)/dn versus ΔK_{eff} curve is more nearly linear. This may be explained by $R_\varepsilon = -1$ being a back and forth straining whereas $R_\varepsilon = 0$ is in the same direction which means for $R_\varepsilon = -1$ interlocking does not occur as much as for $R_\varepsilon = 0$ where the asperities will always catch in the same way and at a relatively high $\Delta\gamma_{max}$. Therefore, at this point, the stress intensity factor is considerably reduced with a resulting large drop in the crack growth rate. An increasing Mode I component with decreasing Mode II loading would be expected to reduce this effect and is observed as the loading goes from torsion to combined to axial. For the axial case at $R_\varepsilon = -1$ and $\Delta\bar{\varepsilon}/2 = 1.0$ percent, slowing of the crack at about 70 percent of the fatigue life is observed. This could be explained by the compressive stress during the lower part of the strain cycle causing a forcing together of the crack surface so the effect of rubbing or interlocking in Mode II in enhanced. The "small crack" effect was observed earlier as less pronounced in certain cases, this was probably due to a smaller Mode I component causing less crack closure.

The reduced growth rate after crack linking can be possibly explained by the need for the new crack to consolidate to the stable semi-elliptical shape. Another explanation would be based on the effect

that two cracks have on the stress intensity factor as the two cracks approach each other. It is observed that crack linking does not appear to affect the overall crack growth behavior, since a change in crack density does not affect the crack growth rate versus ΔK_{eff} plots.

Observation of the data tables (Tables A.1 through A.59) shows, that at most, Mode I type loading is about 60 percent of the Mode II loading. For long crack specimens, crack growth rates have been reported as greater in pure Mode I than for pure Mode III [19] which is similar to Mode II. However, the data reported here does not clearly indicate any dominant effect of Mode I loading on the crack growth rate as a function of ΔK_{eff}. Further experimentation is required to determine the small crack behavior with greater Mode I loadings.

4. CONCLUSIONS

1. The "small crack" effect is observed for all loading cases. For axial loading at $R_\varepsilon = 0$ this effect is very pronounced, i.e. a decrease in crack growth with an increase in the combined stress-intensity factor. At all other loading conditions, combined tension-torsion and torsion at $R_\varepsilon = 0$ and -1 and for axial loading at $R_\varepsilon = -1$ this effect is less pronounced, i.e. the crack-growth rate is increasing at a much slower rate as a function of combined stress-intensity factor compared to the "long crack" behavior.
2. Beyond this "small crack" region, the crack growth increases at a nearly constant rate as a function of stress-intensity factor. This could be the "long crack" behavior since this rate of increase is much higher than in the "small crack" region.
3. An increasing Mode-I loading compared to Mode-II loading on a specimen decreases the life of the specimen. This behavior may be explained by the effect of the rubbing and interlocking of the fracture surfaces under Mode-II loading.
4. Crack linking with the dominant crack is observed throughout the lives of the specimens under all the loading conditions. Even though crack linking affects the immediate behavior of the crack, it does not affect the overall crack behavior as observed on the plot of crack-growth rate versus combined stress-intensity factor.

5. RECOMMENDATIONS FOR FURTHER STUDY

1. A detailed mechanism study should be performed to observe the effects of crack closure, micro-plasticity, crack interaction with the grain boundaries, mechanical interlocking, and rubbing of the fracture surfaces. The effects of these mechanisms on the stress intensity factors should be quantified.
2. The data presented in this paper should be compared with long crack data for both Mode I and II. Some investigators have observed that the transition from small to long crack behavior occurs in the threshold stress-intensity factor region [8].
3. A smaller grain material should be tested under the same conditions to decrease the crack density and determine if the effect of crack linking can be eliminated.
4. Tests should be performed with higher Mode-I loadings compared to Mode II.

Table 1 Material Properties

General Properties	
Modulus of Elasticity	205,500 MPa
Modulus of Rigidity	80,000 MPa
Poisson's Ratio (elastic)	0.28
Poisson's Ratio (plastic)	0.50
Monotonic Properties	
Yield Stress 0.2 percent	1160 MPa
Fracture Stress	1850 MPa
Fracture Strain	0.33
% Reduction in Area	28%
Strength Coefficient	1910 MPa
Strain Hardening Exponent	0.08
Cyclic Properties	
Fatigue Strength Coefficient	1640 MPa
Fatigue Strength Exponent	-0.06
Fatigue Ductility Coefficient	2.67
Fatigue Ductility Exponent	-0.82
Cyclic Strength Coefficient	1530 MPa
Cyclic Strain Hardening Exponent	0.07

Table 2 Fatigue Test Results

Specimen	Nominal Strain Amplitude $\frac{\Delta\varepsilon}{2}$	$\frac{\Delta\gamma}{2}$	Nominal Stress Amplitude $\Delta\sigma/2$(MPa)	$\Delta\tau/2$(MPa)	Mean Stress σ_o(MPa)	τ_o(MPa)	Fatigue Life $N_{0.1}$(*)	$N_{1.0}$(**)	N_f(***)
Axial									
$R_\varepsilon = 0$									
B-5	0.01	0	1,100	0	20	0	240	800	936
B-36	0.005	0	970	0	240	0	2,400	7,000	7,029
$R_\varepsilon = -1$									
B-14	0.010	0	1,050	0	0	0	200	1,050	1,330
B-12	0.005	0	920	0	0	0	2,000	11,000	13,364
Combined									
$R_\varepsilon = 0$									
B-98	0.007	0.012	740	410	100	-70	225	1,050	1,333
B-17	0.0035	0.0063	610	380	60	100	2,000	7,500	9,500
$R_\varepsilon = -1$									
B-35	0.007	0.012	740	430	0	0	200	1,000	1,374
B-26	0.0035	0.0063	630	375	0	0	2,000	8,000	12,899
Torsion									
$R_\varepsilon = 0$									
B-99	0	0.017	0	580	0	10	50	1,000	1,687
B-32	0	0.0085	0	500	0	70	500	4,500	9,526
$R_\varepsilon = -1$									
B-13	0	0.017	0	570	0	0	100	800	1,674
B-8	0	0.0085	0	510	0	0	2,000	7,000	12,942

* Cycles to first crack of length 0.1 mm
** Cycles to first crack of length 1.0 mm
*** Cycles to failure (10% drop in load)

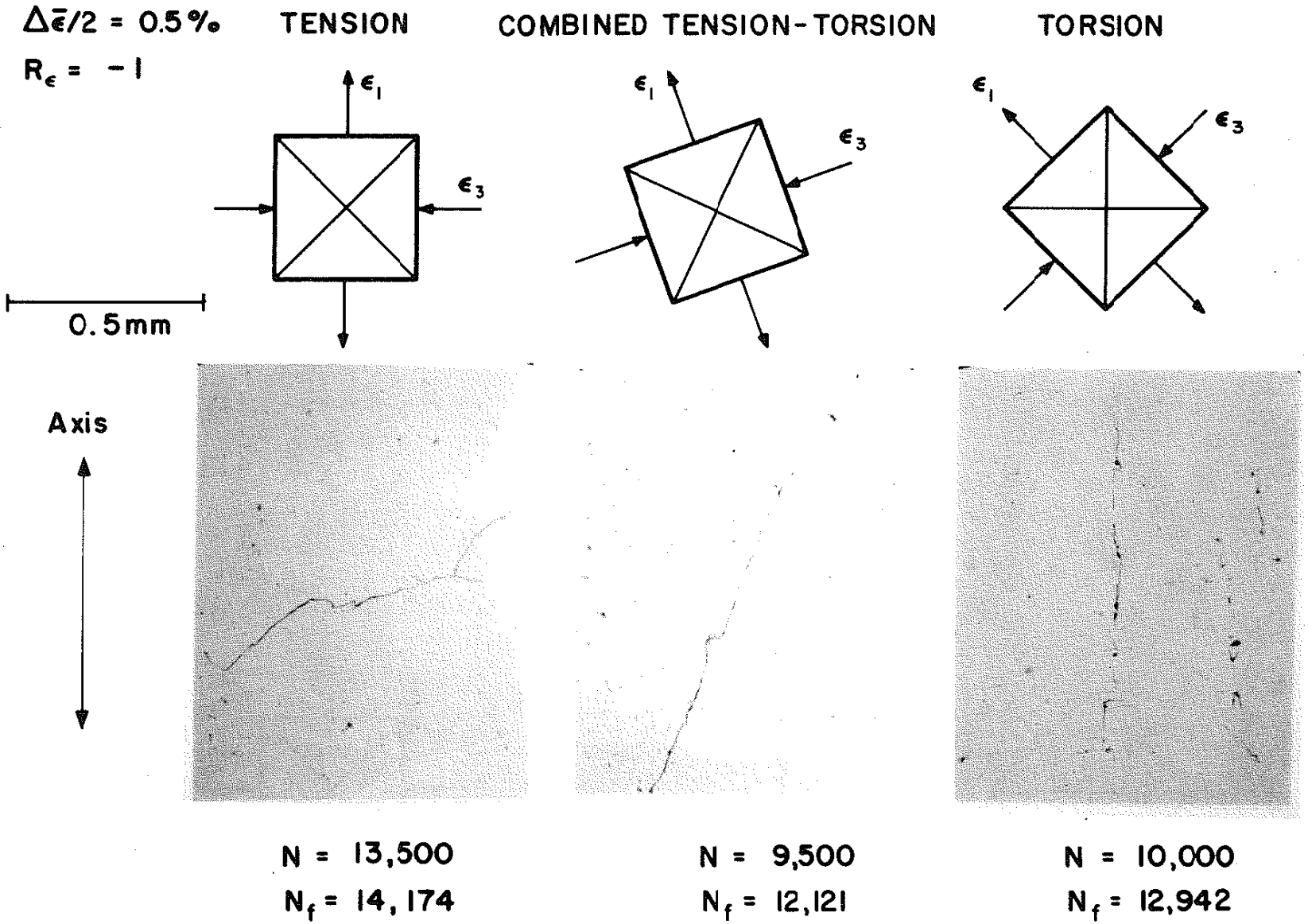

Figure 1 Directions of Crack Growth $\Delta\bar{\varepsilon}/2$ = 0.5%, R_ε = -1

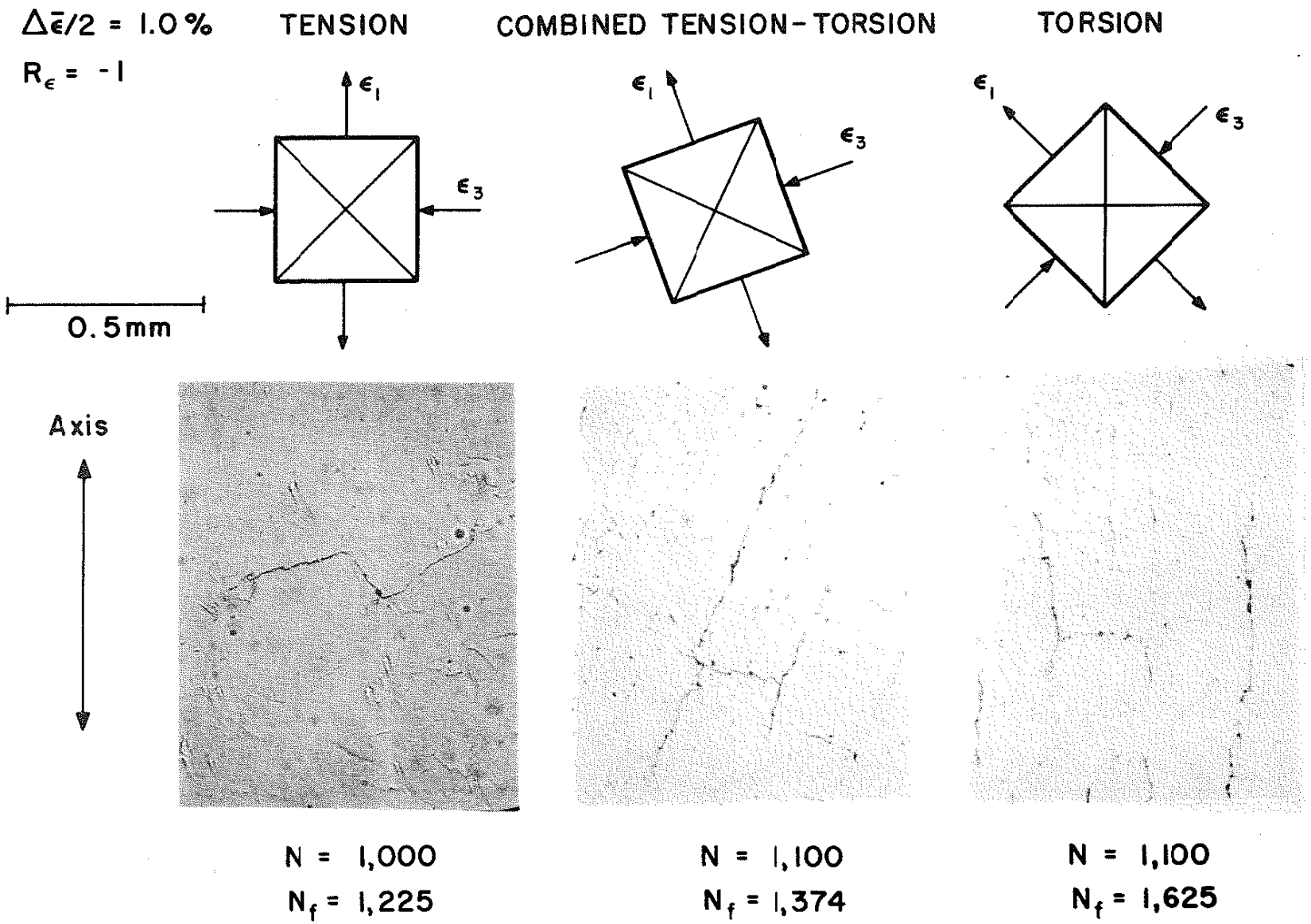

Figure 2 Directions of Crack Growth $\Delta\bar{\varepsilon}/2$ = 1.0%, R_ε = -1

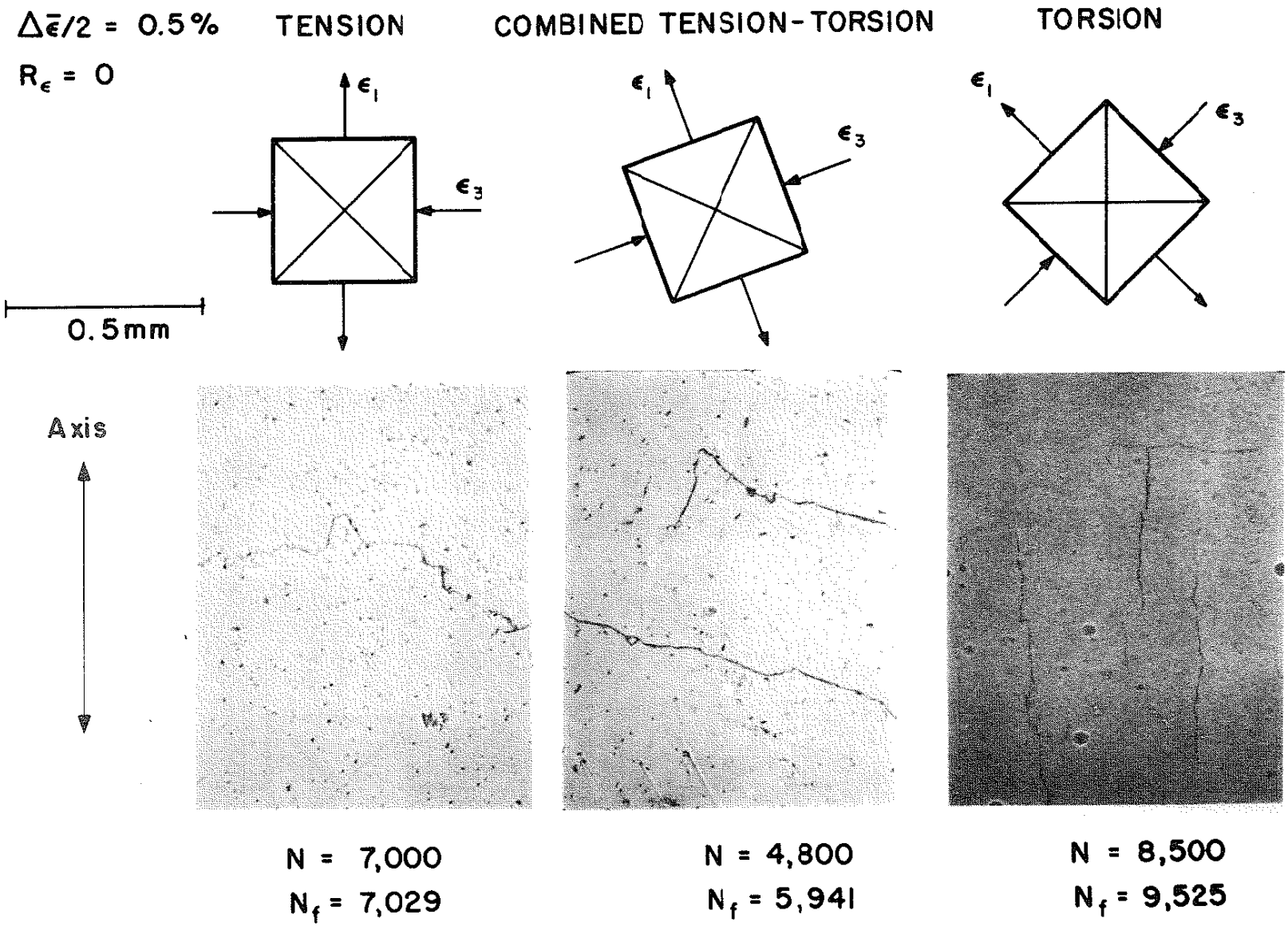

Figure 3 Directions of Crack Growth $\Delta\bar{\varepsilon}/2$ = 0.5%, R_ε = 0

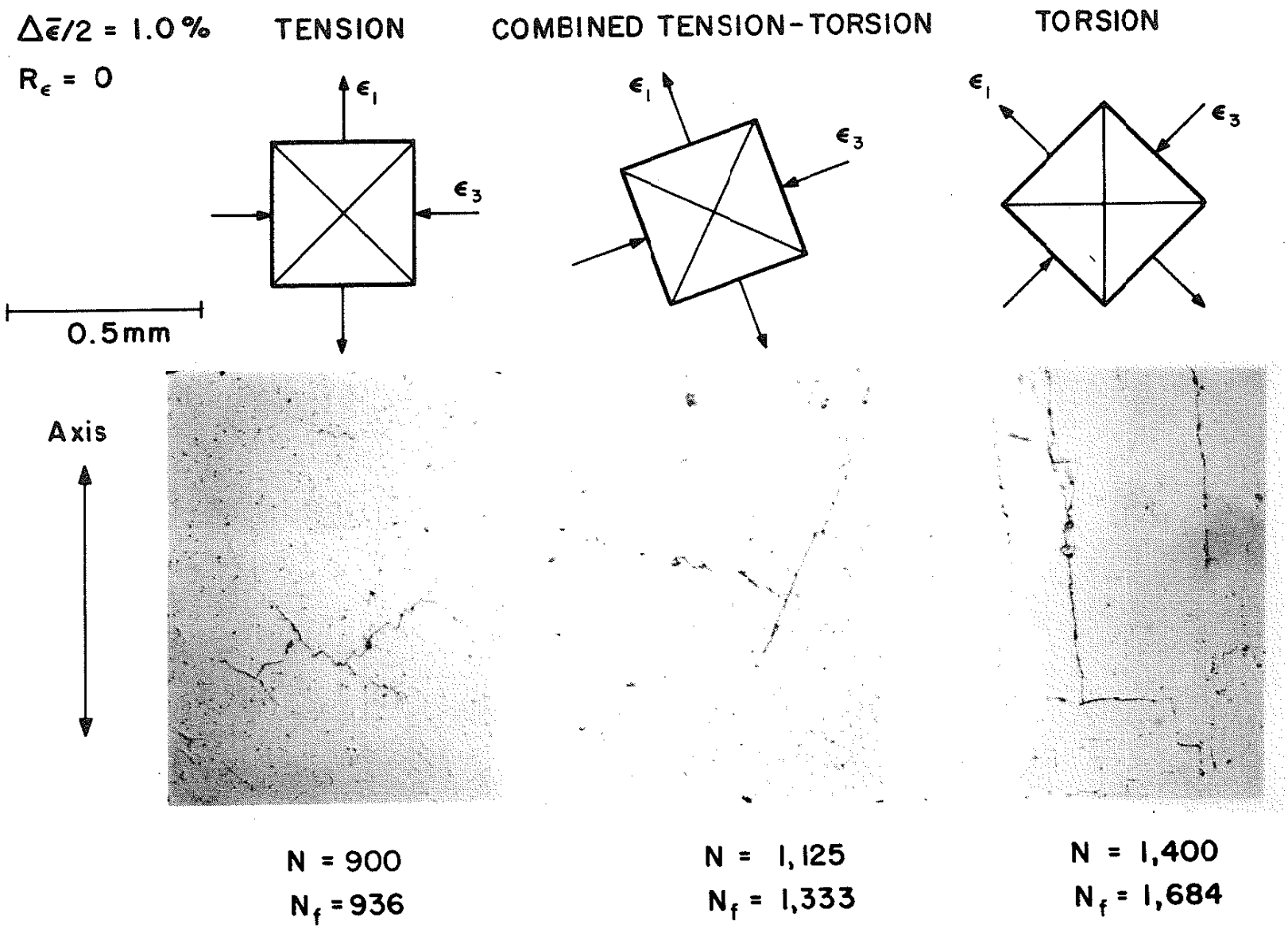

Figure 4 Directions of Crack Growth $\Delta\bar{\varepsilon}/2$ = 1.0%, R_ε = 0

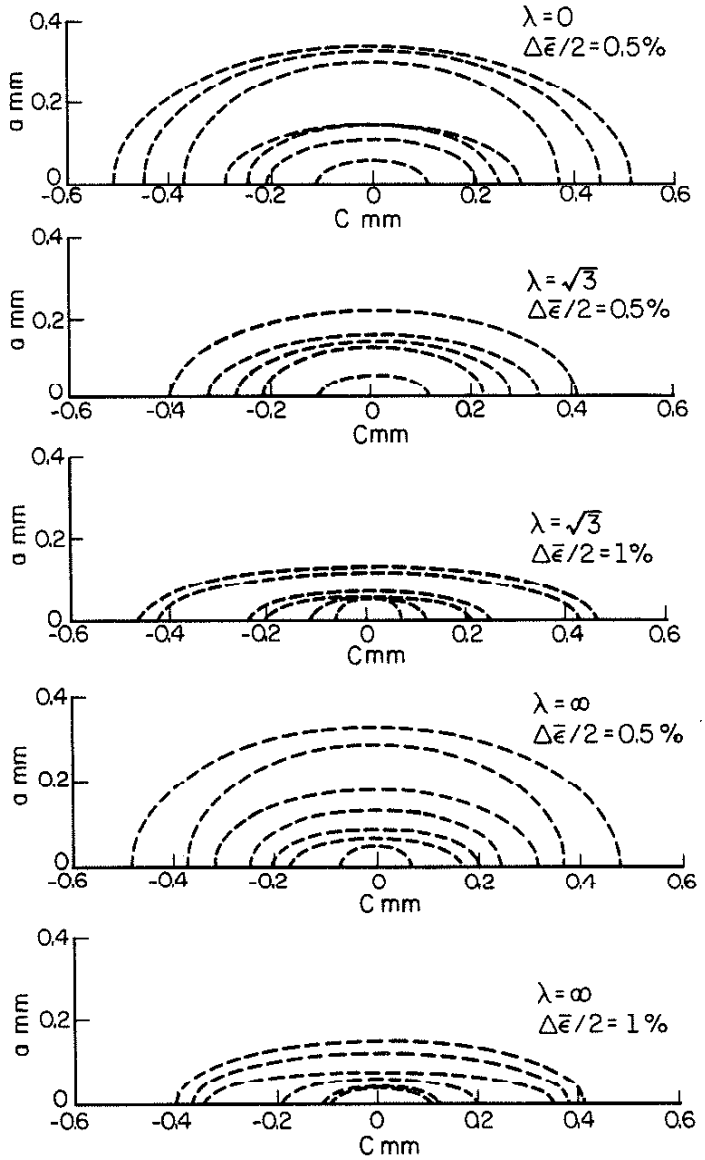

Figure 5 Curve Fitted Crack Profiles

$R_\varepsilon = -1$

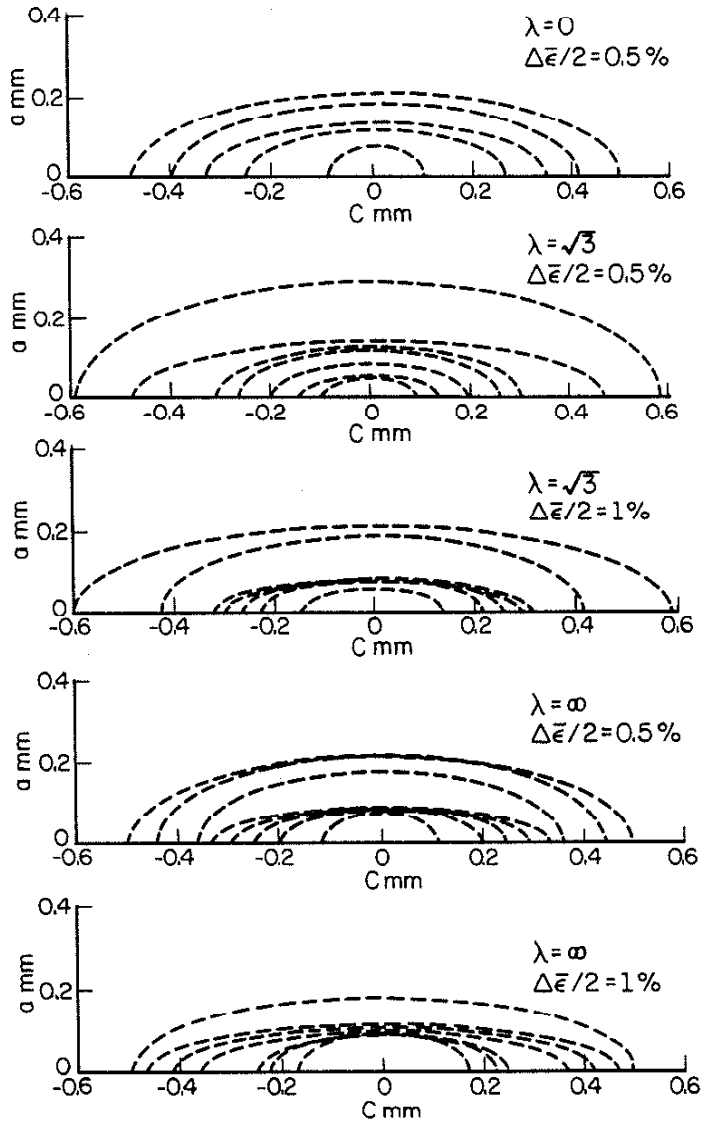

Figure 6 Curve Fitted Crack Profiles

$R_\varepsilon = 0$

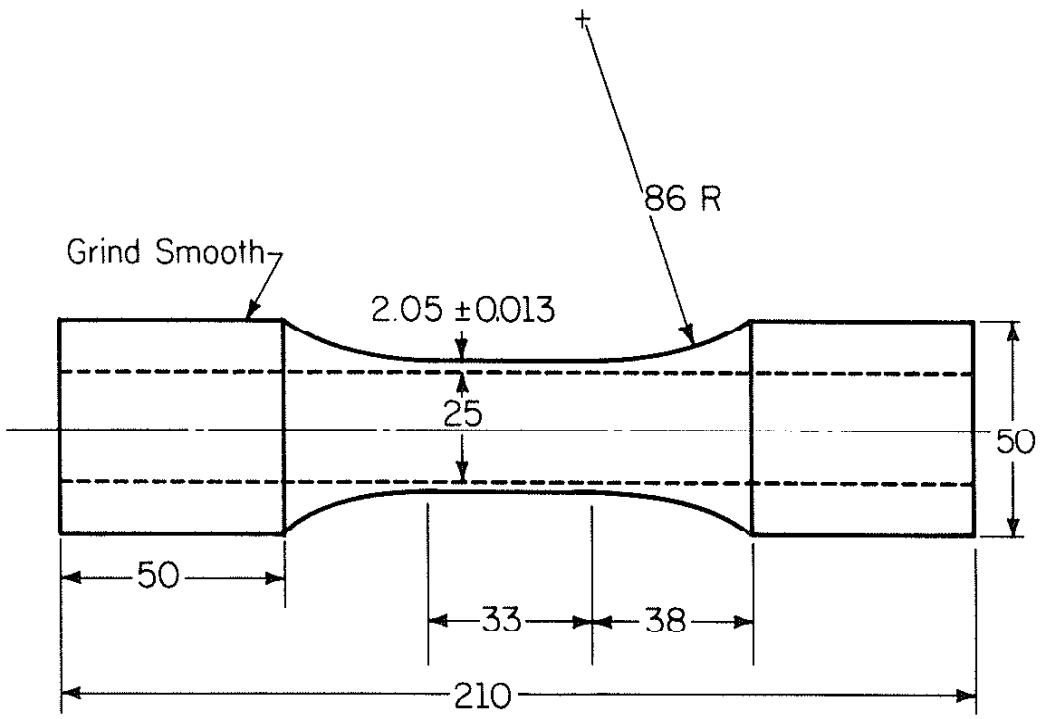

Figure 7 Specimen Dimensions

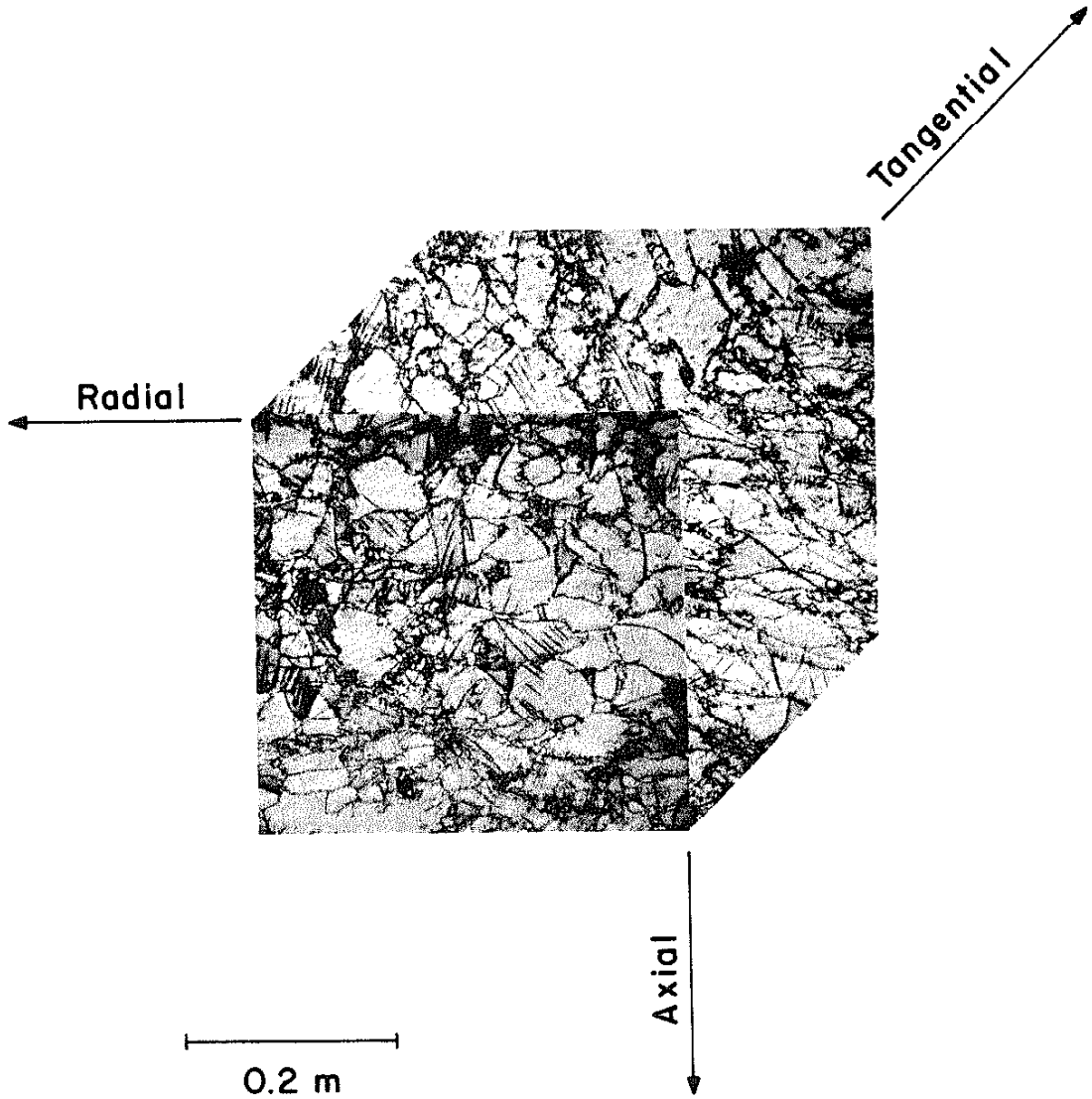

Figure 8 Grain Structure

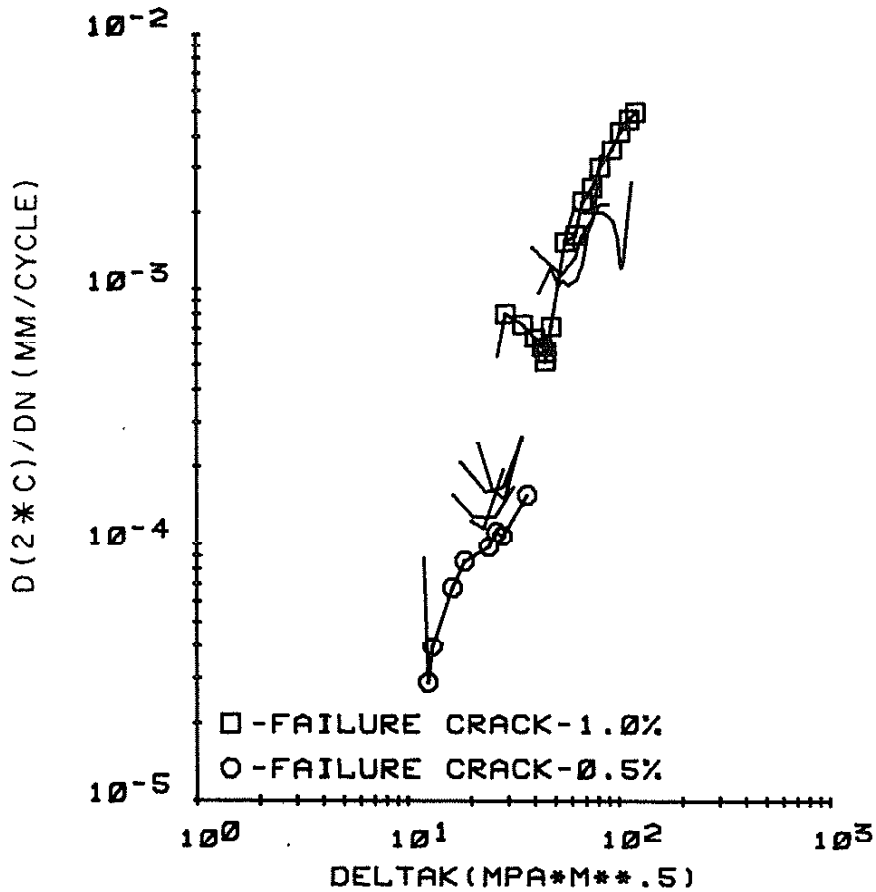

Figure 9 Crack Growth Rate versus ΔK_{eff}
$\lambda = 0$, $\Delta\bar{\varepsilon}/2 = 1.0\%$ and 0.5%, $R_\varepsilon = 0$

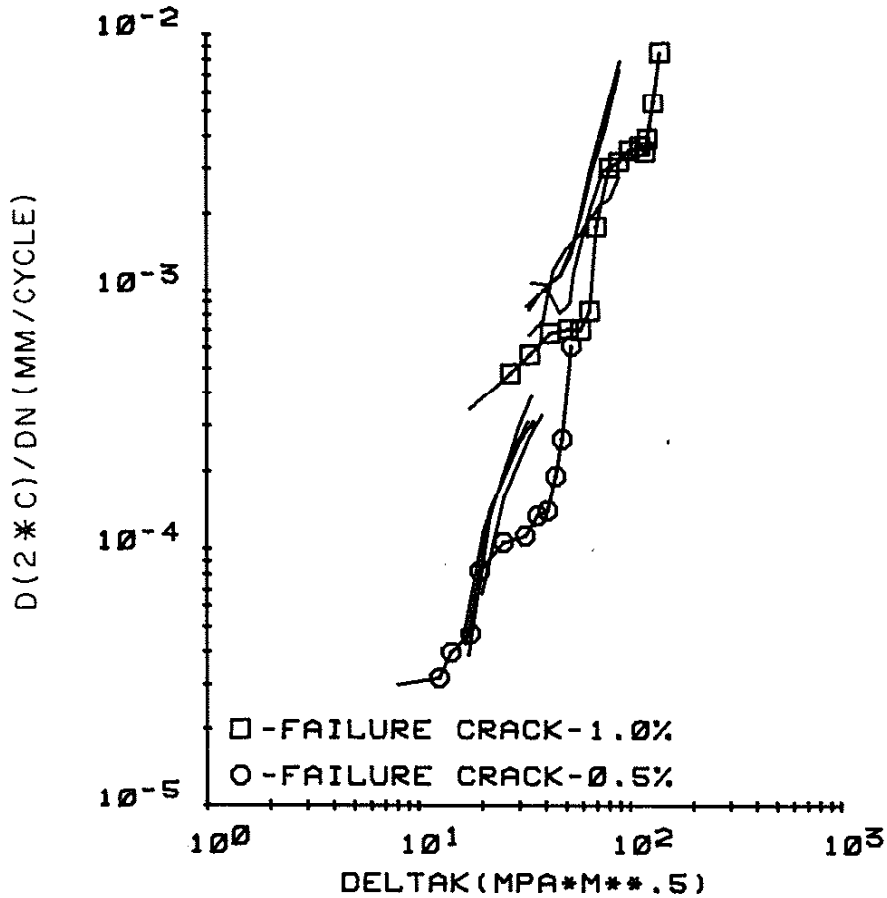

Figure 10 Crack Growth Rate versus ΔK_{eff}
$\lambda = 0$, $\Delta\bar{\varepsilon}/2 = 1.0\%$ and 0.5%, $R_{\varepsilon} = -1$

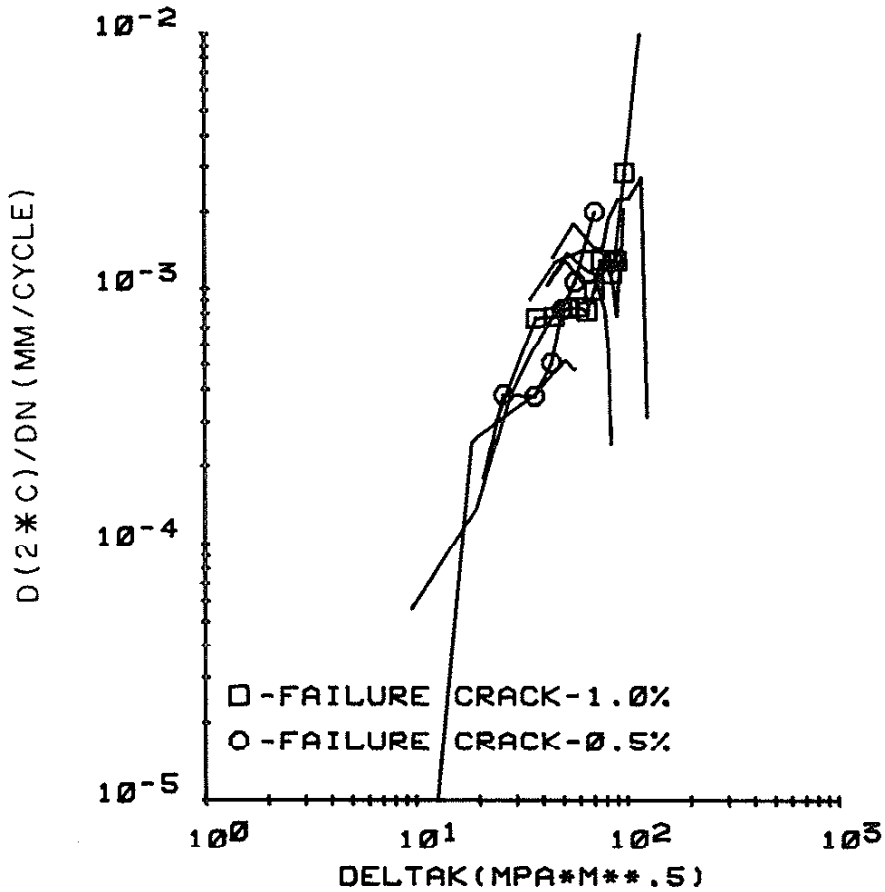

Figure 11 Crack Growth Rate versus ΔK_{eff}
$\lambda = \sqrt{3}$, $\Delta\bar{\varepsilon}/2$ = 1.0% and 0.5%, $R_{\varepsilon} = 0$

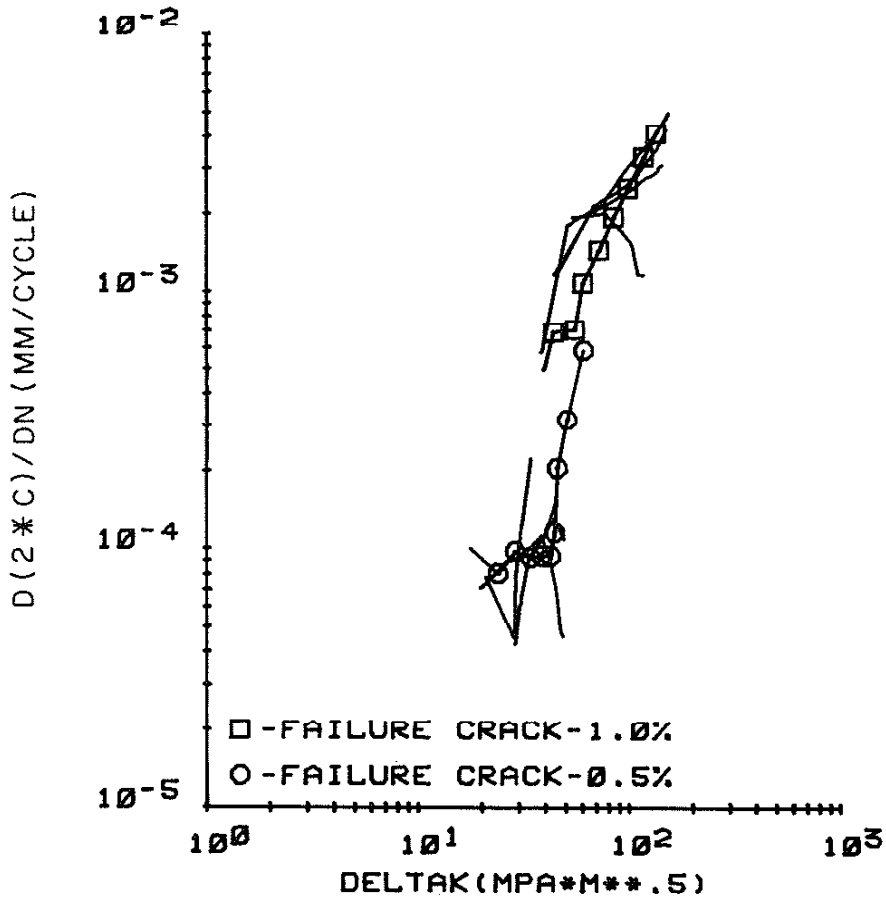

Figure 12 Crack Growth Rate versus ΔK_{eff}
$\lambda = \sqrt{3}$, $\Delta\bar{\varepsilon}/2$ = 1.0% and 0.5%, R_c = -1

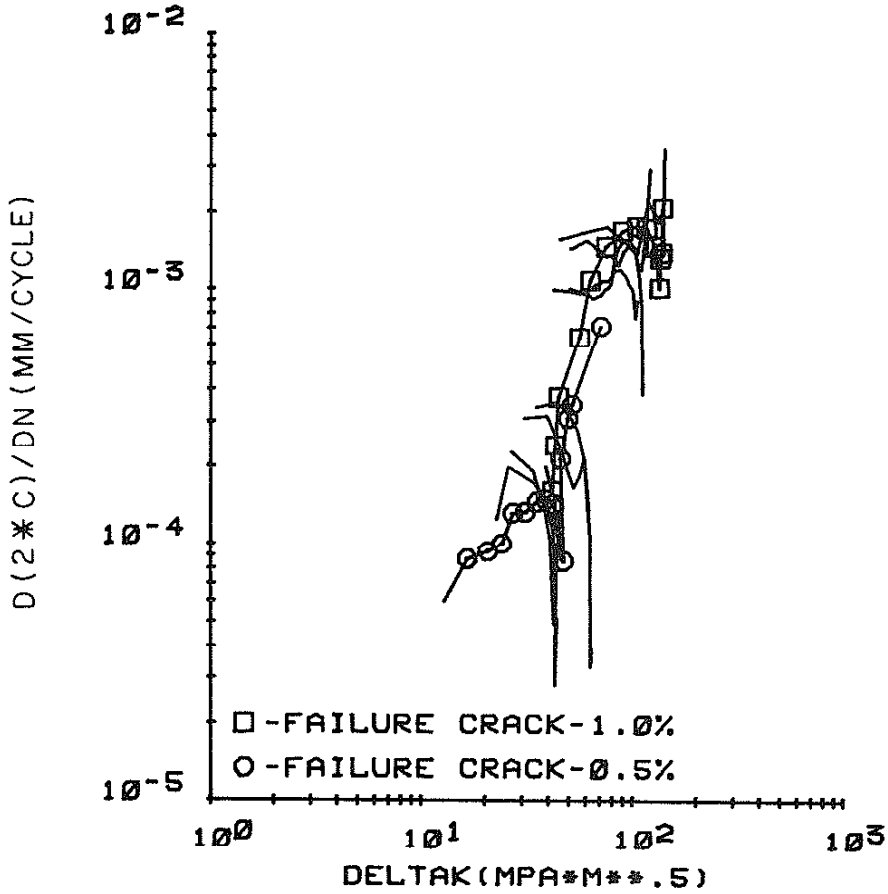

Figure 13 Crack Growth Rate versus ΔK_{eff}
$\lambda = \infty$, $\Delta\bar{\varepsilon}/2$ = 1.0% and 0.5%, $R_{\varepsilon} = 0$

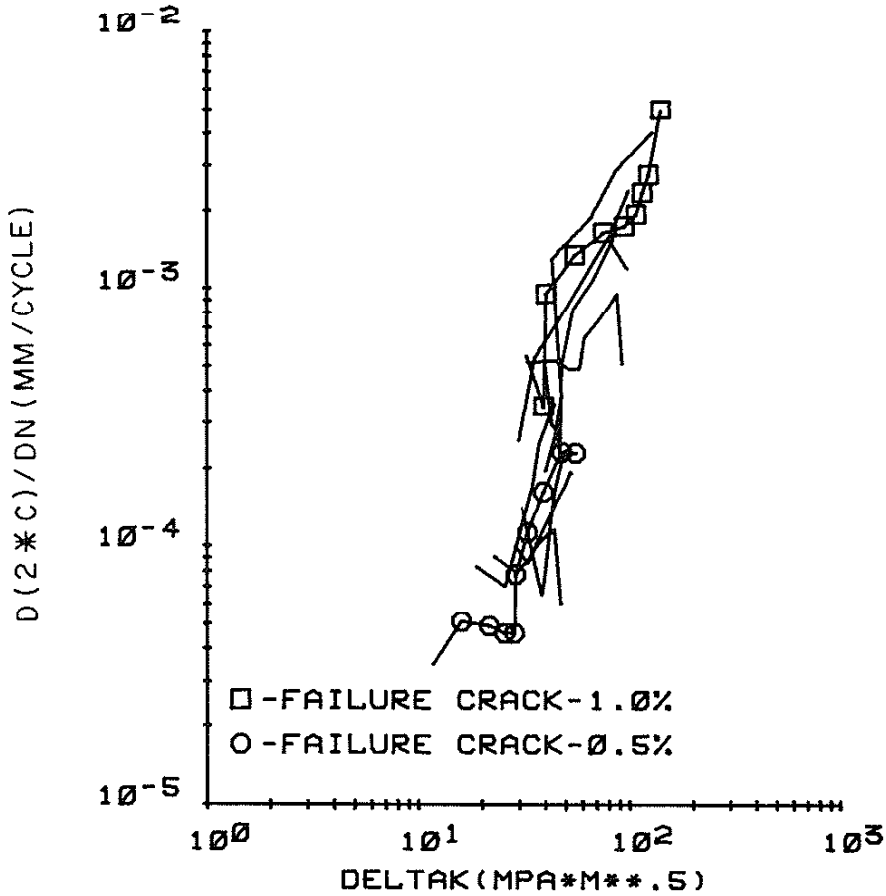

Figure 14 Crack Growth Rate versus ΔK_{eff}
$\lambda = \infty$, $\Delta\bar{\varepsilon}/2$ = 1.0% and 0.5%, R_{ε} = -1

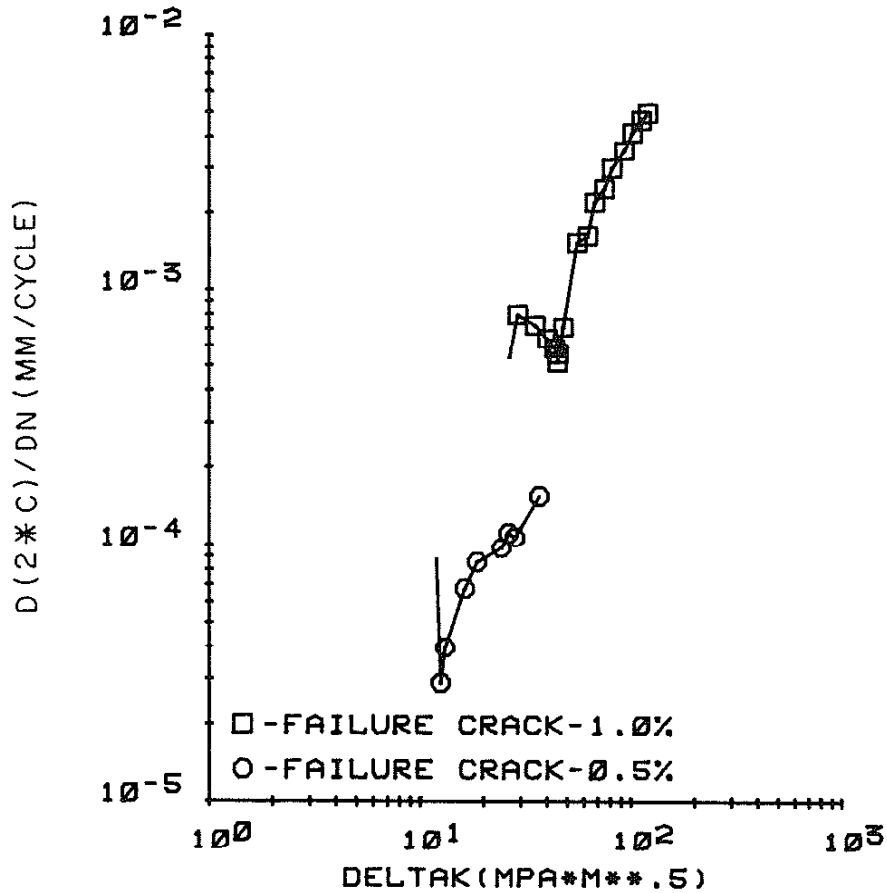

Figure 15 Crack Growth Rate versus ΔK_{eff}, Failure Cracks $\lambda = 0$, $\Delta\bar{\varepsilon}/2 = 1.0\%$ and 0.5%, $R_{\varepsilon} = 0$

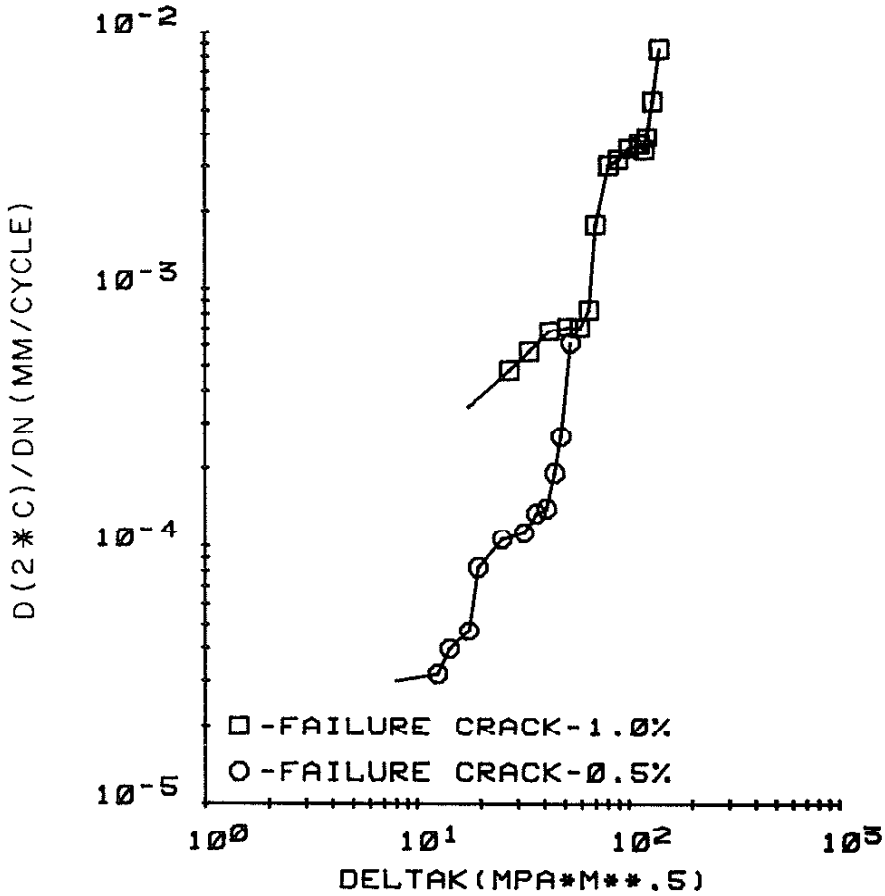

Figure 16 Crack Growth Rate versus ΔK_{eff}, Failure Cracks $\lambda = 0$, $\Delta\bar{\varepsilon}/2 = 1.0\%$ and 0.5%, $R_{\varepsilon} = -1$

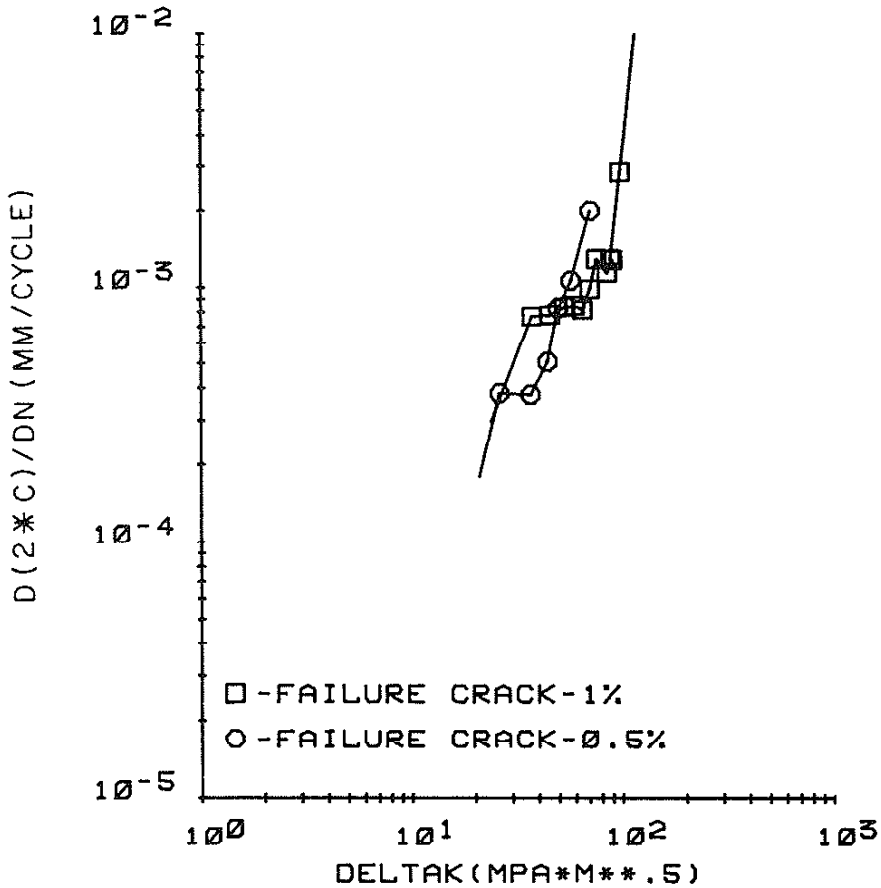

Figure 17 Crack Growth Rate versus ΔK_{eff}, Failure Cracks $\lambda = \sqrt{3}$, $\Delta\bar{\varepsilon}/2$ = 1.0% and 0.5%, $R_{\varepsilon} = 0$

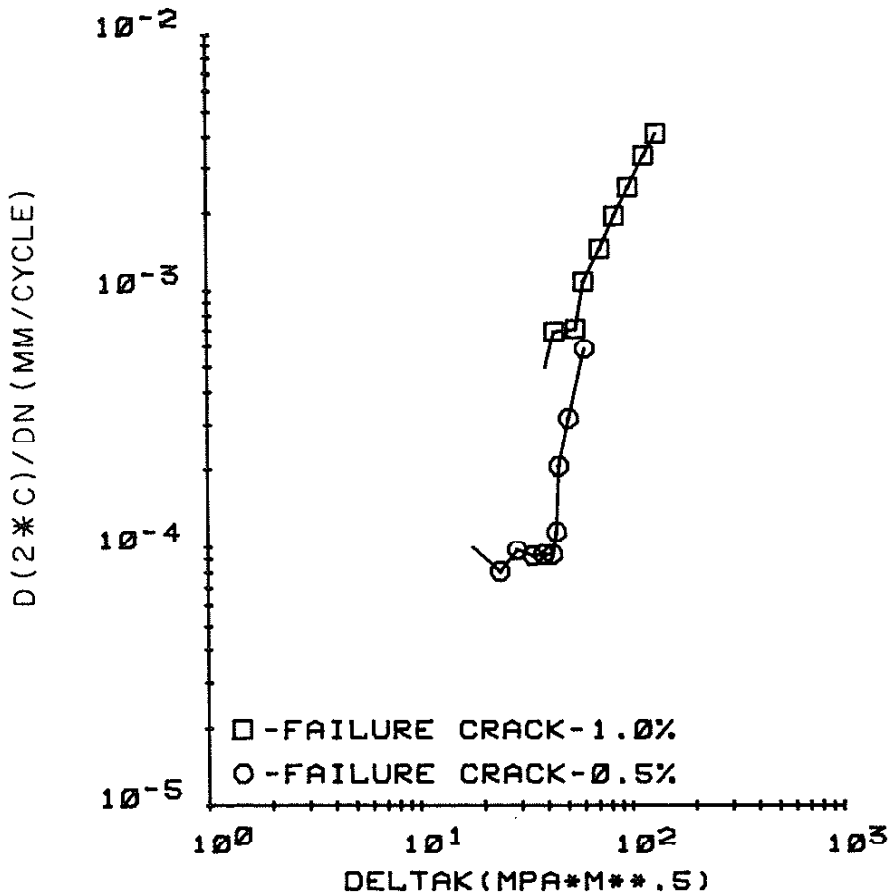

Figure 18 Crack Growth Rate versus ΔK_{eff}, Failure Cracks $\lambda = \sqrt{3}$, $\Delta\bar{\varepsilon}/2 = 1.0\%$ and 0.5%, $R_{\varepsilon} = -1$

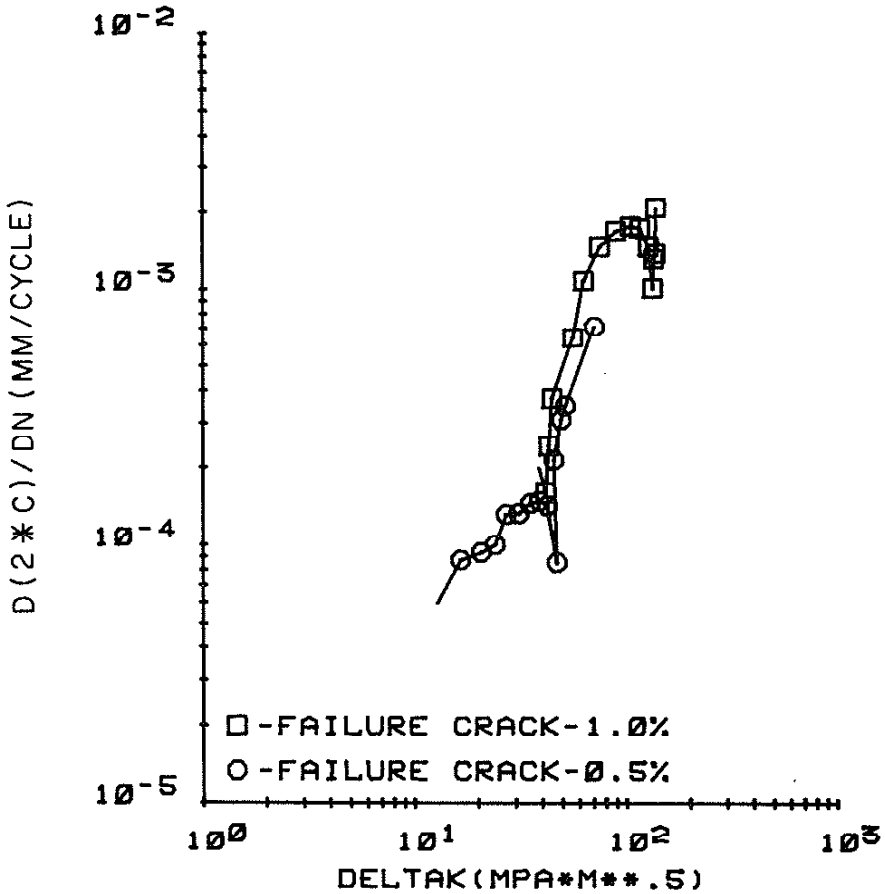

Figure 19 Crack Growth Rate versus ΔK_{eff}, Failure Cracks $\lambda = \infty$, $\Delta\bar{\varepsilon}/2$ = 1.0% and 0.5%, $R_{\varepsilon} = 0$

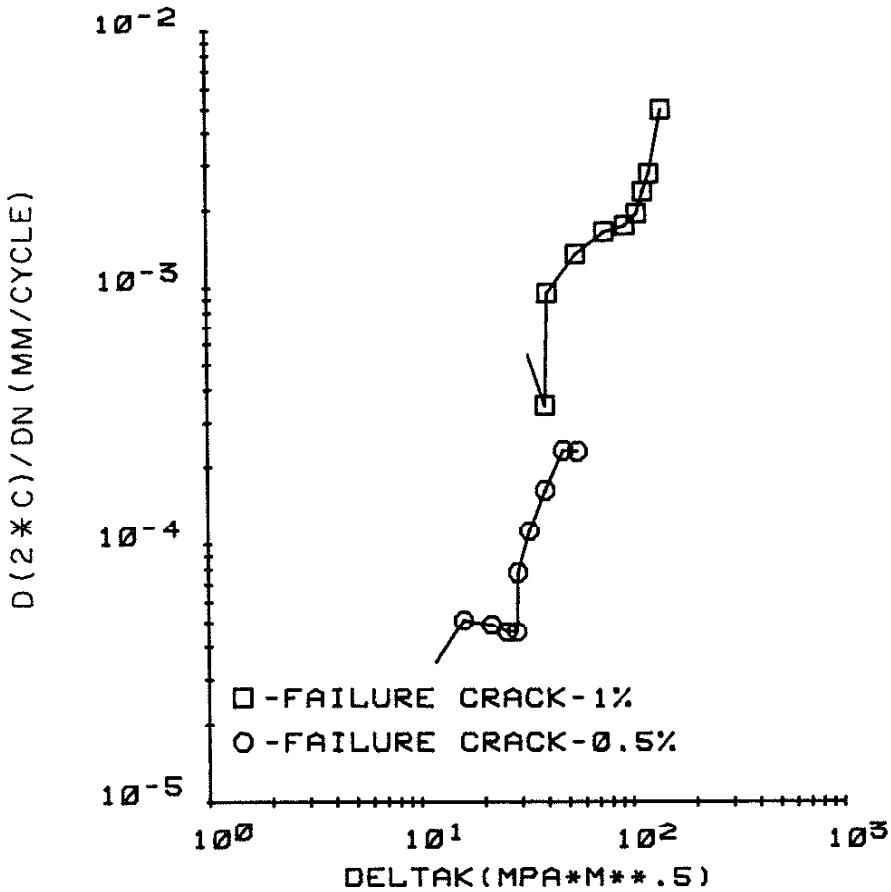

Figure 20 Crack Growth Rate versus ΔK_{eff}, Failure Cracks $\lambda = \infty$, $\Delta\bar{\varepsilon}/2$ = 1.0% and 0.5%, $R_\varepsilon = -1$

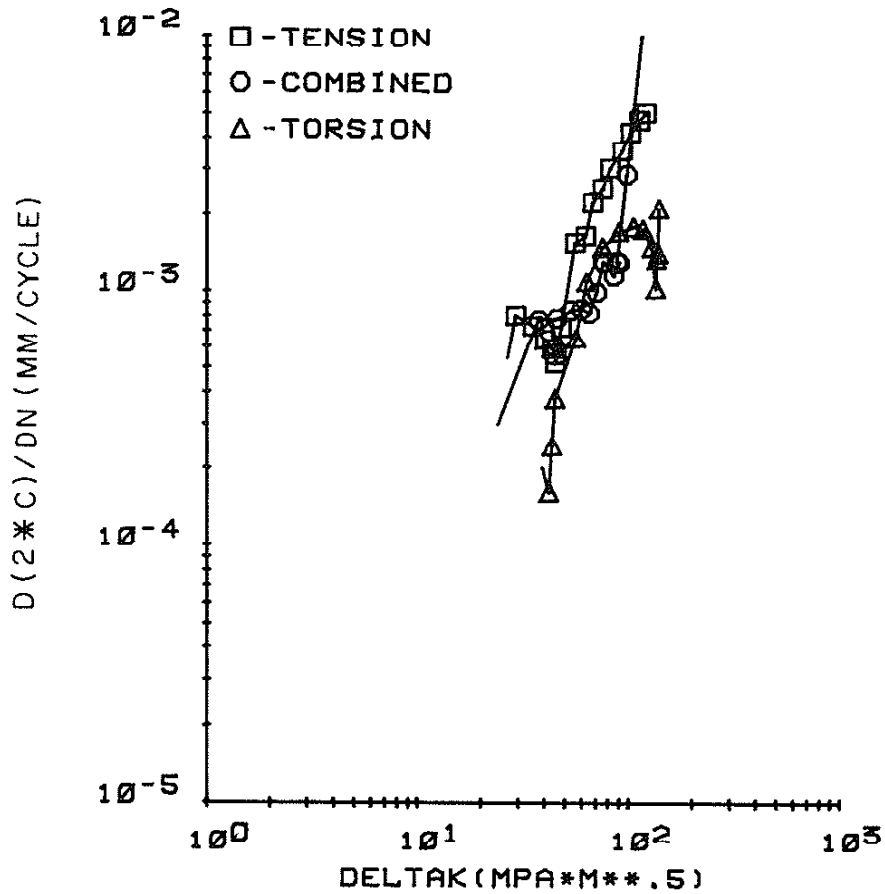

Figure 21 Crack Growth Rate versus ΔK_{eff}, Failure Cracks $\lambda = 0, \sqrt{3}, \infty$; $\Delta\bar{\varepsilon}/2 = 1.0\%$, $R_{\varepsilon} = 0$

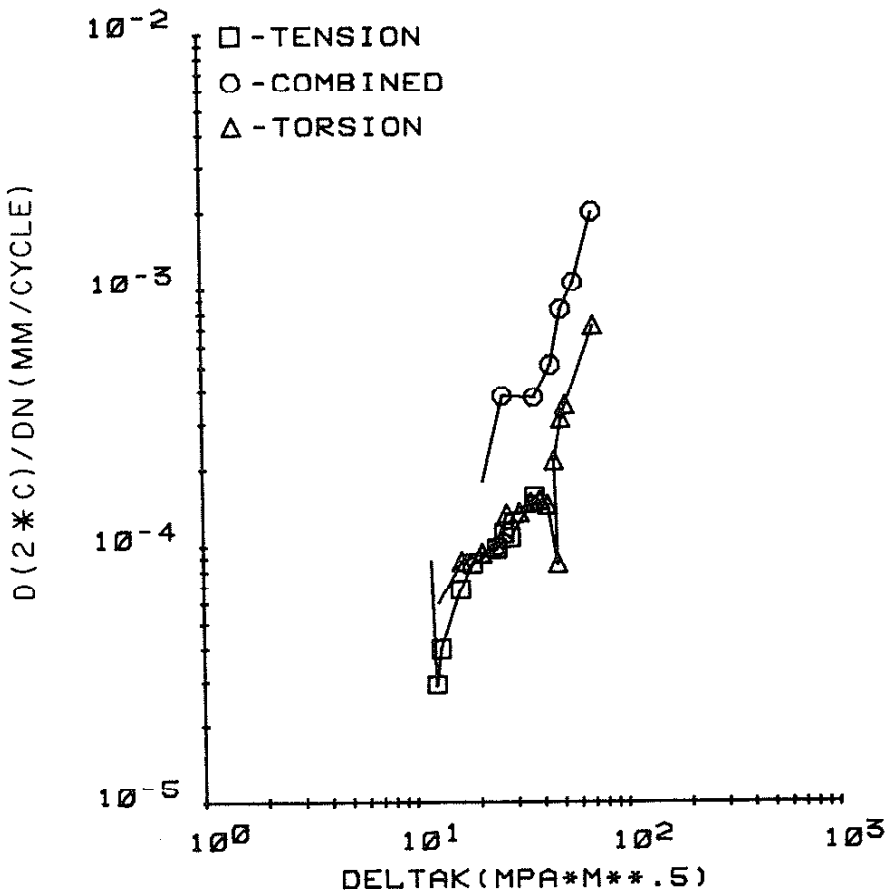

Figure 22 Crack Growth Rate versus ΔK_{eff}, Failure Cracks $\lambda = 0, \sqrt{3}, \infty$; $\Delta\bar{\varepsilon}/2 = 0.5\%$, $R_\varepsilon = 0$

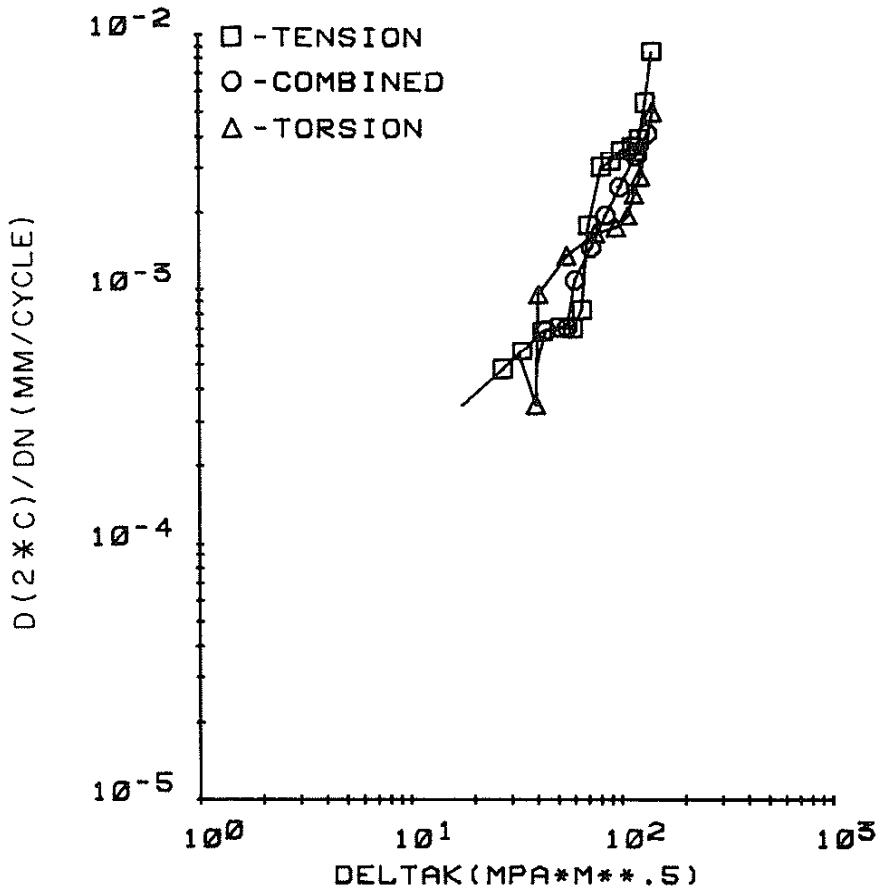

Figure 23 Crack Growth Rate versus ΔK_{eff}, Failure Cracks
$\lambda = 0, \sqrt{3}, \infty$: $\Delta\bar{\varepsilon}/2 = 1.0\%$, $R_{\varepsilon} = -1$

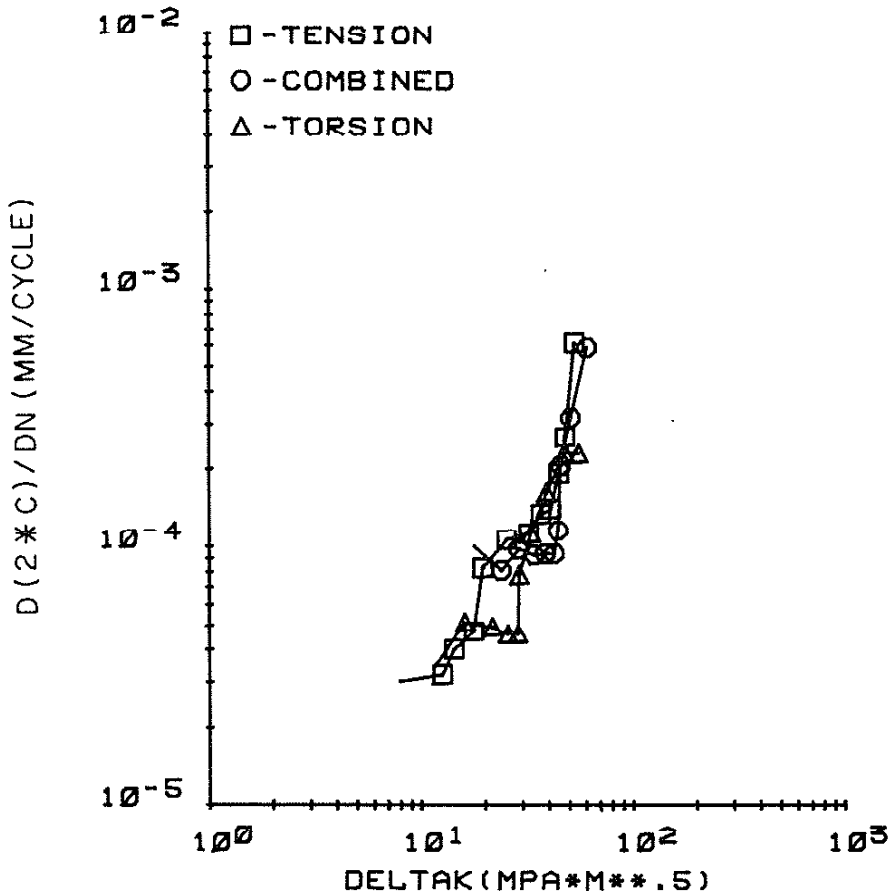

Figure 24 Crack Growth Rate versus ΔK_{eff}, Failure Cracks
$\lambda = 0, \sqrt{3}, \infty$; $\Delta\bar{\varepsilon}/2 = 0.5\%$, $R_{\varepsilon} = -1$

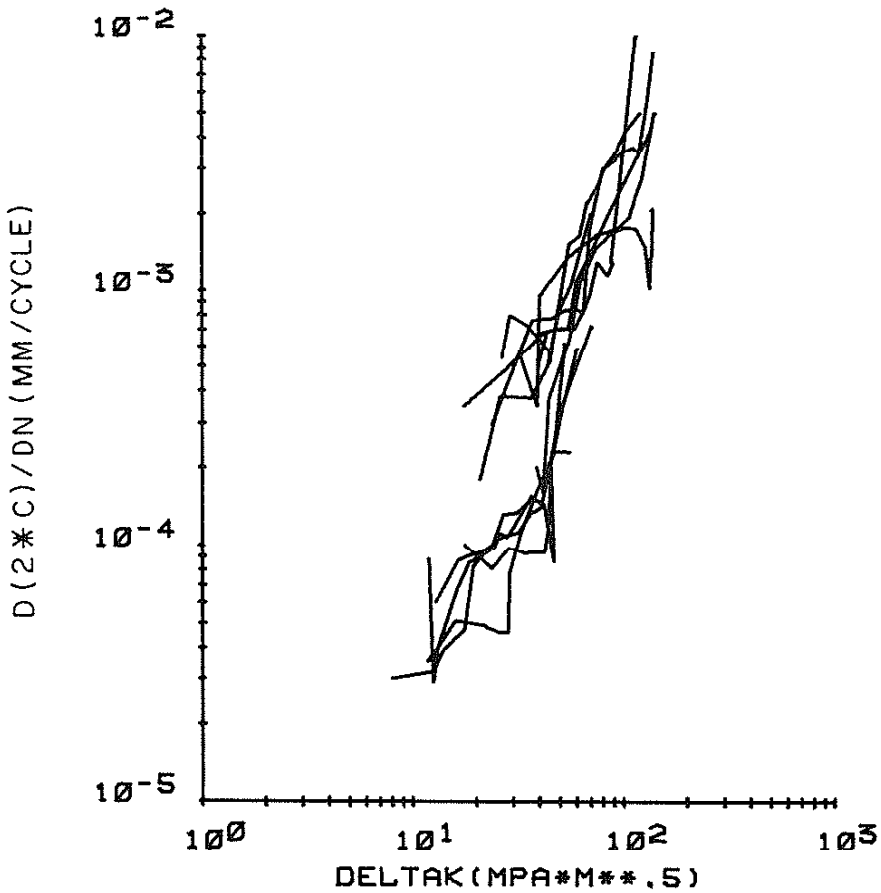

Figure 25 Crack Growth Rate versus ΔK_{eff}, All Failure Cracks

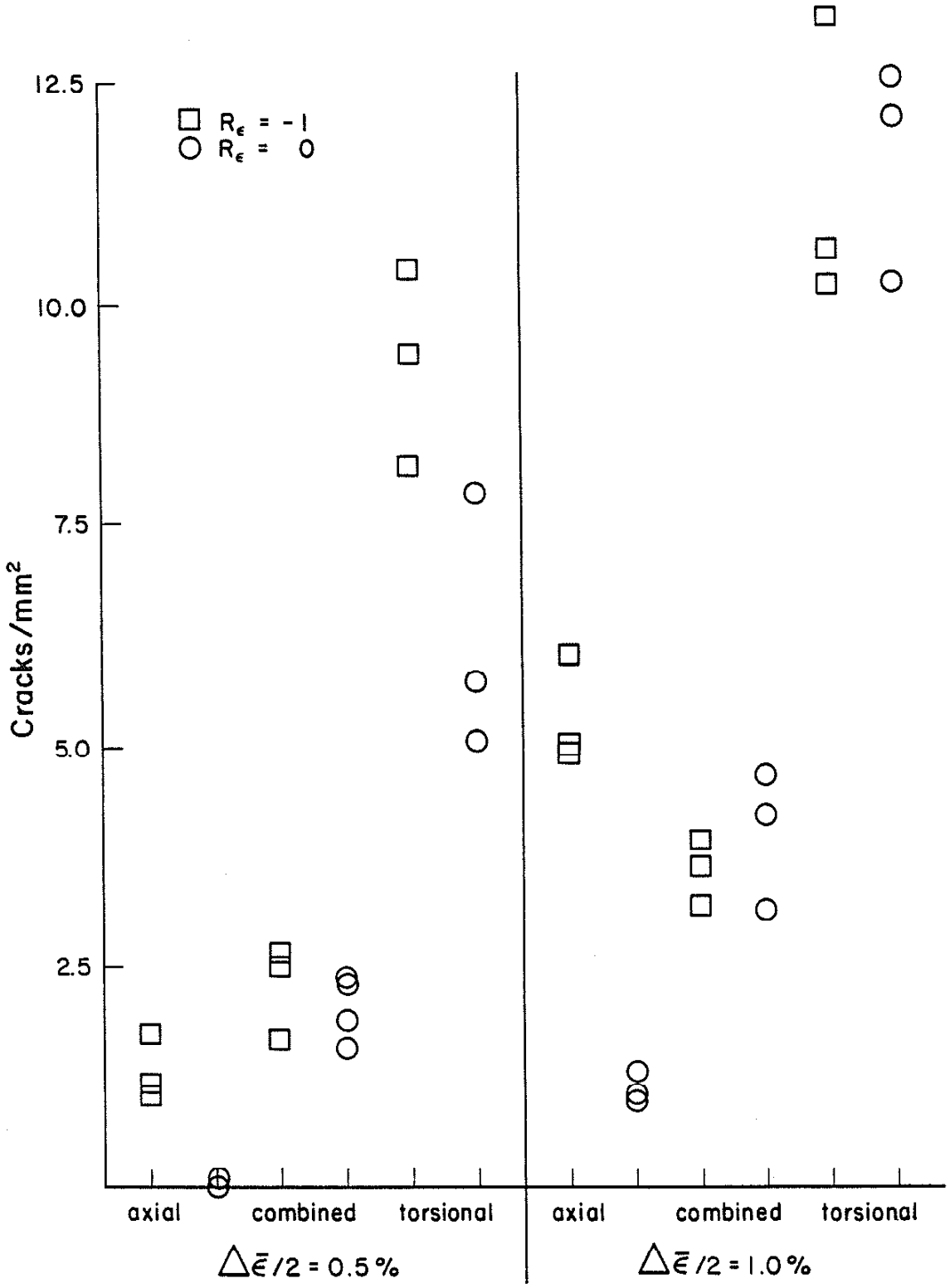

Figure 26 Crack Density at Failure

Table A.1 CRACK GROWTH RATES AS A FUNCTION OF CRACK LENGTH AND OTHER PARAMETERS

TEST: $\lambda = 0$, $\Delta\bar{\varepsilon}/2 = 1.0\%$, $R_\varepsilon = 0$, Failure Crack

Cycles	Crack Length (2c) (mm)	d(2c)/dN mm/cycle	Stress-Intensity Factor (MPa $\sqrt{m}$)					
			MODE I		MODE II		COMBINED	
			Max	Range	Max	Range	Max	Range
40.0	0.020							
120.0	0.070	0.542E-03	13.04	13.04	23.27	23.27	26.67	26.67
160.0	0.090	0.805E-03	14.27	14.27	25.48	25.48	29.21	29.21
200.0	0.090	0.729E-03	17.19	17.19	30.68	30.68	35.17	35.17
240.0	0.180	0.643E-03	19.62	19.62	35.02	35.02	40.15	40.15
280.0	0.200	0.589E-03	21.26	21.26	37.95	37.95	43.50	43.50
320.0	0.200	0.559E-03	22.18	22.18	39.59	39.59	45.38	45.38
360.0	0.200	0.518E-03	21.93	21.93	39.14	39.14	44.86	44.86
400.0	0.230	0.718E-03	23.35	23.35	41.68	41.68	47.78	47.78
480.0	0.270	0.154E-02	27.26	27.26	48.66	48.66	55.78	55.78
520.0	0.430	0.164E-02	30.56	30.56	54.54	54.54	62.52	62.52
560.0	0.430	0.223E-02	33.04	33.04	58.97	58.97	67.59	67.59
600.0	0.580	0.252E-02	36.76	36.76	65.61	65.61	75.21	75.21
650.0	0.620	0.302E-02	40.03	40.03	71.44	71.44	81.89	81.89
700.0	0.900	0.355E-02	45.64	45.64	81.47	81.47	93.38	93.38
750.0	0.980	0.420E-02	50.03	50.03	89.31	89.31	102.36	102.36
800.0	1.350	0.470E-02	55.01	55.01	98.19	98.19	112.55	112.55
850.0	1.430	0.500E-02	58.92	58.92	105.18	105.18	120.56	120.56
900.0	1.850							

Table A.2 CRACK GROWTH RATES AS A FUNCTION OF CRACK LENGTH AND OTHER PARAMETERS

TEST: $\lambda = 0$, $\Delta\bar{\varepsilon}/2 = 1.0\%$, $R_\varepsilon = 0$, Crack A

Cycles	Crack Length (2c) (mm)	d(2c)/dN mm/cycle	Stress-Intensity Factor (MPa $\sqrt{m}$)					
			MODE I		MODE II		COMBINED	
			Max	Range	Max	Range	Max	Range
240.0	0.234							
280.0	0.302	0.156E-02	27.08	27.08	48.33	48.33	55.40	55.40
320.0	0.359	0.210E-02	30.20	30.20	53.91	53.91	61.79	61.79
360.0	0.484	0.201E-02	33.70	33.70	60.15	60.15	68.94	68.94
400.0	0.562	0.202E-02	36.64	36.64	65.39	65.39	74.96	74.96
440.0	0.625	0.202E-02	39.23	39.23	70.02	70.02	80.26	80.26
480.0	0.703	0.202E-02	41.24	41.24	73.61	73.61	84.37	84.37
520.0	0.781	0.194E-02	43.86	43.86	78.28	78.28	89.73	89.73
560.0	0.867	0.186E-02	46.15	46.15	82.38	82.38	94.43	94.43
600.0	0.984	0.163E-02	48.15	48.15	85.95	85.95	98.52	98.52
650.0	1.012	0.124E-02	49.95	49.95	89.17	89.17	102.21	102.21
700.0	1.078	0.122E-02	50.50	50.50	90.13	90.13	103.22	103.22
750.0	1.094	0.130E-02	51.63	51.63	92.16	92.16	105.64	105.64
800.0	1.109	0.164E-02	52.98	52.98	94.57	94.57	108.40	108.40
850.0	1.320	0.266E-02	56.61	56.61	101.05	101.05	115.83	115.83
900.0	1.375							

Table A.3 CRACK GROWTH RATES AS A FUNCTION OF CRACK LENGTH AND OTHER PARAMETERS

TEST: $\lambda = 0$, $\Delta\bar{\varepsilon}/2 = 1.0\%$, $R_\varepsilon = 0$, Crack B

Cycles	Crack Length (2c) (mm)	d(2c)/dN mm/cycle	Stress-Intensity Factor (MPa $\sqrt{m}$)					
			MODE I		MODE II		COMBINED	
			Max	Range	Max	Range	Max	Range
440.0	0.156							
480.0	0.172	0.975E-03	20.44	20.44	36.48	36.48	41.81	41.81
520.0	0.234	0.125E-02	23.53	23.53	42.27	42.27	48.45	48.45
560.0	0.295	0.114E-02	26.26	26.26	46.87	46.87	53.72	53.72
600.0	0.344	0.125E-02	28.23	28.23	50.39	50.39	57.76	57.76
650.0	0.367	0.133E-02	30.47	30.47	54.39	54.39	62.35	62.35
700.0	0.445	0.163E-02	32.82	32.82	58.58	58.58	67.15	67.15
750.0	0.539	0.186E-02	36.27	36.27	64.74	64.74	74.21	74.21
800.0	0.641	0.217E-02	39.96	39.96	71.33	71.33	81.76	81.76
850.0	0.797	0.217E-02	43.99	43.99	78.52	78.52	90.00	90.00
900.0	0.858							

Table A.4 CRACK GROWTH RATES AS A FUNCTION OF CRACK LENGTH AND OTHER PARAMETERS

TEST: $\lambda = 0$, $\Delta\bar{\varepsilon}/2 = 1.0\%$, $R_\varepsilon = 0$, Crack C

Cycles	Crack Length (2c) (mm)	d(2c)/dN mm/cycle	Stress-Intensity Factor (MPa$\sqrt{m}$)					
			MODE I		MODE II		COMBINED	
			Max	Range	Max	Range	Max	Range
400.0	0.117							
440.0	0.148	0.146E-02	18.96	18.96	33.84	33.84	37.78	38.78
480.0	0.234	0.126E-02	23.20	23.20	41.42	41.42	47.47	47.47
520.0	0.273	0.104E-02	25.32	25.32	45.20	45.20	51.81	51.81
560.0	0.306	0.109E-02	26.78	26.78	47.79	47.79	54.78	54.78
600.0	0.313	0.104E-02	28.29	28.29	50.49	50.49	57.88	57.88
650.0	0.375	0.110E-02	31.01	31.01	55.36	55.36	63.45	63.45
700.0	0.480	0.127E-02	33.14	33.14	59.16	59.16	67.81	67.81
750.0	0.539	0.170E-02	35.16	35.16	62.76	62.76	71.94	71.94
800.0	0.547	0.188E-02	37.04	37.04	66.12	66.12	75.79	75.79
850.0	0.675	0.336E-02	40.48	40.48	72.26	72.26	82.83	82.83
900.0	0.883							

Table A.5 CRACK GROWTH RATES AS A FUNCTION OF CRACK LENGTH AND OTHER PARAMETERS

TEST: $\lambda = 0$, $\Delta\bar{\varepsilon}/2 = 0.5\%$, $R_\varepsilon = 0$, Failure Crack

Cycles	Crack Length (2c) (mm)	d(2c)/dN mm/cycle	Stress-Intensity Factor (MPa$\sqrt{m}$)					
			MODE I		MODE II		COMBINED	
			Max	Range	Max	Range	Max	Range
200.0	0.030							
400.0	0.055	0.875E-04	6.44	6.44	10.02	10.02	11.91	11.91
800.0	0.060	0.286E-04	6.73	6.73	10.47	10.47	12.45	12.45
1200.0	0.065	0.404E-04	7.07	7.07	11.00	11.00	13.08	13.08
2000.0	0.070	0.679E-04	8.80	8.80	13.70	13.70	16.28	16.28
2400.0	0.175	0.861E-04	10.05	10.05	15.65	15.65	18.60	18.60
3200.0	0.200	0.984E-04	13.09	13.09	20.39	20.39	24.23	24.23
3600.0	0.280	0.112E-03	14.20	14.20	22.10	22.10	26.27	26.27
4000.0	0.330	0.108E-03	15.21	15.21	23.68	23.68	28.14	28.14
6000.0	0.525	0.156E-03	19.89	19.89	30.97	30.97	35.80	36.80
7000.0	0.710							

Table A.6 CRACK GROWTH RATES AS A FUNCTION OF CRACK LENGTH AND OTHER PARAMETERS

TEST: $\lambda = 0$, $\Delta\bar{\varepsilon}/2 = 0.5\%$, $R_\varepsilon = 0$, Crack A

Cycles	Crack Length (2c) (mm)	d(2c)/dN mm/cycle	Stress-Intensity Factor (MPa $\sqrt{m}$)					
			MODE I		MODE II		COMBINED	
			Max	Range	Max	Range	Max	Range
3600.0	0.099							
4000.0	0.156	0.124E-03	10.84	10.84	16.88	16.88	20.06	20.06
5000.0	0.234	0.116E-03	12.37	12.37	19.26	19.26	22.89	22.89
6000.0	0.313	0.196E-03	15.36	15.36	23.91	23.91	28.42	28.42
7000.0	0.625							

Table A.7 CRACK GROWTH RATES AS A FUNCTION OF CRACK LENGTH AND OTHER PARAMETERS

TEST: $\lambda = 0$, $\Delta\bar{\varepsilon}/2 = 0.5\%$, $R_\varepsilon = 0$, Crack B

Cycles	Crack Length (2c) (mm)	d(2c)/dN mm/cycle	Stress-Intensity Factor (MPa $\sqrt{m}$)					
			MODE I		MODE II		COMBINED	
			Max	Range	Max	Range	Max	Range
3200.0	0.050							
3600.0	0.105	0.156E-03	8.89	8.89	13.85	13.85	16.46	16.46
4000.0	0.175	0.129E-03	11.04	11.04	17.18	17.18	20.42	20.42
5000.0	0.273	0.129E-03	14.09	14.09	21.94	21.94	26.08	26.08
6000.0	0.391	0.168E-03	17.16	17.16	26.73	26.73	31.76	31.76
7000.0	0.609							

Table A.8 CRACK GROWTH RATES AS A FUNCTION OF CRACK LENGTH AND OTHER PARAMETERS

TEST: $\lambda = 0$, $\Delta\bar{\varepsilon}/2 = 0.5\%$, $R_\varepsilon = 0$, Crack C

Cycles	Crack Length (2c) (mm)	d(2c)/dN mm/cycle	Stress-Intensity Factor (MPa $\sqrt{m}$)					
			MODE I		MODE II		COMBINED	
			Max	Range	Max	Range	Max	Range
3200.0	0.078							
3600.0	0.123	0.209E-03	9.63	9.63	14.99	14.99	17.81	17.81
4000.0	0.245	0.160E-03	12.69	12.69	19.77	19.77	23.49	23.49
5000.0	0.342	0.168E-03	15.38	15.38	23.95	23.95	28.46	28.46
6000.0	0.469	0.259E-03	18.80	18.80	29.27	29.27	34.79	34.79
7000.0	0.859							

Table A.9 CRACK GROWTH RATES AS A FUNCTION OF CRACK LENGTH AND OTHER PARAMETERS

TEST: $\lambda = 0$, $\Delta\bar{\varepsilon}/2 = 0.5\%$, $R_\varepsilon = 0$, Crack D

Cycles	Crack Length (2c) (mm)	d(2c)/dN mm/cycle	Stress-Intensity Factor (MPa $\sqrt{m}$)					
			MODE I		MODE II		COMBINED	
			Max	Range	Max	Range	Max	Range
3200.0	0.082							
3600.0	0.181	0.248E-03	11.68	11.68	18.18	18.18	21.61	21.61
4000.0	0.280	0.164E-03	13.65	13.65	21.26	21.26	25.26	25.26
5000.0	0.352	0.151E-03	15.58	15.58	24.26	24.26	28.83	28.83
6000.0	0.472	0.266E-03	18.86	18.86	29.36	29.36	34.90	34.90
7000.0	0.883							

Table A.10 CRACK GROWTH RATES AS A FUNCTION OF CRACK LENGTH AND OTHER PARAMETERS

TEST: $\lambda = 0$, $\Delta\bar{\varepsilon}/2 = 1.0\%$ $R_\varepsilon = -1$, Failure Crack

Cycles	Crack Length (2c) (mm)	d(2c)/dN mm/cycle	Stress-Intensity Factor (MPa $\sqrt{m}$)					
			MODE I		MODE II		COMBINED	
			Max	Range	Max	Range	Max	Range
0.0	0.000							
100.0	0.030	0.350E-03	4.27	8.54	7.69	15.38	8.80	17.59
200.0	0.070	0.480E-03	6.64	13.29	11.96	23.92	13.68	27.36
300.0	0.130	0.568E-03	8.20	16.39	14.75	29.51	16.88	33.76
400.0	0.190	0.686E-03	10.25	20.50	18.46	36.91	21.11	42.22
500.0	0.180	0.711E-03	12.49	24.98	22.49	44.98	25.73	51.45
600.0	0.390	0.704E-03	14.34	28.68	25.81	51.62	29.53	59.05
700.0	0.440	0.832E-03	15.78	31.55	28.40	56.80	32.49	64.98
800.0	0.460	0.179E-02	16.99	33.98	30.58	61.17	34.99	69.97
900.0	0.520	0.305E-02	19.61	39.23	35.31	70.62	40.39	80.79
950.0	0.680	0.321E-02	21.79	43.59	39.23	78.47	44.88	89.76
1000.0	1.200	0.356E-02	24.43	48.86	43.98	87.96	50.31	100.62
1050.0	1.240	0.369E-02	27.50	55.00	49.51	99.01	56.63	113.26
1100.0	1.300	0.350E-02	29.05	58.10	52.30	104.60	59.83	119.65
1150.0	1.560	0.395E-02	29.75	59.51	53.56	107.12	61.27	122.54
1200.0	1.620	0.545E-02	31.75	63.50	57.15	114.30	65.38	130.76
1250.0	1.925	0.860E-02	34.21	68.42	61.59	123.18	70.45	140.90
1300.0	2.480							

Table A.11 CRACK GROWTH RATES AS A FUNCTION OF CRACK LENGTH AND OTHER PARAMETERS

TEST: $\lambda = 0$, $\Delta\bar{\varepsilon}/2 = 1.0\%$, $R_\varepsilon = -1$, Crack A

Cycles	Crack Length (2c) (mm)	d(2c)/dN mm/cycle	Stress-Intensity Factor (MPa $\sqrt{m}$)					
			MODE I		MODE II		COMBINED	
			Max	Range	Max	Range	Max	Range
900.0	0.080							
950.0	0.109	0.840E-03	8.14	16.28	14.66	29.31	16.76	33.53
1000.0	0.164	0.103E-02	9.61	19.21	17.29	34.58	19.78	39.56
1050.0	0.195	0.116E-02	11.42	22.85	20.57	41.13	23.53	47.05
1100.0	0.295	0.141E-02	12.93	25.87	23.28	46.57	26.64	53.27
1150.0	0.352	0.196E-02	14.26	28.53	25.68	51.36	29.38	58.75
1200.0	0.417	0.305E-02	16.07	32.13	28.92	57.84	33.08	66.17
1250.0	0.547	0.445E-02	18.27	36.54	32.89	65.77	37.62	75.24
1300.0	0.803	0.798E-02	22.10	44.19	39.78	79.55	45.50	91.00
1330.0	1.094							

Table A.12 CRACK GROWTH RATES AS A FUNCTION OF CRACK LENGTH AND OTHER PARAMETERS

TEST: $\lambda = 0$, $\Delta\bar{\varepsilon}/2 = 1.0\%$, $R_\varepsilon = -1$, Crack B

Cycles	Crack Length (2c) (mm)	d(2c)/dN mm/cycle	Stress-Intensity Factor (MPa $\sqrt{m}$)					
			MODE I		MODE II		COMBINED	
			Max	Range	Max	Range	Max	Range
800.0	0.063							
900.0	0.109	0.673E-03	8.14	16.28	14.66	29.31	16.76	33.53
950.0	0.148	0.764E-03	9.48	18.97	17.07	34.14	19.53	39.06
1000.0	0.195	0.122E-02	10.65	21.30	19.17	38.34	21.93	43.86
1050.0	0.234	0.148E-02	12.29	24.59	22.13	44.26	25.31	50.63
1100.0	0.312	0.169E-02	14.32	28.64	25.78	51.56	29.49	58.98
1150.0	0.469	0.198E-02	16.20	32.40	29.16	58.32	33.36	66.71
1200.0	0.547	0.223E-02	18.17	36.34	32.71	65.42	37.42	74.83
1250.0	0.625	0.231E-02	19.70	39.40	35.46	70.92	40.57	81.13
1300.0	0.781	0.280E-02	21.79	43.58	39.23	78.46	44.87	89.75
1330.0	0.859							

Table A.13 CRACK GROWTH RATES AS A FUNCTION OF CRACK LENGTH AND OTHER PARAMETERS

TEST: $\lambda = 0$, $\Delta\bar{\epsilon}/2 = 1.0\%$, $R_\epsilon = -1$, Crack C

Cycles	Crack Length (2c) (mm)	d(2c)/dN mm/cycle	Stress-Intensity Factor (MPa $\sqrt{m}$)					
			MODE I		MODE II		COMBINED	
			Max	Range	Max	Range	Max	Range
800.0	0.055							
900.0	0.103	0.867E-03	7.91	15.83	14.25	28.49	16.30	32.59
950.0	0.156	0.103E-02	9.83	19.65	17.69	35.38	20.23	40.47
1000.0	0.234	0.816E-03	11.42	22.84	20.56	41.13	23.52	47.04
1050.0	0.273	0.889E-03	12.69	25.38	22.84	45.68	26.13	52.26
1100.0	0.304	0.117E-02	13.22	26.43	23.79	47.58	27.21	54.43
1150.0	0.313	0.151E-02	14.30	28.59	25.73	51.47	29.44	58.88
1200.0	0.390	0.210E-02	15.96	31.93	28.74	57.48	32.88	65.75
1250.0	0.586	0.297E-02	18.38	36.76	33.09	66.17	37.85	75.70
1300.0	0.703	0.312E-02	20.67	41.35	37.22	74.44	42.58	85.15
1350.0	0.898							

Table A.14 CRACK GROWTH RATES AS A FUNCTION OF CRACK LENGTH AND OTHER PARAMETERS

TEST: $\lambda = 0$, $\Delta\bar{\varepsilon} = 1.0\%$, $R_\varepsilon = -1$, Crack D

Cycles	Crack Length (2c) (mm)	d(2c)/dN mm/cycle	Stress-Intensity Factor (MPa $\sqrt{m}$)					
			MODE I		MODE II		COMBINED	
			Max	Range	Max	Range	Max	Range
900.0	0.071							
950.0	0.117	0.108E-02	8.43	16.87	15.18	30.37	17.37	34.74
1000.0	0.179	0.107E-02	10.06	20.12	18.11	36.22	20.72	41.44
1050.0	0.206	0.118E-02	11.64	23.28	20.96	41.91	23.97	47.95
1100.0	0.293	0.148E-02	12.96	25.92	23.33	46.66	26.69	53.38
1150.0	0.352	0.198E-02	14.48	28.96	26.07	52.14	29.82	59.65
1200.0	0.429	0.301E-02	16.38	32.75	29.48	58.96	33.72	67.44
1250.0	0.594	0.426E-02	18.75	37.49	33.74	67.49	38.60	77.20
1300.0	0.797	0.738E-02	22.01	44.03	39.63	79.26	45.33	90.66
1330.0	1.078							

Table A.15 CRACK GROWTH RATES AS A FUNCTION OF CRACK LENGTH AND OTHER PARAMETERS

TEST: $\lambda = 0$, $\Delta\bar{\varepsilon}/2 = 0.5\%$, $R_\varepsilon = -1$, Failure Crack

Cycles	Crack Length (2c) (mm)	d(2c)/dN mm/cycle	Stress-Intensity Factor (MPa $\sqrt{m}$)					
			MODE I		MODE II		COMBINED	
			Max	Range	Max	Range	Max	Range
0.0	0.000							
1000.0	0.025	0.300E-04	2.19	4.39	3.31	6.63	3.97	7.95
2000.0	0.060	0.315E-04	3.45	6.89	5.21	10.41	6.24	12.49
3000.0	0.100	0.396E-04	3.93	7.86	5.94	11.87	7.12	14.24
4000.0	0.120	0.473E-04	4.85	9.71	7.33	14.66	8.79	17.59
5000.0	0.130	0.829E-04	5.37	10.73	8.10	16.21	9.72	19.44
6000.0	0.280	0.107E-03	6.97	13.94	10.53	21.06	12.63	25.25
7000.0	0.310	0.113E-03	8.85	17.71	13.37	26.75	16.04	32.08
8000.0	0.640	0.135E-03	10.09	20.17	15.24	30.47	18.27	36.55
9000.0	0.690	0.141E-03	11.28	22.56	17.04	34.08	20.43	40.87
10000.0	0.680	0.193E-03	12.31	24.61	18.59	37.18	22.29	44.58
11000.0	1.000	0.267E-03	13.19	26.39	19.93	39.86	23.90	47.81
12000.0	1.120	0.613E-03	14.68	29.37	22.18	44.36	26.60	53.20
12500.0	1.550							

Table A.16 CRACK GROWTH RATES AS A FUNCTION OF CRACK LENGTH AND OTHER PARAMETERS

TEST: $\lambda = 0$, $\Delta\bar{\varepsilon}/2 = 0.5\%$, $R_\varepsilon = -1$. Crack A

Cycles	Crack Length (2c) (mm)	d(2c)/dN mm/cycle	Stress-Intensity Factor (MPa $\sqrt{m}$)					
			MODE I		MODE II		COMBINED	
			Max	Range	Max	Range	Max	Range
9000.0	0.078							
10000.0	0.117	0.390E-04	4.75	9.49	7.17	14.34	8.60	17.19
11000.0	0.156	0.134E-03	6.02	12.04	9.09	18.19	10.90	21.81
12000.0	0.391	0.302E-03	8.31	16.62	12.55	25.10	15.05	30.11
12500.0	0.469	0.390E-03	9.50	19.00	14.35	28.71	17.21	34.43
13000.0	0.781							

Table A.17 CRACK GROWTH RATES AS A FUNCTION OF CRACK LENGTH AND OTHER PARAMETERS

TEST: $\lambda = 0$, $\Delta\bar{\varepsilon}/2 = 0.5\%$, $R_\varepsilon = -1$, Crack B

Cycles	Crack Length (2c) (mm)	d(2c)/dN mm/cycle	Stress-Intensity Factor (MPa $\sqrt{m}$)					
			MODE I		MODE II		COMBINED	
			Max	Range	Max	Range	Max	Range
9000.0	0.060							
10000.0	0.103	0.440E-04	4.45	8.91	6.73	13.45	8.07	16.13
11000.0	0.148	0.119E-03	5.62	11.24	8.49	16.97	10.18	20.35
12000.0	0.313	0.238E-03	7.73	15.46	11.68	23.35	14.00	28.01
12500.0	0.430	0.312E-03	9.10	18.20	13.74	27.49	16.48	32.96
13000.0	0.625							

Table A.18 CRACK GROWTH RATES AS A FUNCTION OF CRACK LENGTH AND OTHER PARAMETERS

TEST: $\lambda = 0$, $\Delta\bar{\varepsilon}/2 = 0.5\%$, $R_\varepsilon = -1$. Crack C

Cycles	Crack Length (2c) (mm)	d(2c)/dN mm/cycle	Stress-Intensity Factor (MPa $\sqrt{m}$)					
			MODE I		MODE II		COMBINED	
			Max	Range	Max	Range	Max	Range
9000.0	0.100							
10000.0	0.156	0.670E-04	5.48	10.96	8.28	16.56	9.93	19.85
11000.0	0.234	0.159E-03	7.00	14.01	10.58	21.16	12.69	25.38
12000.0	0.468	0.276E-03	9.32	18.64	14.08	28.15	16.88	33.76
12500.0	0.586	0.329E-03	10.62	21.24	16.04	32.09	19.24	38.48
13000.0	0.797							

Table A.19 CRACK GROWTH RATES AS A FUNCTION OF CRACK LENGTH AND OTHER PARAMETERS

TEST: $\lambda = 0$, $\Delta\bar{\varepsilon}/2 = 0.5\%$, $R_\varepsilon = -1$, Crack D

Cycles	Crack Length (2c) (mm)	d(2c)/dN mm/cycle	Stress-Intensity Factor (MPa $\sqrt{m}$)					
			MODE I		MODE II		COMBINED	
			Max	Range	Max	Range	Max	Range
9000.0	0.070							
10000.0	0.109	0.430E-04	4.58	9.16	6.92	13.84	8.30	16.60
11000.0	0.156	0.141E-03	5.97	11.94	9.02	18.03	10.81	21.63
12000.0	0.391	0.264E-03	8.36	16.71	12.62	25.25	15.14	30.28
12500.0	0.484	0.312E-03	9.65	19.30	14.58	29.16	17.49	34.97
13000.0	0.703							

Table A.20 CRACK GROWTH RATES AS A FUNCTION OF CRACK LENGTH AND OTHER PARAMETERS

TEST: $\lambda = \sqrt{3}$, $\Delta\bar{\varepsilon}/2 = 1.0\%$, $R_\varepsilon = 0$, Failure Crack

Cycles	Crack Length (2c) (mm)	d(2c)/dN mm/cycle	Stress-Intensity Factor (MPa $\sqrt{m}$)					
			MODE I		MODE II		COMBINED	
			Max	Range	Max	Range	Max	Range
75.0	0.040							
125.0	0.050	0.300E-03	6.24	6.24	23.13	23.13	23.95	23.95
225.0	0.100	0.771E-03	9.74	9.74	36.11	36.11	37.40	37.40
300.0	0.220	0.782E-03	11.84	11.84	43.88	43.88	45.45	45.45
375.0	0.250	0.839E-03	13.84	13.84	51.30	51.30	53.13	53.13
450.0	0.270	0.852E-03	15.61	15.61	57.85	57.85	59.92	59.92
525.0	0.400	0.819E-03	16.93	16.93	62.75	62.75	64.99	64.99
600.0	0.440	0.990E-03	18.35	18.35	68.01	68.01	70.44	70.44
675.0	0.500	0.130E-02	19.79	19.79	73.35	73.35	75.97	75.97
750.0	0.570	0.115E-02	22.10	22.10	81.94	81.94	84.87	84.87
825.0	0.710	0.129E-02	23.52	23.52	87.18	87.18	90.29	90.29
875.0	0.880	0.130E-02	22.88	22.88	84.79	84.79	87.83	87.83
1050.0	0.925	0.286E-02	25.53	25.53	94.62	94.62	98.00	98.00
1200.0	1.240	0.121E-01	31.07	31.07	115.17	115.17	119.29	119.29
1260.0	2.210							

Table A.21 CRACK GROWTH RATES AS A FUNCTION OF CRACK LENGTH AND OTHER PARAMETERS

TEST: $\lambda = \sqrt{3}$, $\Delta\bar{\varepsilon}/2 = 1.0\%$, $R_\varepsilon = 0$, Crack A

Cycles	Crack Length (2c) (mm)	d(2c)/dN mm/cycle	Stress-Intensity Factor (MPa $\sqrt{m}$)					
			MODE I		MODE II		COMBINED	
			Max	Range	Max	Range	Max	Range
600.0	0.078							
675.0	0.156	0.104E-02	11.02	11.02	40.85	40.85	42.31	42.31
750.0	0.234	0.130E-02	13.34	13.34	49.44	49.44	51.20	51.20
825.0	0.313	0.107E-02	16.15	16.15	59.88	59.88	62.02	62.02
875.0	0.440	0.107E-02	17.41	17.41	64.55	64.55	66.86	66.86
975.0	0.469	0.111E-02	19.34	19.34	71.70	71.70	74.26	74.26
1050.0	0.547	0.119E-02	20.77	20.77	76.99	76.99	79.75	79.75
1125.0	0.625	0.124E-02	22.37	22.37	82.93	82.93	85.90	85.90
1200.0	0.781	0.144E-02	24.41	24.41	90.49	90.49	93.73	93.73
1260.0	0.859	0.120E-02	25.86	25.86	95.86	95.86	99.29	99.29
1333.0	0.938							

Table A.22 CRACK GROWTH RATES AS A FUNCTION OF CRACK LENGTH AND OTHER PARAMETERS

TEST: $\lambda = \sqrt{3}$, $\Delta\bar{\varepsilon}/2 = 1.0\%$, $R_\varepsilon = 0$, Crack B

Cycles	Crack Length (2c) (mm)	d(2c)/dN mm/cycle	Stress-Intensity Factor (MPa $\sqrt{m}$)					
			MODE I		MODE II		COMBINED	
			Max	Range	Max	Range	Max	Range
600.0	0.090							
675.0	0.160	0.107E-02	11.16	11.16	41.37	41.37	42.85	42.85
750.0	0.250	0.139E-02	13.77	13.77	51.04	51.04	52.87	52.87
825.0	0.344	0.119E-02	16.87	16.87	62.54	62.54	64.77	64.77
875.0	0.469	0.114E-02	18.49	18.49	68.54	68.54	70.99	70.99
975.0	0.547	0.820E-03	20.61	20.61	76.42	76.42	79.15	79.15
1050.0	0.590	0.532E-03	21.49	21.49	79.68	79.68	82.53	82.53
1125.0	0.609	0.347E-03	21.76	21.76	80.64	80.64	83.53	83.53
1200.0	0.620	0.244E-03	21.93	21.93	81.29	81.29	84.20	84.20
1260.0	0.625	0.287E-03	22.06	22.06	81.77	81.77	84.69	84.69
1333.0	0.664							

Table A.23 CRACK GROWTH RATES AS A FUNCTION OF CRACK LENGTH AND OTHER PARAMETERS

TEST: $\lambda = \sqrt{3}$, $\Delta\bar{\varepsilon}/2 = 1.0\%$, $R_\varepsilon = 0$, Crack C

Cycles	Crack Length (2c) (mm)	d(2c)/dN mm/cycle	Stress-Intensity Factor (MPa $\sqrt{m}$)					
			MODE I		MODE II		COMBINED	
			Max	Range	Max	Range	Max	Range
525.0	0.050							
600.0	0.107	0.920E-03	9.13	9.13	33.83	33.83	35.04	35.04
675.0	0.188	0.129E-02	12.10	12.10	44.84	44.84	46.45	46.45
750.0	0.297	0.141E-02	15.81	15.81	58.61	58.61	60.71	60.71
825.0	0.438	0.141E-02	18.63	18.63	69.06	69.06	71.53	71.53
875.0	0.578	0.139E-02	20.21	20.21	74.90	74.90	77.59	77.58
975.0	0.625	0.105E-02	22.56	22.56	83.62	83.62	86.61	86.61
1050.0	0.703	0.778E-03	23.53	23.53	87.21	87.21	90.32	90.32
1125.0	0.778	0.103E-02	23.89	23.89	88.57	88.57	91.73	91.73
1200.0	0.781	0.129E-02	24.65	24.65	91.36	91.36	94.62	94.62
1260.0	0.820	0.205E-02	25.27	25.27	93.66	93.66	97.01	97.01
1333.0	1.094							

Table A.24 CRACK GROWTH RATES AS A FUNCTION OF CRACK LENGTH AND OTHER PARAMETERS

TEST: $\lambda = \sqrt{3}$, $\Delta\bar{\varepsilon}/2 = 1.0\%$, $R_\varepsilon = 0$, Crack D

Cycles	Crack Length (2c) (mm)	d(2c)/dN mm/cycle	Stress-Intensity Factor (MPa $\sqrt{m}$)					
			MODE I		MODE II		COMBINED	
			Max	Range	Max	Range	Max	Range
600.0	0.095							
675.0	0.175	0.133E-02	11.67	11.67	43.27	43.27	44.81	44.81
750.0	0.295	0.181E-02	14.66	14.66	54.34	54.34	56.28	56.28
825.0	0.391	0.144E-02	18.48	18.48	68.48	68.48	70.93	70.93
875.0	0.594	0.144E-02	20.11	20.11	74.55	74.55	77.21	77.21
975.0	0.644	0.190E-02	21.50	21.50	79.71	79.71	82.55	82.55
1050.0	0.688	0.225E-02	23.90	23.90	88.60	88.60	91.77	91.77
1125.0	0.781	0.226E-02	26.92	26.92	99.80	99.80	103.37	103.37
1200.0	1.359	0.275E-02	30.84	30.84	114.31	114.31	118.40	118.40
1260.0	1.367	0.314E-02	32.62	32.62	120.93	120.93	125.25	125.25
1333.0	1.406							

Table A.25 CRACK GROWTH RATES AS A FUNCTION OF CRACK LENGTH AND OTHER PARAMETERS

TEST: $\lambda = \sqrt{3}$, $\Delta\bar{\varepsilon}/2 = 0.5\%$, $R_\varepsilon = 0$, Failure Crack

Cycles	Crack Length (2c) (mm)	d(2c)/dN mm/cycle	Stress-Intensity Factor (MPa $\sqrt{m}$)					
			MODE I		MODE II		COMBINED	
			Max	Range	Max	Range	Max	Range
4500.0	0.016							
5500.0	0.152	0.181E-03	6.10	6.10	20.08	20.08	20.98	20.98
6000.0	0.254	0.383E-03	7.62	7.62	25.08	25.08	26.21	26.21
6500.0	0.348	0.378E-03	10.70	10.70	35.24	35.24	36.83	36.83
7000.0	0.849	0.507E-03	12.84	12.84	42.27	42.27	44.18	44.18
7500.0	0.966	0.833E-03	14.50	14.50	47.74	47.74	49.90	49.90
8000.0	1.116	0.107E-02	16.61	16.61	54.71	54.71	57.18	57.18
8500.0	1.739	0.201E-02	20.62	20.62	67.90	67.90	70.96	70.96
9000.0	3.125							

Table A.26 CRACK GROWTH RATES AS A FUNCTION OF CRACK LENGTH AND OTHER PARAMETERS

TEST: $\lambda = \sqrt{3}$, $\Delta\bar{\varepsilon}/2 = 0.5\%$, $R_\varepsilon = 0$, Crack A

Cycles	Crack Length (2c) (mm)	d(2c)/dN mm/cycle	Stress-Intensity Factor (MPa $\sqrt{m}$)					
			MODE I		MODE II		COMBINED	
			Max	Range	Max	Range	Max	Range
5000.0	0.023							
5500.0	0.032	0.560E-04	2.78	2.78	9.15	9.15	9.57	9.57
6000.0	0.079	0.108E-03	4.64	4.54	15.27	15.27	15.96	15.96
6500.0	0.174	0.138E-03	5.65	5.65	18.61	18.61	19.45	19.45
7000.0	0.221	0.228E-03	6.79	6.79	22.35	22.35	23.36	23.36
7500.0	0.493	0.385E-03	8.28	8.28	27.26	27.26	28.49	28.49
8000.0	0.493	0.574E-03	10.56	10.56	34.76	34.76	36.33	36.33
8500.0	0.806	0.871E-03	14.04	14.04	46.23	46.23	48.31	48.31
9000.0	1.364							

Table A.27 CRACK GROWTH RATES AS A FUNCTION OF CRACK LENGTH AND OTHER PARAMETERS

TEST: $\lambda = \sqrt{3}$, $\Delta\bar{\varepsilon}/2 = 0.5\%$, $R_\varepsilon = 0$, Crack B

Cycles	Crack Length (2c) (mm)	d(2c)/dN mm/cycle	Stress-Intensity Factor (MPa $\sqrt{m}$)					
			MODE I		MODE II		COMBINED	
			Max	Range	Max	Range	Max	Range
7500.0	0.087	INSUFFICIENT DATA FOR CRACK GROWTH CALCULATIONS						
8000.0	0.290							
8500.0	0.322							
9000.0	0.546							

Table A.28 CRACK GROWTH RATES AS A FUNCTION OF CRACK LENGTH AND OTHER PARAMETERS

TEST: $\lambda = \sqrt{3}$, $\Delta\bar{\varepsilon}/2 = 0.5\%$, $R_\varepsilon = 0$, Crack C

Cycles	Crack Length (2c) (mm)	d(2c)/dN mm/cycle	Stress-Intensity Factor (MPa $\sqrt{m}$)					
			MODE I		MODE II		COMBINED	
			Max	Range	Max	Range	Max	Range
5000.0	0.047							
5500.0	0.053	0.950E-05	3.61	3.61	11.89	11.89	12.42	12.42
6000.0	0.057	0.254E-03	5.37	5.37	17.67	17.67	18.46	18.46
6500.0	0.354	0.326E-03	8.07	8.07	26.58	26.58	27.78	27.78
7000.0	0.531	0.384E-03	10.92	10.92	35.95	35.95	37.57	37.57
7500.0	0.557	0.468E-03	13.09	13.09	43.11	43.11	45.05	45.05
8000.0	1.073	0.519E-03	14.97	14.97	49.29	49.29	51.52	51.52
8500.0	1.116	0.477E-03	16.52	16.52	54.40	54.40	56.85	56.85
9000.0	1.550							

Table A.29 CRACK GROWTH RATES AS A FUNCTION OF CRACK LENGTH AND OTHER PARAMETERS

TEST: $\lambda = \sqrt{3}$, $\Delta\bar{\varepsilon}/2 = 0.5\%$, $R_\varepsilon = 0$, Crack D

Cycles	Crack Length (2c) (mm)	d(2c)/dN mm/cycle	Stress-Intensity Factor (MPa $\sqrt{m}$)					
			MODE I		MODE II		COMBINED	
			Max	Range	Max	Range	Max	Range
7500.0	0.055	INSUFFICIENT DATA FOR CRACK GROWTH CALCULATIONS						
8000.0	0.596							
8500.0	0.837							
9000.0	0.967							

Table A.30 CRACK GROWTH RATES AS A FUNCTION OF CRACK LENGTH AND OTHER PARAMETERS

TEST: $\lambda = \sqrt{3}$, $\Delta\bar{\varepsilon}/2 = 1.0\%$, $R_\varepsilon = -1$, Failure Crack

Cycles	Crack Length (2c) (mm)	d(2c)/dN mm/cycle	Stress-Intensity Factor (MPa $\sqrt{m}$)					
			MODE I		MODE II		COMBINED	
			Max	Range	Max	Range	Max	Range
200.0	0.060							
300.0	0.125	0.500E-03	7.35	14.70	18.44	36.88	19.85	39.70
400.0	0.160	0.695E-03	8.11	16.22	20.35	40.71	21.91	43.82
500.0	0.200	0.711E-03	10.24	20.48	25.69	51.38	27.66	55.31
600.0	0.370	0.109E-02	11.19	22.39	28.09	56.18	30.24	60.47
700.0	0.400	0.146E-02	13.34	26.38	33.47	66.95	36.03	72.07
800.0	0.470	0.196E-02	15.64	31.28	39.25	78.49	42.25	84.50
900.0	0.870	0.254E-02	18.22	36.45	45.73	91.47	49.23	98.46
1000.0	1.040	0.336E-02	21.71	43.43	54.49	108.98	58.66	117.31
1100.0	1.425	0.415E-02	24.81	49.62	62.26	124.52	67.02	134.05
1200.0	1.870							

Table A.31 CRACK GROWTH RATES AS A FUNCTION OF CRACK LENGTH AND OTHER PARAMETERS

TEST: $\lambda = \sqrt{3}$, $\Delta\bar{\epsilon}/2 = 1.0\%$, $R_\epsilon = -1$, Crack A

Cycles	Crack Length (2c) (mm)	d(2c)/dN mm/cycle	Stress-Intensity Factor (MPa $\sqrt{m}$)					
			MODE I		MODE II		COMBINED	
			Max	Range	Max	Range	Max	Range
600.0	0.078							
700.0	0.234	0.195E-02	10.05	20.11	25.23	50.46	27.16	54.32
800.0	0.468	0.203E-02	14.22	28.45	35.69	71.38	38.42	76.84
900.0	0.703	0.173E-02	17.00	34.01	42.67	85.34	45.93	91.87
1000.0	0.859	0.154E-02	19.10	38.20	47.93	95.86	51.59	103.19
1100.0	0.938	0.117E-02	20.41	40.83	51.22	102.45	55.14	110.28
1200.0	1.094	0.117E-02	21.74	43.48	54.55	109.11	58.73	117.45
1300.0	1.172							

Table A.32 CRACK GROWTH RATES AS A FUNCTION OF CRACK LENGTH AND OTHER PARAMETERS

TEST: $\lambda = \sqrt{3}$, $\Delta\bar{\varepsilon}/2 = 1.0\%$, $R_\varepsilon = -1$, Crack B

Cycles	Crack Length (2c) (mm)	d(2c)/cN mm/cycle	Stress-Intensity Factor (MPa $\sqrt{m}$)					
			MODE I		MODE II		COMBINED	
			Max	Range	Max	Range	Max	Range
500.0	0.078							
600.0	0.156	0.118E-02	8.21	16.42	20.60	41.20	22.18	44.35
700.0	0.314	0.230E-02	12.12	24.24	30.41	60.82	32.74	65.47
800.0	0.625	0.229E-02	15.84	31.68	39.75	79.49	42.79	85.57
900.0	0.859	0.254E-02	19.19	38.37	48.14	96.29	51.83	103.65
1000.0	1.094	0.276E-02	21.92	43.84	55.01	110.02	59.61	118.43
1100.0	1.406	0.289E-02	24.36	48.71	61.12	122.23	65.79	131.58
1200.0	1.641	0.312E-02	26.63	53.25	66.81	133.63	71.92	143.85
1300.0	2.030							

Table A.33 CRACK GROWTH RATES AS A FUNCTION OF CRACK LENGTH AND OTHER PARAMETERS

TEST: $\lambda = \sqrt{3}$, $\Delta\bar{\varepsilon}/2 = 1.0\%$, $R_\varepsilon = -1$, Crack C

Cycles	Crack Length (2c) (mm)	d(2c)/dN mm/cycle	Stress-Intensity Factor (MPa $\sqrt{m}$)					
			MODE I		MODE II		COMBINED	
			Max	Range	Max	Range	Max	Range
500.0	0.103							
600.0	0.172	0.121E-02	8.62	17.24	21.63	43.26	23.29	46.57
700.0	0.344	0.218E-02	12.64	25.27	31.71	63.42	34.14	68.27
800.0	0.679	0.246E-02	16.37	32.74	41.08	82.16	44.22	88.45
900.0	0.938	0.277E-02	19.89	39.77	49.90	99.80	53.72	107.43
1000.0	1.133	0.325E-02	22.60	45.21	56.72	113.45	61.06	122.12
1100.0	1.563	0.363E-02	25.25	50.50	63.36	126.73	68.21	136.42
1200.0	1.797	0.429E-02	27.86	55.73	69.92	139.84	75.27	150.53
1300.0	2.420							

Table A.34 CRACK GROWTH RATES AS A FUNCTION OF CRACK LENGTH AND OTHER PARAMETERS

TEST: $\lambda = \sqrt{3}$, $\Delta\bar{\varepsilon}/2 = 1.0\%$, $R_\varepsilon = -1$, Crack D

Cycles	Crack Length (2c) (mm)	d(2c)/dN mm/cycle	Stress-Intensity Factor (MPa $\sqrt{m}$)					
			MODE I		MODE II		COMBINED	
			Max	Range	Max	Range	Max	Range
500.0	0.040							
600.0	0.117	0.580E-03	7.11	14.22	17.84	35.68	19.21	38.41
700.0	0.156	0.183E-02	9.44	18.88	23.69	47.38	25.50	51.01
800.0	0.469	0.222E-02	13.94	27.88	34.98	69.97	37.66	75.32
900.0	0.781	0.290E-02	17.33	34.67	43.50	86.99	46.82	93.65
1000.0	0.976	0.354E-02	21.04	42.09	52.81	105.61	56.85	113.69
1100.0	1.328	0.402E-02	24.19	48.39	60.71	121.43	65.36	130.71
1200.0	1.875	0.506E-02	28.46	56.92	71.42	142.84	76.88	153.76
1300.0	2.340							

Table A.35 CRACK GROWTH RATES AS A FUNCTION OF CRACK LENGTH AND OTHER PARAMETERS

TEST: $\lambda = \sqrt{3}$, $\Delta\bar{\varepsilon}/2 = 0.5\%$, $R_{\varepsilon} = -1$, Failure Crack

Cycles	Crack Length (2c) (mm)	d(2c)/dN mm/cycle	Stress-Intensity Factor (MPa $\sqrt{m}$)					
			MODE I		MODE II		COMBINED	
			Max	Range	Max	Range	Max	Range
0.0	0.000							
1000.0	0.100	0.100E-03	3.76	7.52	7.98	15.96	8.82	17.65
2000.0	0.200	0.810E-04	5.06	10.12	10.74	21.48	11.87	23.75
3000.0	0.230	0.975E-04	6.12	12.24	12.99	25.98	14.36	28.72
4000.0	0.340	0.934E-04	7.25	14.50	15.39	30.78	17.01	34.03
5000.0	0.525	0.943E-04	8.15	16.30	17.30	34.60	19.12	38.24
6000.0	0.580	0.941E-04	9.02	18.05	19.15	38.30	21.17	42.34
7000.0	0.620	0.116E-03	9.44	18.87	20.03	40.06	22.14	44.28
8000.0	0.740	0.207E-03	9.71	19.43	20.61	41.23	22.79	45.58
9000.0	0.810	0.318E-03	10.82	21.64	22.97	45.93	25.39	50.77
10000.0	1.180	0.590E-03	12.92	25.83	27.42	54.83	30.31	60.61
11000.0	1.990							

Table A.36 CRACK GROWTH RATES AS A FUNCTION OF CRACK LENGTH AND OTHER PARAMETERS

TEST: $\lambda = \sqrt{3}$, $\Delta\bar{\varepsilon}/2 = 0.5\%$, $R_\varepsilon = -1$, Crack A

Cycles	Crack Length (2c) (mm)	d(2c)/dN mm/cycle	Stress-Intensity Factor (MPa $\sqrt{m}$)					
			MODE I		MODE II		COMBINED	
			Max	Range	Max	Range	Max	Range
5000.0	0.075							
6000.0	0.125	0.710E-04	4.20	8.41	8.92	17.85	9.86	19.73
7000.0	0.217	0.895E-04	5.58	11.17	11.85	23.70	13.10	26.20
8000.0	0.334	0.935E-04	6.60	13.20	14.00	28.01	15.48	30.96
9000.0	0.418	0.106E-03	7.58	15.16	16.09	32.17	17.78	35.56
10000.0	0.466	0.112E-03	8.39	16.79	17.81	35.63	19.69	39.39
11000.0	0.653	0.156E-03	9.61	19.22	20.39	40.79	22.55	45.09
12000.0	0.778							

Table A.37 CRACK GROWTH RATES AS A FUNCTION OF CRACK LENGTH AND OTHER PARAMETERS

TEST: $\lambda = \sqrt{3}$, $\Delta\bar{\varepsilon}/2 = 0.5\%$, $R_\varepsilon = -1$, Crack B

Cycles	Crack Length (2c) (mm)	d(2c)/dN mm/cycle	Stress-Intensity Factor (MPa $\sqrt{m}$)					
			MODE I		MODE II		COMBINED	
			Max	Range	Max	Range	Max	Range
5000.0	0.095							
6000.0	0.140	0.775E-04	4.45	8.90	9.44	18.89	10.44	20.88
7000.0	0.250	0.496E-04	5.70	11.41	12.10	24.21	13.38	26.76
8000.0	0.270	0.449E-04	6.11	12.22	12.96	25.93	14.33	28.66
9000.0	0.278	0.799E-04	6.14	12.28	13.04	26.07	14.41	28.82
10000.0	0.334	0.112E-03	6.47	12.94	13.73	27.46	15.18	30.36
11000.0	0.375	0.224E-03	7.28	14.56	15.46	30.91	17.08	34.17
12000.0	0.781							

Table A.38 CRACK GROWTH RATES AS A FUNCTION OF CRACK LENGTH AND OTHER PARAMETERS

TEST: $\lambda = \sqrt{3}$, $\Delta\bar{\varepsilon}/2 = 0.5\%$, $R_\varepsilon = -1$, Crack C

Cycles	Crack Length (2c) (mm)	d(2c)/dN mm/cycle	Stress-Intensity Factor (MPa $\sqrt{m}$)					
			MODE I		MODE II		COMBINED	
			Max	Range	Max	Range	Max	Range
5000.0	0.195							
6000.0	0.266	0.430E-04	6.13	12.27	13.02	26.03	14.39	28.78
7000.0	0.281	0.597E-04	6.42	12.83	13.62	27.23	15.05	30.11
8000.0	0.347	0.979E-04	7.16	14.31	15.19	30.38	16.79	33.58
9000.0	0.453	0.108E-03	8.19	16.39	17.39	34.78	19.22	38.45
10000.0	0.634	0.133E-03	9.39	18.79	19.94	39.88	22.04	44.08
11000.0	0.769	0.109E-03	10.43	20.86	22.13	44.26	24.47	48.93
12000.0	0.852							

Table A.39 CRACK GROWTH RATES AS A FUNCTION OF CRACK LENGTH AND OTHER PARAMETERS

TEST: $\lambda = \sqrt{3}$, $\Delta\bar{\varepsilon}/2 = 0.5\%$, $R_\varepsilon = -1$, Crack D

Cycles	Crack Length (2c) (mm)	d(2c)/dN mm/cycle	Stress-Intensity Factor (MPa $\sqrt{m}$)					
			MODE I		MODE II		COMBINED	
			Max	Range	Max	Range	Max	Range
5000.0	0.219							
6000.0	0.406	0.106E-03	7.58	15.15	16.08	32.16	17.78	35.55
7000.0	0.431	0.112E-03	8.17	16.34	17.35	34.69	19.17	38.35
8000.0	0.588	0.875E-04	9.08	18.15	19.26	38.53	21.29	42.59
9000.0	0.689	0.689E-04	9.61	19.23	20.40	40.81	22.55	45.11
10000.0	0.706	0.479E-04	10.07	20.15	21.38	42.76	23.63	47.27
11000.0	0.750	0.455E-04	10.30	20.60	21.86	43.71	24.16	48.32
12000.0	0.797							

Table A.40 CRACK GROWTH RATES AS A FUNCTION OF CRACK LENGTH AND OTHER PARAMETERS

TEST: $\lambda = \infty$, $\Delta\bar{\varepsilon}/2 = 1.0\%$, $R_\varepsilon = 0$, Failure Crack

Cycles	Crack Length (2c) (mm)	d(2c)/dN mm/cycle	Stress-Intensity Factor (MPa $\sqrt{m}$)					
			MODE I		MODE II		COMBINED	
			Max	Range	Max	Range	Max	Range
50.0	0.100							
100.0	0.110	0.200E-03	0.00	0.00	38.87	38.87	38.87	38.87
200.0	0.130	0.161E-03	0.00	0.00	41.66	41.66	41.66	41.66
250.0	0.130	0.244E-03	0.00	0.00	43.03	43.03	43.03	43.03
350.0	0.150	0.377E-03	0.00	0.00	44.55	44.55	44.55	44.55
500.0	0.240	0.648E-03	0.00	0.00	56.18	56.18	56.18	56.18
600.0	0.260	0.109E-02	0.00	0.00	63.08	63.08	63.08	63.08
700.0	0.460	0.148E-02	0.00	0.00	75.03	75.03	75.03	75.03
800.0	0.490	0.170E-02	0.00	0.00	89.83	89.83	89.83	89.83
900.0	0.840	0.178E-02	0.00	0.00	105.34	105.34	105.34	105.34
1000.0	1.050	0.174E-02	0.00	0.00	116.81	116.81	116.81	116.81
1100.0	1.170	0.148E-02	0.00	0.00	128.28	128.28	128.28	128.28
1200.0	1.260	0.102E-02	0.00	0.00	133.77	133.77	133.77	133.77
1250.0	1.400	0.133E-02	0.00	0.00	135.76	135.76	135.76	135.76
1300.0	1.400	0.140E-02	0.00	0.00	138.36	138.36	138.36	138.36
1350.0	1.400	0.210E-02	0.00	0.00	138.66	138.66	138.66	138.66
1400.0	1.610							

Table A.41 CRACK GROWTH RATES AS A FUNCTION OF CRACK LENGTH AND OTHER PARAMETERS

TEST: $\lambda = \infty$, $\Delta\bar{\varepsilon}/2 = 1.0\%$, $R_\varepsilon = 0$, Crack A

Cycles	Crack Length (2c) (mm)	d(2c)/dN mm/cycle	Stress-Intensity Factor (MPa $\sqrt{m}$)					
			MODE I		MODE II		COMBINED	
			Max	Range	Max	Range	Max	Range
749.0	0.104							
800.0	0.185	0.101E-02	0.00	0.00	50.40	50.40	50.40	50.40
850.0	0.207	0.990E-03	0.00	0.00	54.61	54.61	54.61	54.61
900.0	0.260	0.926E-03	0.00	0.00	60.36	60.36	60.36	60.36
950.0	0.315	0.928E-03	0.00	0.00	65.03	65.03	65.03	65.03
1000.0	0.359	0.958E-03	0.00	0.00	70.29	70.29	70.29	70.29
1050.0	0.402	0.101E-02	0.00	0.00	74.33	74.33	74.33	74.33
1100.0	0.455	0.105E-02	0.00	0.00	78.84	78.84	78.84	78.84
1150.0	0.495	0.134E-02	0.00	0.00	82.66	82.66	82.66	82.66
1200.0	0.580	0.154E-02	0.00	0.00	88.68	88.68	88.68	88.68
1250.0	0.625	0.159E-02	0.00	0.00	95.59	95.59	95.59	95.59
1300.0	0.795	0.146E-02	0.00	0.00	102.42	102.42	102.42	102.42
1350.0	0.850	0.115E-02	0.00	0.00	107.41	107.41	107.41	107.41
1400.0	0.889	0.861E-02	0.00	0.00	110.50	110.50	110.50	110.50
1450.0	0.895	0.386E-03	0.00	0.00	110.98	110.98	110.98	110.98
1500.0	0.906	0.430E-03	0.00	0.00	111.54	111.54	110.54	111.54
1550.0	0.938							

Table A.42 CRACK GROWTH RATES AS A FUNCTION OF CRACK LENGTH AND OTHER PARAMETERS

TEST: $\lambda = \infty$, $\Delta\bar{\varepsilon}/2 = 1.0\%$, $R_\varepsilon = 0$, Crack B

Cycles	Crack Length (2c) (mm)	d(2c)/dN mm/cycle	Stress-Intensity Factor (MPa $\sqrt{m}$)					
			MODE I		MODE II		COMBINED	
			Max	Range	Max	Range	Max	Range
650.0	0.095							
700.0	0.149	0.158E-02	0.00	0.00	45.24	45.24	45.24	45.24
749.0	0.250	0.167E-02	0.00	0.00	57.51	57.51	57.51	57.51
800.0	0.331	0.173E-02	0.00	0.00	67.36	67.36	67.36	67.36
850.0	0.422	0.177E-02	0.00	0.00	76.31	76.31	76.31	76.31
900.0	0.510	0.163E-02	0.00	0.00	84.12	84.12	84.12	84.12
950.0	0.604	0.158E-02	0.00	0.00	90.50	90.50	90.50	90.50
1000.0	0.682	0.149E-02	0.00	0.00	95.95	95.95	95.95	95.95
1050.0	0.720	0.143E-02	0.00	0.00	100.74	100.74	100.74	100.74
1100.0	0.810	0.137E-02	0.00	0.00	105.21	105.21	105.21	105.21
1150.0	0.878	0.156E-02	0.00	0.00	109.07	109.07	109.07	109.07
1200.0	0.950	0.186E-02	0.00	0.00	114.01	114.01	114.01	114.01
1250.0	1.010	0.223E-02	0.00	0.00	119.21	119.21	119.21	119.21
1300.0	1.171	0.201E-02	0.00	0.00	127.66	127.66	127.66	127.66
1350.0	1.302	0.184E-02	0.00	0.00	133.75	133.75	133.75	133.75
1400.0	1.492	0.199E-02	0.00	0.00	137.42	137.42	137.42	137.42
1450.0	1.359	0.163E-02	0.00	0.00	139.50	139.50	139.50	139.50
1500.0	1.471	0.360E-02	0.00	0.00	142.13	142.13	142.13	142.13
1550.0	1.719							

Table A.43 CRACK GROWTH RATES AS A FUNCTION OF CRACK LENGTH AND OTHER PARAMETERS

TEST: $\lambda = \infty$, $\Delta\bar{\varepsilon}/2 = 1.0\%$, $R_\varepsilon = 0$, Crack C

Cycles	Crack Length (2c) (mm)	d(2c)/dN mm/cycle	Stress-Intensity Factor (MPa $\sqrt{m}$)					
			MODE I		MODE II		COMBINED	
			Max	Range	Max	Range	Max	Range
800.0	0.095							
850.0	0.130	0.100E-02	0.00	0.00	42.25	42.25	42.25	42.25
900.0	0.195	0.990E-03	0.00	0.00	49.92	49.92	49.92	49.92
950.0	0.221	0.969E-03	0.00	0.00	56.40	56.40	56.40	56.40
1000.0	0.297	0.101E-02	0.00	0.00	62.15	62.15	62.15	62.15
1050.0	0.315	0.105E-02	0.00	0.00	67.24	67.24	67.24	67.24
1100.0	0.390	0.109E-02	0.00	0.00	72.96	72.96	72.96	72.96
1150.0	0.442	0.109E-02	0.00	0.00	77.78	77.78	77.78	77.78
1200.0	0.506	0.120E-02	0.00	0.00	82.80	82.80	82.80	82.80
1250.0	0.550	0.121E-02	0.00	0.00	87.29	87.29	87.29	87.29
1300.0	0.610	0.115E-02	0.00	0.00	92.46	92.46	92.46	92.46
1350.0	0.690	0.105E-02	0.00	0.00	96.89	96.89	96.89	96.89
1400.0	0.755	0.995E-03	0.00	0.00	100.54	100.54	100.54	100.54
1450.0	0.768	0.774E-03	0.00	0.00	103.15	103.15	103.15	103.15
1500.0	0.804	0.940E-03	0.00	0.00	105.08	105.08	105.08	105.08
1550.0	0.859							

Table A.44 CRACK GROWTH RATES AS A FUNCTION OF CRACK LENGTH AND OTHER PARAMETERS

TEST: $\lambda = \infty$, $\Delta\bar{\varepsilon}/2 = 1.0\%$, $R_\varepsilon = 0$, Crack D

Cycles	Crack Length (2c) (mm)	d(2c)/dN mm/cycle	Stress-Intensity Factor (MPa $\sqrt{m}$)					
			MODE I		MODE II		COMBINED	
			Max	Range	Max	Range	Max	Range
800.0	0.105							
850.0	0.190	0.145E-02	0.00	0.00	51.08	51.08	51.08	51.08
900.0	0.250	0.157E-02	0.00	0.00	60.62	60.62	60.62	60.62
950.0	0.365	0.144E-02	0.00	0.00	68.86	68.86	68.86	68.86
1000.0	0.410	0.136E-02	0.00	0.00	75.43	75.43	75.43	75.43
1050.0	0.479	0.136E-02	0.00	0.00	80.91	80.91	80.91	80.91
1100.0	0.531	0.125E-02	0.00	0.00	85.96	85.96	85.96	85.96
1150.0	0.598	0.142E-02	0.00	0.00	90.68	90.68	90.68	90.68
1200.0	0.689	0.149E-02	0.00	0.00	96.12	96.12	96.12	96.12
1250.0	0.723	0.145E-02	0.00	0.00	102.14	102.14	102.14	102.14
1300.0	0.859	0.125E-02	0.00	0.00	107.38	107.38	107.38	107.38
1350.0	0.916	0.120E-02	0.00	0.00	110.57	110.57	110.57	110.57
1400.0	0.938	0.146E-02	0.00	0.00	113.22	113.22	113.22	113.22
1450.0	0.950	0.160E-02	0.00	0.00	115.07	115.07	115.07	115.07
1500.0	1.070	0.300E-02	0.00	0.00	121.22	121.22	121.22	121.22
1550.0	1.250							

Table A.45 CRACK GROWTH RATES AS A FUNCTION OF CRACK LENGTH AND OTHER PARAMETERS

TEST: $\lambda = \infty$, $\Delta\bar{\varepsilon}/2 = 0.5\%$, $R_\varepsilon = 0$, Failure Crack

Cycles	Crack Length (2c) (mm)	d(2c)/dN mm/cycle	Stress-Intensity Factor (MPa $\sqrt{m}$)					
			MODE I		MODE II		COMBINED	
			Max	Range	Max	Range	Max	Range
500.0	0.000							
1000.0	0.050	0.660E-04	0.00	0.00	12.82	12.82	12.82	12.82
1500.0	0.060	0.880E-04	0.00	0.00	16.53	16.53	16.53	16.53
2000.0	0.150	0.936E-04	0.00	0.00	20.59	20.59	20.59	20.59
2500.0	0.170	0.101E-03	0.00	0.00	24.03	24.03	24.03	24.03
3000.0	0.230	0.133E-03	0.00	0.00	27.03	27.03	27.03	27.03
3500.0	0.280	0.134E-03	0.00	0.00	31.05	31.05	31.05	31.05
4000.0	0.350	0.147E-03	0.00	0.00	35.19	35.19	35.19	35.19
4500.0	0.510	0.150E-03	0.00	0.00	38.78	38.78	38.78	38.78
5000.0	0.510	0.144E-03	0.00	0.00	42.34	42.34	42.34	42.34
6000.0	0.670	0.861E-04	0.00	0.00	46.93	46.93	46.93	46.93
6500.0	0.720	0.215E-03	0.00	0.00	45.59	45.59	45.59	45.59
7000.0	0.720	0.312E-03	0.00	0.00	49.32	49.32	49.32	49.32
7500.0	0.720	0.353E-03	0.00	0.00	51.48	51.48	51.48	51.48
8500.0	1.520	0.720E-03	0.00	0.00	70.68	70.68	70.68	70.68
9000.0	1.860							

Table A.46 CRACK GROWTH RATES AS A FUNCTION OF CRACK LENGTH AND OTHER PARAMETERS

TEST: $\lambda = \infty$, $\Delta\bar{\varepsilon}/2 = 0.5\%$, $R_\varepsilon = 0$, Crack A

Cycles	Crack Length (2c) (mm)	d(2c)/dN mm/cycle	Stress-Intensity Factor (MPa $\sqrt{m}$)					
			MODE I		MODE II		COMBINED	
			Max	Range	Max	Range	Max	Range
4000.0	0.093							
4500.0	0.156	0.126E-03	0.00	0.00	22.64	22.64	22.64	22.64
5000.0	0.219	0.200E-03	0.00	0.00	25.81	25.81	25.81	25.81
5500.0	0.281	0.175E-03	0.00	0.00	33.79	33.79	33.79	33.79
6000.0	0.531	0.150E-03	0.00	0.00	38.71	38.71	38.71	38.71
6500.0	0.547	0.115E-03	0.00	0.00	41.86	41.86	41.86	41.86
7000.0	0.547	0.714E-04	0.00	0.00	43.28	43.28	43.28	43.28
7500.0	0.547	0.276E-04	0.00	0.00	42.67	42.67	42.67	42.67
8000.0	0.573	0.390E-04	0.00	0.00	43.14	43.14	43.14	43.14
8500.0	0.586	0.520E-04	0.00	0.00	43.88	43.88	43.88	43.88
9000.0	0.625							

Table A.47 CRACK GROWTH RATES AS A FUNCTION OF CRACK LENGTH AND OTHER PARAMETERS

TEST: $\lambda = \infty$, $\Delta\bar{\varepsilon}/2 = 0.5\%$, $R_\varepsilon = 0$, Crack B

Cycles	Crack Length (2c) (mm)	d(2c)/dN mm/cycle	Stress-Intensity Factor (MPa $\sqrt{m}$)					
			MODE I		MODE II		COMBINED	
			Max	Range	Max	Range	Max	Range
4000.0	0.125							
4500.0	0.288	0.313E-03	0.00	0.00	30.76	30.76	30.76	30.76
5000.0	0.438	0.318E-03	0.00	0.00	39.51	39.51	39.51	39.51
5500.0	0.688	0.241E-03	0.00	0.00	45.30	45.30	45.30	45.30
6000.0	0.719	0.196E-03	0.00	0.00	48.92	48.92	48.92	48.92
6500.0	0.794	0.180E-03	0.00	0.00	50.87	50.87	50.87	50.87
7000.0	0.820	0.166E-03	0.00	0.00	52.64	52.64	52.64	52.64
7500.0	0.914	0.183E-03	0.00	0.00	55.78	55.78	55.78	55.78
8000.0	1.094	0.216E-03	0.00	0.00	59.32	59.32	59.32	59.32
8500.0	1.172	0.136E-03	0.00	0.00	62.06	62.06	62.06	62.06
9000.0	1.230							

Table A.48 CRACK GROWTH RATES AS A FUNCTION OF CRACK LENGTH AND OTHER PARAMETERS

TEST: $\lambda = \infty$, $\Delta\bar{\varepsilon}/2 = 0.5\%$, $R_\varepsilon = 0$, Crack C

Cycles	Crack Length (2c) (mm)	d(2c)/dN mm/cycle	Stress-Intensity Factor (MPa $\sqrt{m}$)					
			MODE I		MODE II		COMBINED	
			Max	Range	Max	Range	Max	Range
4000.0	0.131							
4500.0	0.219	0.228E-03	0.00	0.00	26.83	26.83	26.83	26.83
5000.0	0.359	0.194E-03	0.00	0.00	33.67	33.67	33.67	33.67
5500.0	0.438	0.144E-03	0.00	0.00	37.84	37.84	37.84	37.84
6000.0	0.506	0.104E-03	0.00	0.00	40.62	40.62	40.62	40.62
6500.0	0.531	0.622E-04	0.00	0.00	41.76	41.76	41.76	41.76
7000.0	0.547	0.494E-04	0.00	0.00	42.20	42.20	42.20	42.20
7500.0	0.547	0.551E-04	0.00	0.00	42.52	42.52	42.52	42.52
8000.0	0.563	0.748E-04	0.00	0.00	43.24	43.24	43.24	43.24
8500.0	0.625	0.132E-03	0.00	0.00	45.32	45.32	45.32	45.32
9000.0	0.695							

Table A.49 CRACK GROWTH RATES AS A FUNCTION OF CRACK LENGTH AND OTHER PARAMETERS

TEST: $\lambda = \infty$, $\Delta\bar{\epsilon}/2 = 0.5\%$, $R_\epsilon = 0$, Crack D

Cycles	Crack Length (2c) (mm)	d(2c)/dN mm/cycle	Stress-Intensity Factor (MPa $\sqrt{m}$)					
			MODE I		MODE II		COMBINED	
			Max	Range	Max	Range	Max	Range
4000.0	0.218							
4500.0	0.375	0.345E-03	0.00	0.00	35.10	35.10	35.10	35.10
5000.0	0.563	0.363E-03	0.00	0.00	43.82	43.82	43.82	43.82
5500.0	0.813	0.324E-03	0.00	0.00	49.81	49.81	49.81	49.81
6000.0	0.906	0.279E-03	0.00	0.00	55.11	55.11	55.11	55.11
6500.0	1.013	0.214E-03	0.00	0.00	58.85	58.85	58.85	58.85
7000.0	1.188	0.147E-03	0.00	0.00	61.05	61.05	61.05	61.05
7500.0	1.195	0.107E-03	0.00	0.00	62.78	62.78	62.78	62.78
8000.0	1.211	0.326E-04	0.00	0.00	63.11	63.11	63.11	63.11
8500.0	1.234	0.391E-04	0.00	0.00	63.68	63.68	63.68	63.68
9000.0	1.250							

Table A.50 CRACK GROWTH RATES AS A FUNCTION OF CRACK LENGTH AND OTHER PARAMETERS

TEST: $\lambda = \infty$, $\Delta\bar{\varepsilon}/2 = 1.0\%$, $R_\varepsilon = -1$, Failure Crack

Cycles	Crack Length (2c) (mm)	d(2c)/dN mm/cycle	Stress-Intensity Factor (MPa $\sqrt{m}$)					
			MODE I		MODE II		COMBINED	
			Max	Range	Max	Range	Max	Range
0.0	0.000							
100.0	0.075	0.550E-03	0.00	0.00	16.27	32.54	16.27	32.54
200.0	0.110	0.350E-03	0.00	0.00	19.63	39.26	19.63	39.26
300.0	0.125	0.961E-03	0.00	0.00	20.25	40.51	20.25	40.51
400.0	0.150	0.136E-02	0.00	0.00	27.66	55.32	27.66	55.32
500.0	0.380	0.166E-02	0.00	0.00	37.71	75.43	37.71	75.43
600.0	0.680	0.176E-02	0.00	0.00	47.34	94.68	47.34	94.68
700.0	0.875	0.195E-02	0.00	0.00	53.83	107.66	53.83	107.66
800.0	0.980	0.238E-02	0.00	0.00	57.77	115.54	57.77	115.54
900.0	1.050	0.279E-02	0.00	0.00	61.81	123.62	61.81	123.62
1000.0	1.420	0.500E-02	0.00	0.00	70.81	141.61	70.81	141.61
1100.0	2.050							

Table A.51 CRACK GROWTH RATES AS A FUNCTION OF CRACK LENGTH AND OTHER PARAMETERS

TEST: $\lambda = \infty$, $\Delta\bar{\varepsilon}/2 = 1.0\%$, $R_\varepsilon = -1$, Crack A

Cycles	Crack Length (2c) (mm)	d(2c)/dN mm/cycle	Stress-Intensity Factor (MPa $\sqrt{m}$)					
			MODE I		MODE II		COMBINED	
			Max	Range	Max	Range	Max	Range
500.0	0.032							
600.0	0.063	0.258E-03	0.00	0.00	14.94	29.88	14.94	29.88
700.0	0.083	0.541E-03	0.00	0.00	17.78	35.57	17.78	35.57
800.0	0.155	0.732E-03	0.00	0.00	22.61	45.22	22.61	45.22
1000.0	0.380	0.130E-02	0.00	0.00	34.39	68.78	34.39	68.78
1100.0	0.393	0.164E-02	0.00	0.00	40.79	81.57	40.79	81.57
1200.0	0.694	0.241E-02	0.00	0.00	49.50	99.00	49.50	99.00
1300.0	0.874							

Table A.52 CRACK GROWTH RATES AS A FUNCTION OF CRACK LENGTH AND OTHER PARAMETERS

TEST: $\lambda = \infty$, $\Delta\bar{\varepsilon}/2 = 1.0\%$, $R_\varepsilon = -1$, Crack B

Cycles	Crack Length (2c) (mm)	d(2c)/dN mm/cycle	Stress-Intensity Factor (MPa $\sqrt{m}$)					
			MODE I		MODE II		COMBINED	
			Max	Range	Max	Range	Max	Range
500.0	0.097							
600.0	0.113	0.197E-03	0.00	0.00	19.97	39.95	19.97	39.95
700.0	0.136	0.277E-03	0.00	0.00	22.40	44.80	22.40	44.80
800.0	0.183	0.389E-03	0.00	0.00	23.87	47.74	23.87	47.74
900.0	0.200	0.132E-02	0.00	0.00	21.56	43.13	21.56	43.13
1000.0	0.225	0.189E-02	0.00	0.00	32.84	65.68	32.84	65.68
1100.0	0.364	0.291E-02	0.00	0.00	43.65	87.30	43.65	87.30
1200.0	1.178	0.407E-02	0.00	0.00	64.49	128.98	64.49	128.98
1300.0	1.178							

Table A.53 CRACK GROWTH RATES AS A FUNCTION OF CRACK LENGTH AND OTHER PARAMETERS

TEST: $\lambda = \infty$, $\Delta\bar{\varepsilon}/2 = 1.0\%$, $R_\varepsilon = -1$, Crack C

Cycles	Crack Length (2c) (mm)	d(2c)/dN mm/cycle	Stress-Intensity Factor (MPa $\sqrt{m}$)					
			MODE I		MODE II		COMBINED	
			Max	Range	Max	Range	Max	Range
300.0	0.035							
400.0	0.079	0.516E-03	0.00	0.00	16.70	33.40	16.70	33.40
500.0	0.138	0.524E-03	0.00	0.00	22.46	44.92	22.46	44.92
600.0	0.209	0.485E-03	0.00	0.00	26.04	52.08	26.04	52.08
700.0	0.232	0.486E-03	0.00	0.00	28.98	57.96	28.98	57.96
800.0	0.277	0.646E-03	0.00	0.00	30.68	61.37	30.68	61.37
900.0	0.324	0.724E-03	0.00	0.00	34.51	69.02	34.51	69.02
1000.0	0.386	0.827E-03	0.00	0.00	38.90	77.80	38.90	77.80
1100.0	0.592	0.962E-03	0.00	0.00	43.71	87.41	43.71	87.41
1200.0	0.608	0.510E-03	0.00	0.00	46.33	92.66	46.33	92.66
1300.0	0.694							

Table A.54 CRACK GROWTH RATES AS A FUNCTION OF CRACK LENGTH AND OTHER PARAMETERS

TEST: $\lambda = \infty$, $\Delta\bar{\varepsilon}/2 = 1.0\%$, $R_\varepsilon = -1$, Crack D

Cycles	Crack Length (2c) (mm)	d(2c)/dN mm/cycle	Stress-Intensity Factor (MPa $\sqrt{m}$)					
			MODE I		MODE II		COMBINED	
			Max	Range	Max	Range	Max	Range
300.0	0.011							
400.0	0.111	0.525E-03	0.00	0.00	19.80	39.59	19.80	39.59
500.0	0.116	0.293E-03	0.00	0.00	21.42	42.84	21.42	42.84
600.0	0.142	0.279E-03	0.00	0.00	22.63	45.27	22.63	45.27
700.0	0.142	0.226E-03	0.00	0.00	23.52	47.04	23.52	47.04
800.0	0.200	0.509E-03	0.00	0.00	23.89	47.78	23.89	47.78
900.0	0.203	0.839E-03	0.00	0.00	27.19	54.39	27.19	54.39
1000.0	0.245	0.109E-02	0.00	0.00	33.77	67.54	33.77	67.54
1100.0	0.502	0.151E-02	0.00	0.00	41.01	82.02	41.01	82.02
1200.0	0.670	0.121E-02	0.00	0.00	48.64	97.27	48.64	97.27
1300.0	0.744							

Table A.55 CRACK GROWTH RATES AS A FUNCTION OF CRACK LENGTH AND OTHER PARAMETERS

TEST: $\lambda = \infty$, $\Delta\bar{\varepsilon}/2 = 0.5\%$, $R_\varepsilon = -1$, Failure Crack

Cycles	Crack Length (2c) (mm)	d(2c)/dN mm/cycle	Stress-Intensity Factor (MPa $\sqrt{m}$)					
			MODE I		MODE II		COMBINED	
			Max	Range	Max	Range	Max	Range
0.0	0.000							
1000.0	0.040	0.350E-04	0.00	0.00	5.85	11.71	5.85	11.71
2000.0	0.070	0.510E-04	0.00	0.00	7.98	15.95	7.98	15.95
3000.0	0.130	0.486E-04	0.00	0.00	10.76	21.52	10.76	21.52
4000.0	0.210	0.464E-04	0.00	0.00	12.77	25.54	12.77	25.54
5000.0	0.230	0.457E-04	0.00	0.00	14.25	28.50	14.25	28.50
6000.0	0.280	0.775E-04	0.00	0.00	14.46	28.93	14.46	28.93
7000.0	0.300	0.113E-03	0.00	0.00	16.41	32.81	16.41	32.81
8000.0	0.360	0.163E-03	0.00	0.00	19.58	39.16	19.58	39.16
9000.0	0.730	0.232E-03	0.00	0.00	23.75	47.51	23.75	47.51
10000.0	0.900	0.230E-03	0.00	0.00	27.76	55.53	27.76	55.53
11000.0	1.190							

Table A.56 CRACK GROWTH RATES AS A FUNCTION OF CRACK LENGTH AND OTHER PARAMETERS

TEST: $\lambda = \infty$, $\Delta\bar{\varepsilon}/2 = 0.5\%$, $R_\varepsilon = -1$. Crack A

Cycles	Crack Length (2c) (mm)	d(2c)/dN mm/cycle	Stress-Intensity Factor (MPa $\sqrt{m}$)					
			MODE I		MODE II		COMBINED	
			Max	Range	Max	Range	Max	Range
6000.0	0.109							
7000.0	0.275	0.144E-03	0.00	0.00	15.35	30.69	15.35	30.69
8000.0	0.397	0.824E-04	0.00	0.00	17.95	35.89	17.95	35.89
9000.0	0.401	0.654E-04	0.00	0.00	19.19	38.39	19.19	38.39
10000.0	0.458	0.755E-04	0.00	0.00	19.85	39.70	19.85	39.70
11000.0	0.507	0.124E-03	0.00	0.00	21.18	42.37	21.18	42.37
11500.0	0.547	0.164E-03	0.00	0.00	22.14	44.28	22.14	44.28
12000.0	0.703	0.234E-03	0.00	0.00	24.54	49.07	24.54	49.07
12500.0	0.781							

Table A.57 CRACK GROWTH RATES AS A FUNCTION OF CRACK LENGTH AND OTHER PARAMETERS

TEST: $\lambda = \infty$, $\Delta\bar{\varepsilon}/2 = 0.5\%$, $R_\varepsilon = -1$, Crack B

Cycles	Crack Length (2c) (mm)	d(2c)/dN mm/cycle	Stress-Intensity Factor (MPa $\sqrt{m}$)					
			MODE I		MODE II		COMBINED	
			Max	Range	Max	Range	Max	Range
7000.0	0.040							
8000.0	0.105	0.835E-04	0.00	0.00	9.48	18.97	9.48	18.97
9000.0	0.207	0.695E-04	0.00	0.00	12.87	25.74	12.87	25.74
10000.0	0.254	0.103E-03	0.00	0.00	14.67	29.34	14.67	29.34
11000.0	0.313	0.178E-03	0.00	0.00	17.48	34.96	17.48	34.96
11500.0	0.390	0.250E-03	0.00	0.00	18.68	37.37	18.68	37.37
12000.0	0.575	0.360E-03	0.00	0.00	22.19	44.38	22.19	44.38
12500.0	0.750							

Table A.58 CRACK GROWTH RATES AS A FUNCTION OF CRACK LENGTH AND OTHER PARAMETERS

TEST: $\lambda = \infty$, $\Delta\bar{\varepsilon}/2 = 0.5\%$, $R_\varepsilon = -1$, Crack C

Cycles	Crack Length (2c) (mm)	d(2c)/cN mm/cycle	Stress-Intensity Factor (MPa $\sqrt{m}$)					
			MODE I		MODE II		COMBINED	
			Max	Range	Max	Range	Max	Range
6000.0	0.078							
7000.0	0.155	0.910E-04	0.00	0.00	11.52	23.04	11.52	23.04
8000.0	0.260	0.790E-04	0.00	0.00	14.61	29.23	14.61	29.23
9000.0	0.321	0.887E-04	0.00	0.00	16.47	32.95	16.47	32.95
10000.0	0.390	0.103E-03	0.00	0.00	18.56	37.11	18.56	37.11
11000.0	0.469	0.112E-03	0.00	0.00	20.75	41.51	20.75	41.51
11500.0	0.604	0.116E-03	0.00	0.00	22.16	44.32	22.16	44.32
12000.0	0.650	0.600E-04	0.00	0.00	23.59	47.19	23.59	47.19
12500.0	0.664							

Table A.59 CRACK GROWTH RATES AS A FUNCTION OF CRACK LENGTH AND OTHER PARAMETERS

TEST: $\lambda = \infty$, $\Delta\bar{\varepsilon}/2 = 0.5\%$, $R_\varepsilon = -1$, Crack D

Cycles	Crack Length (2c) (mm)	d(2c)/dN mm/cycle	Stress-Intensity Factor (MPa $\sqrt{m}$)					
			MODE I		MODE II		COMBINED	
			Max	Range	Max	Range	Max	Range
6000.0	0.115							
7000.0	0.241	0.100E-03	0.00	0.00	14.37	28.73	14.37	28.73
8000.0	0.315	0.857E-04	0.00	0.00	16.54	33.07	16.54	33.07
9000.0	0.390	0.105E-03	0.00	0.00	18.45	36.90	18.45	36.90
10000.0	0.469	0.126E-03	0.00	0.00	20.55	41.09	20.55	41.09
11000.0	0.650	0.157E-03	0.00	0.00	23.20	46.41	23.20	46.41
11500.0	0.703	0.172E-03	0.00	0.00	24.83	49.66	24.83	49.66
12000.0	0.810	0.195E-03	0.00	0.00	26.34	52.68	26.34	52.68
12500.0	0.898							

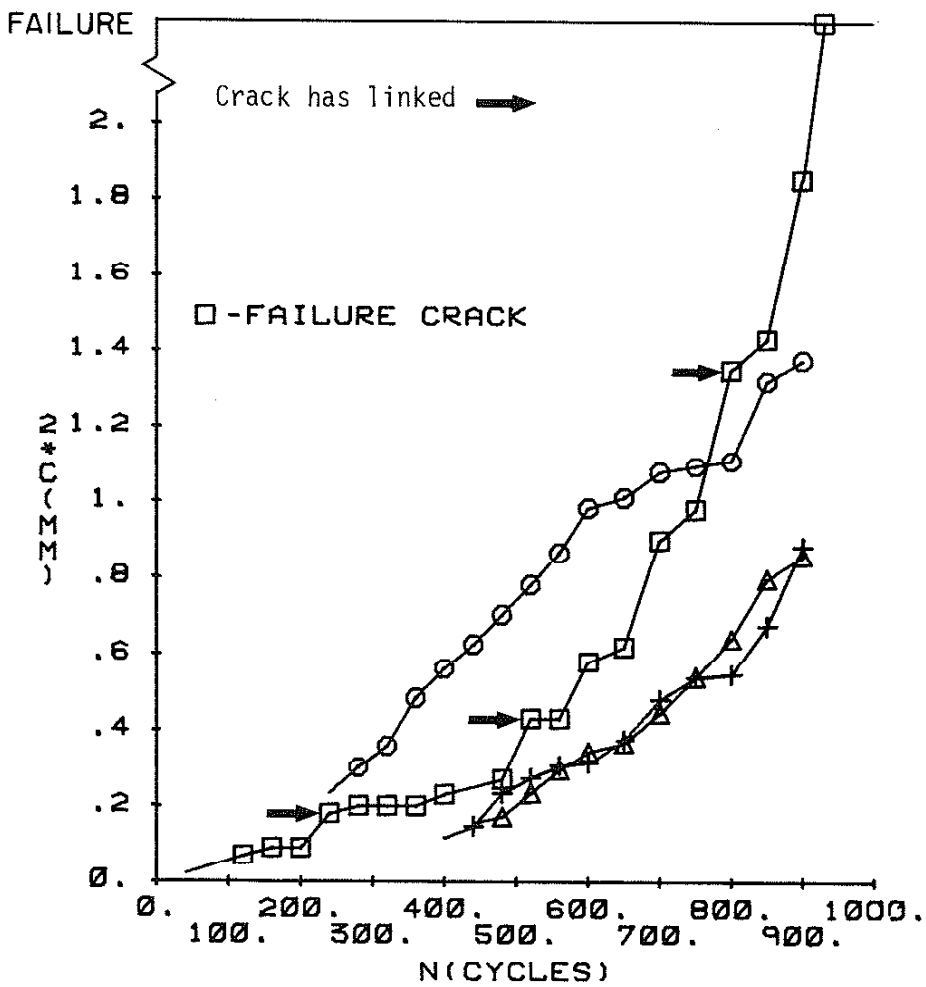

Figure A.1 Crack Length versus Cycles
$\lambda = 0$, $\Delta\bar{\varepsilon}/2 = 1.0\%$, $R_\varepsilon = 0$

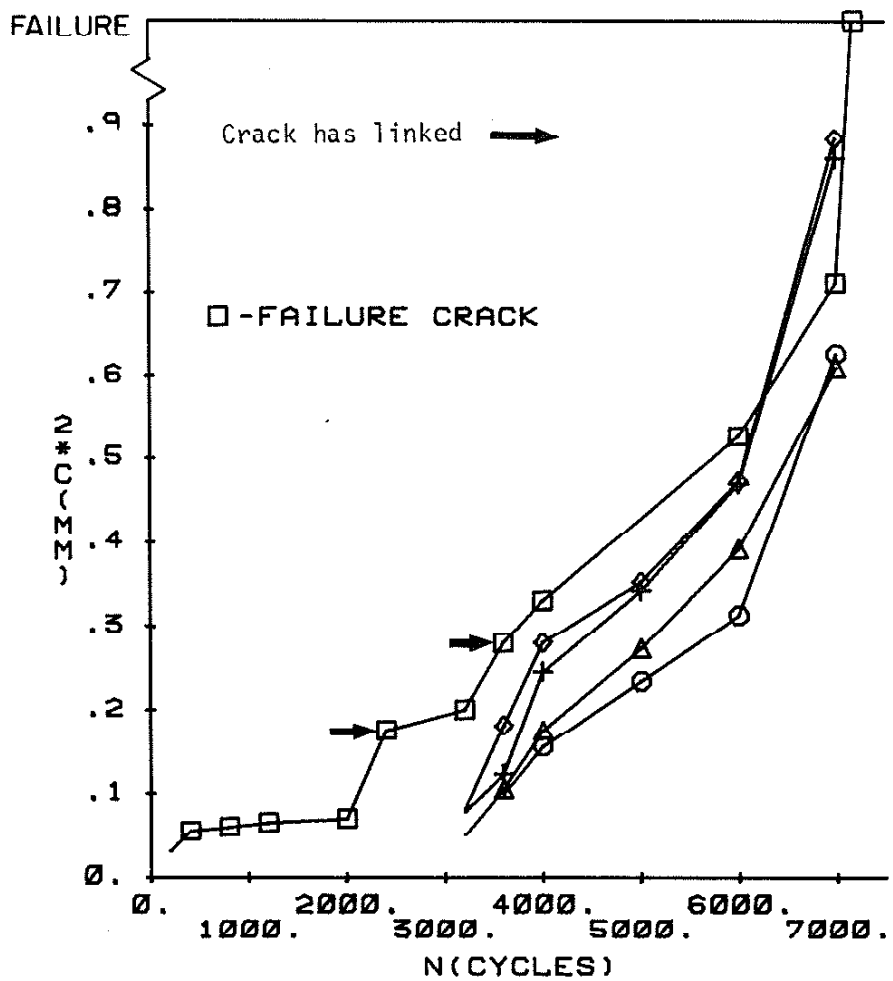

Figure A.2 Crack Length versus Cycles
$\lambda = 0$, $\Delta\bar{\varepsilon}/2 = 0.5\%$, $R_\varepsilon = 0$

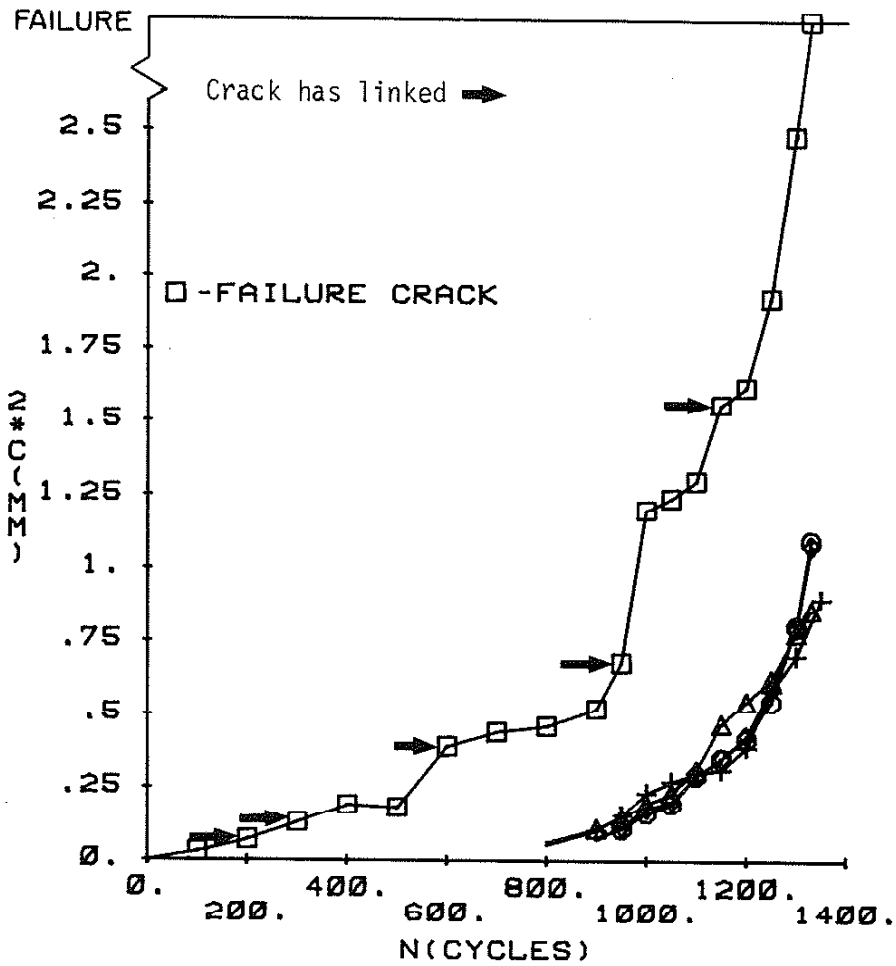

Figure A.3 Crack Length versus Cycles
$\lambda = 0$, $\Delta\varepsilon/2 = 1.0\%$, $R_\varepsilon = -1$

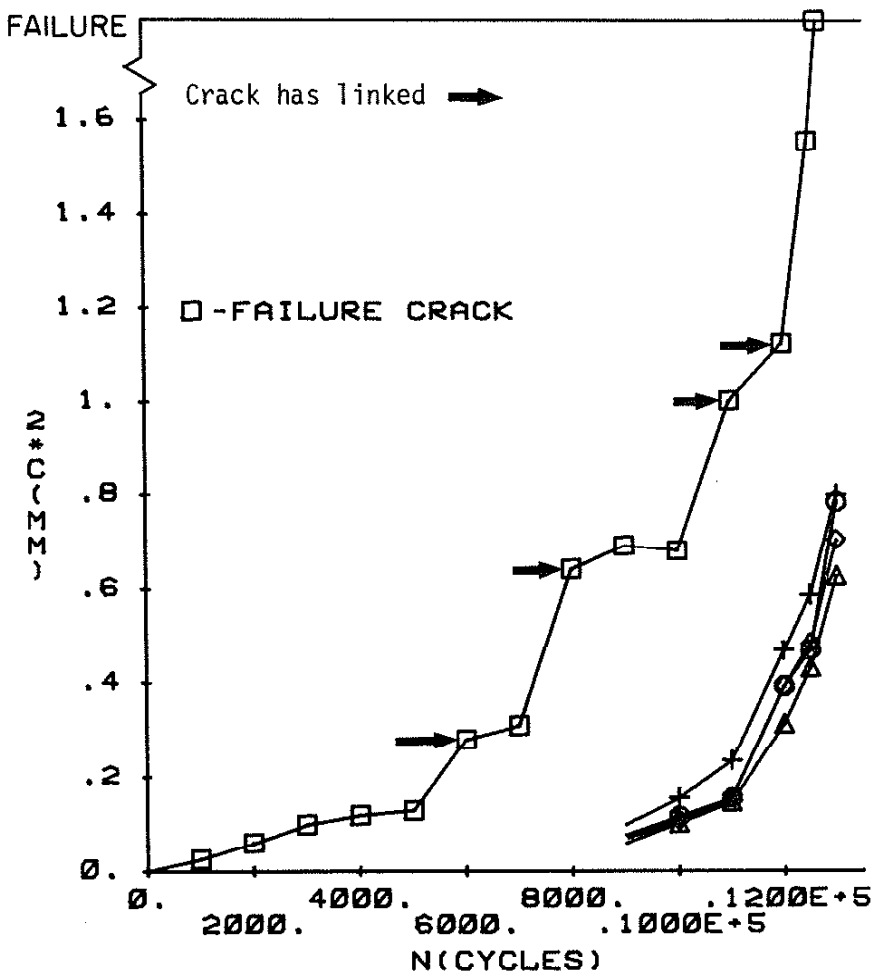

Figure A.4 Crack Length versus Cycles
$\lambda = 0$, $\Delta\bar{\varepsilon}/2 = 0.5\%$, $R_\varepsilon = -1$

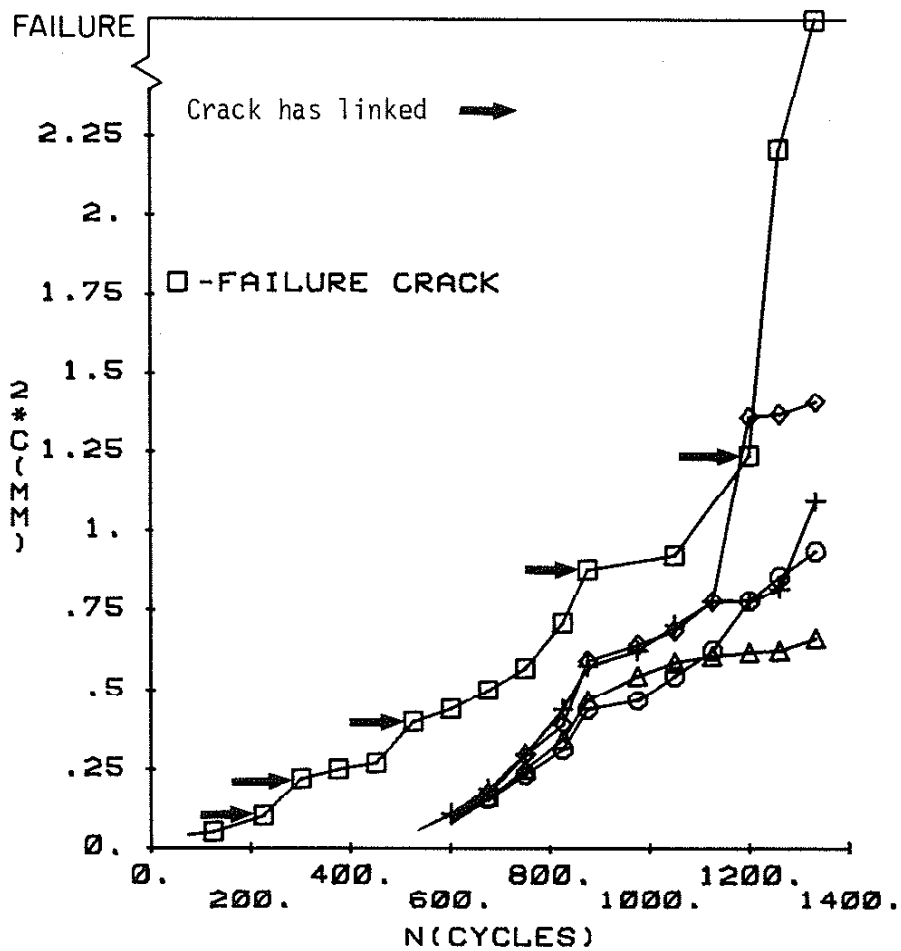

Figure A.5 Crack Length versus Cycles
$\lambda = \sqrt{3}$, $\Delta\varepsilon/2 = 1.0\%$, $R_\varepsilon = 0$

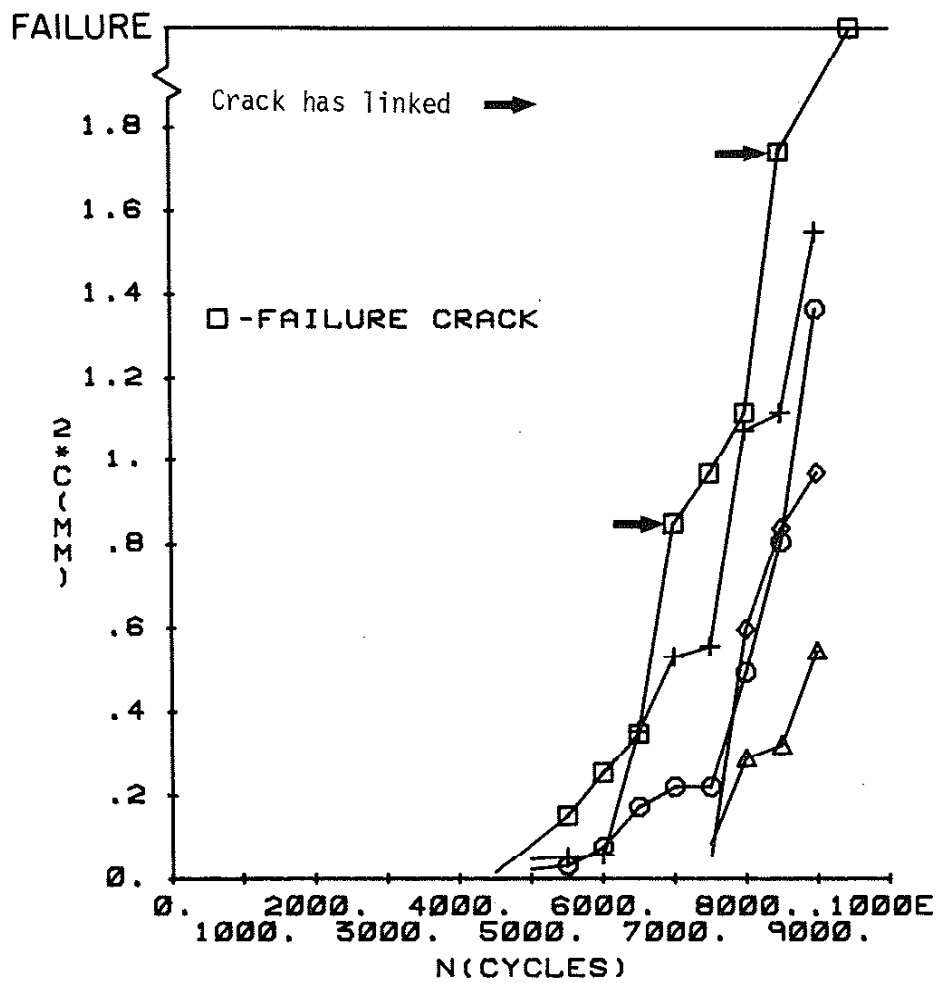

Figure A.6 Crack Length versus Cycles
$\lambda = \sqrt{3}$, $\Delta\varepsilon/2 = 0.5\%$, $R_\varepsilon = 0$

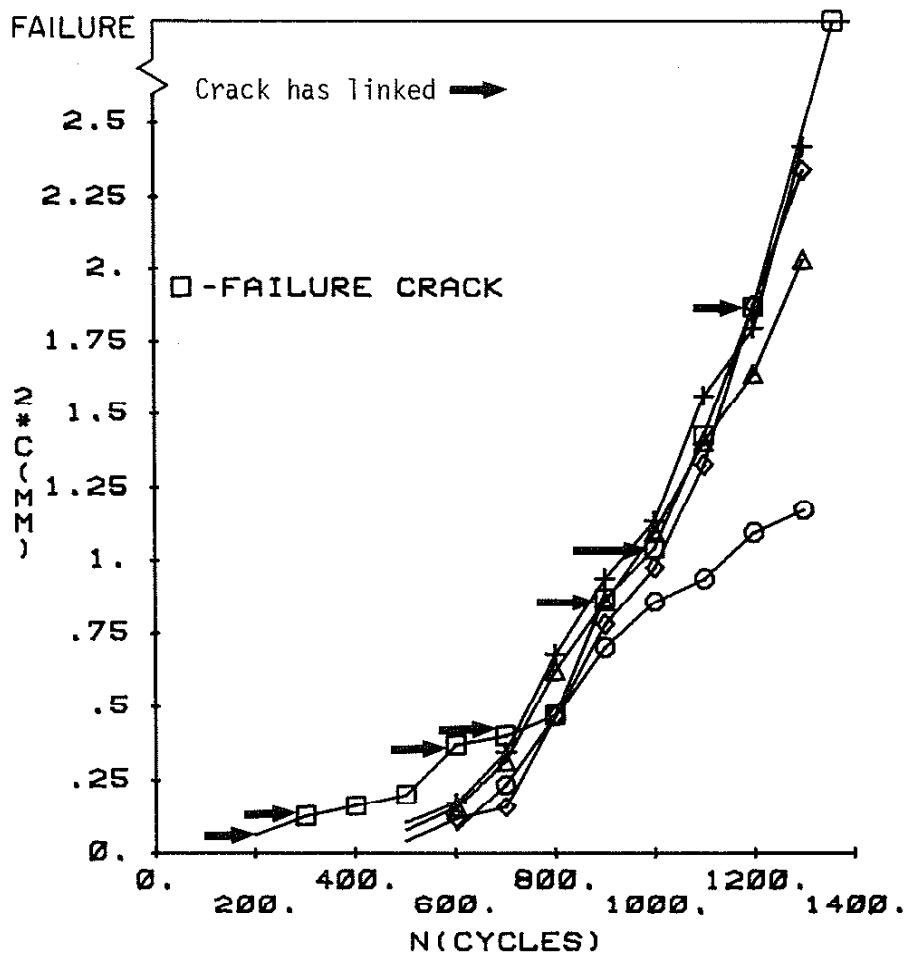

Figure A.7 Crack Length versus Cycles
$\lambda = \sqrt{3}$, $\Delta\varepsilon/2 = 1.0\%$, $R_\varepsilon = -1$

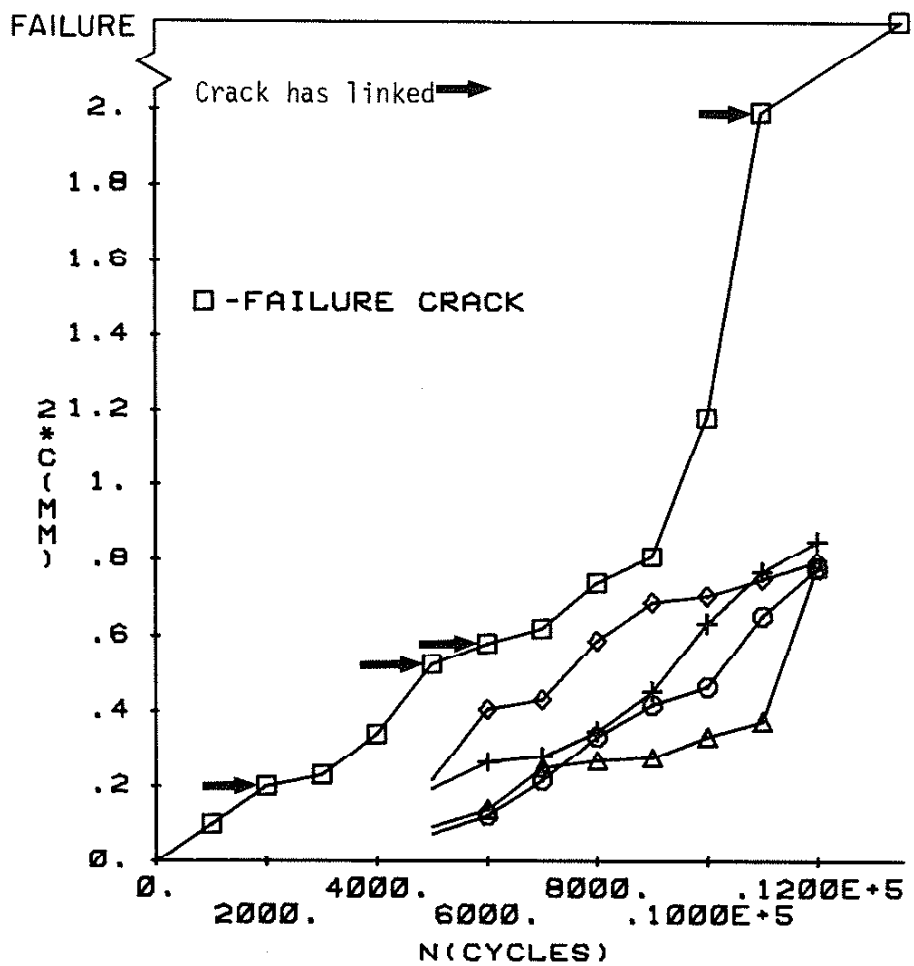

Figure A.8 Crack Length versus Cycles
$\lambda = \sqrt{3}$, $\Delta\bar{\varepsilon}/2 = 0.5\%$, $R_\varepsilon = -1$

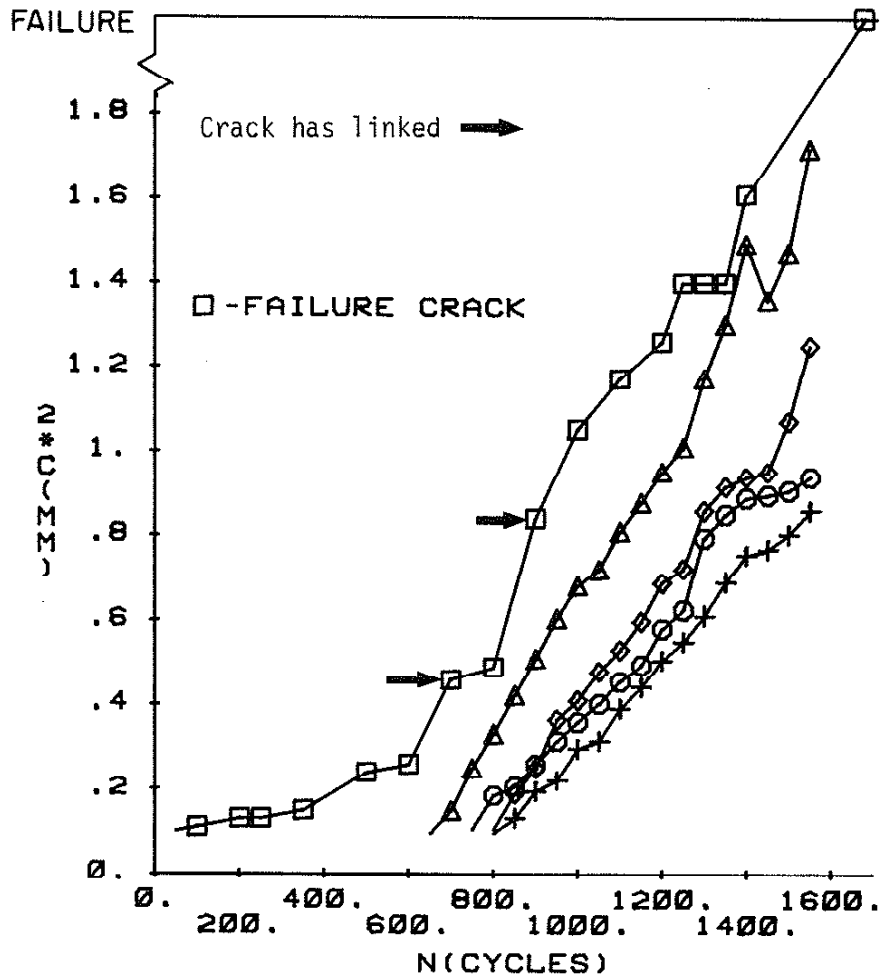

Figure A.9 Crack Length versus Cycles

$\lambda = \infty$, $\Delta\bar{\varepsilon}/2 = 1.0\%$, $R_\varepsilon = 0$

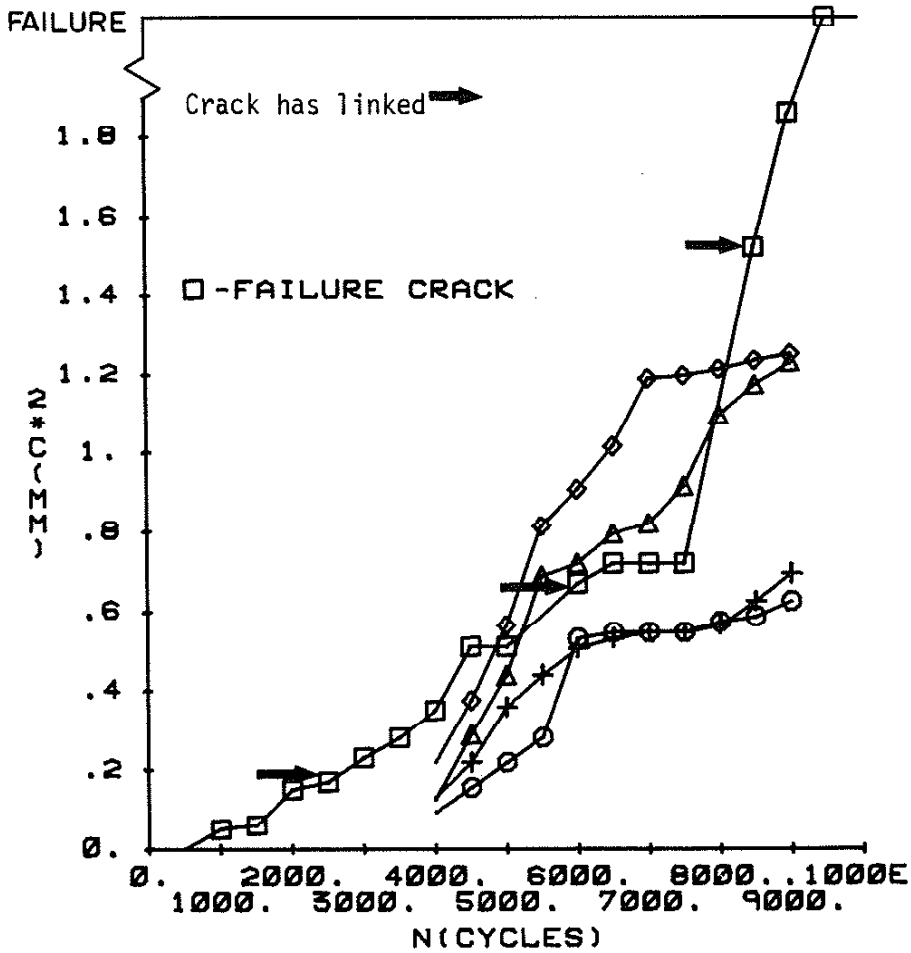

Figure A.10 Crack Length versus Cycles
$\lambda = \infty$, $\Delta\bar{\varepsilon}/2 = 0.5\%$, $R_\varepsilon = 0$

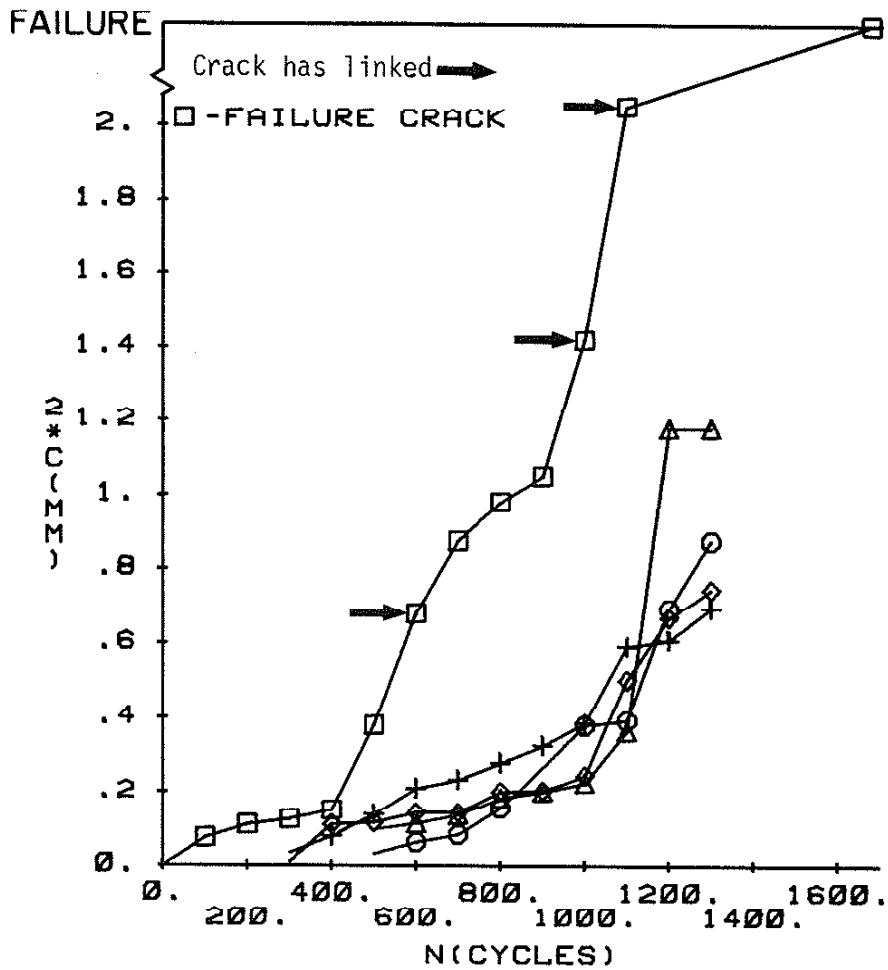

Figure A.11 Crack Length versus Cycles

$\lambda = \infty$, $\Delta\bar{\varepsilon}/2 = 1.0\%$, $R_\varepsilon = -1$

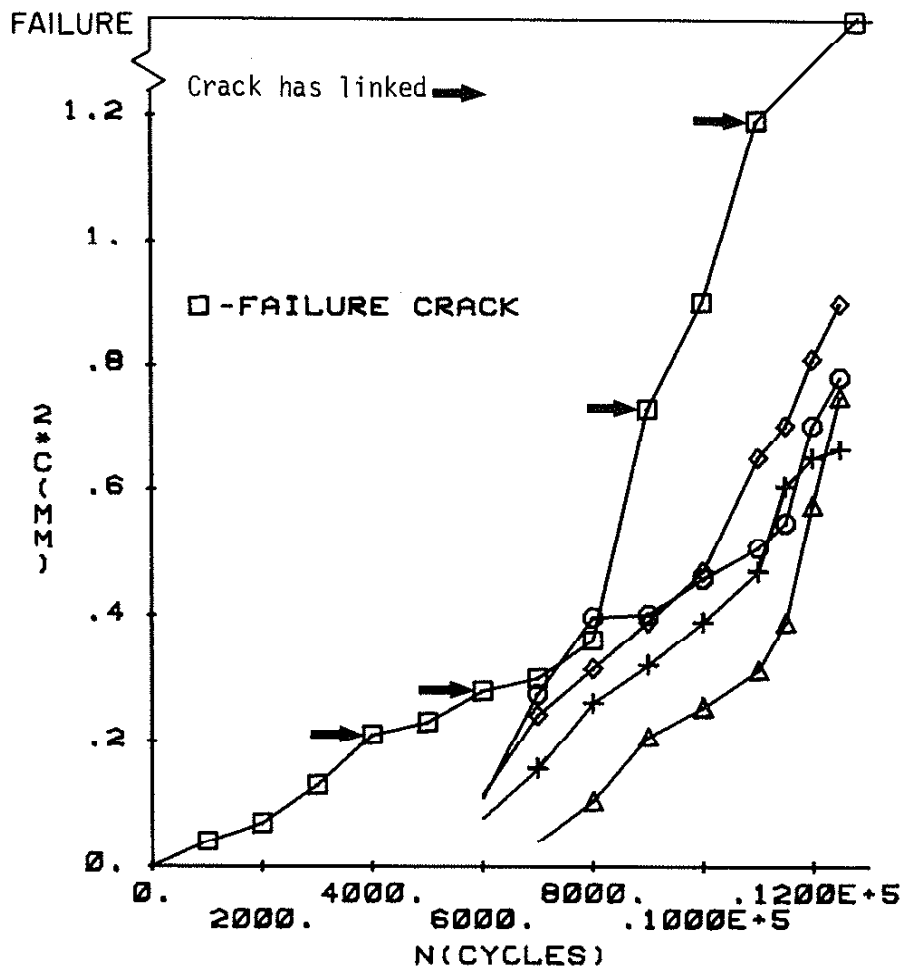

Figure A.12 Crack Length versus Cycles

$\lambda = \infty$, $\Delta\bar{\varepsilon}/2 = 0.5\%$, $R_\varepsilon = -1$

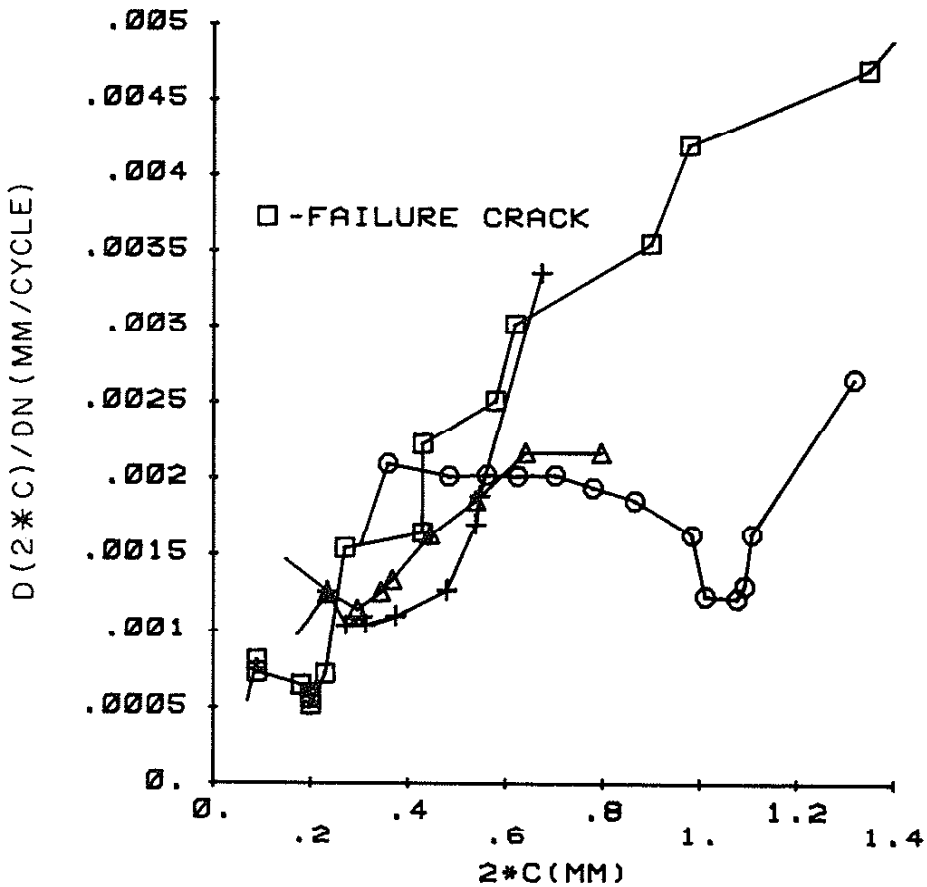

Figure A.13 Crack Growth Rate versus Crack Length
$\lambda = 0$, $\Delta\bar{\varepsilon}/2 = 1.0\%$, $R_\varepsilon = 0$

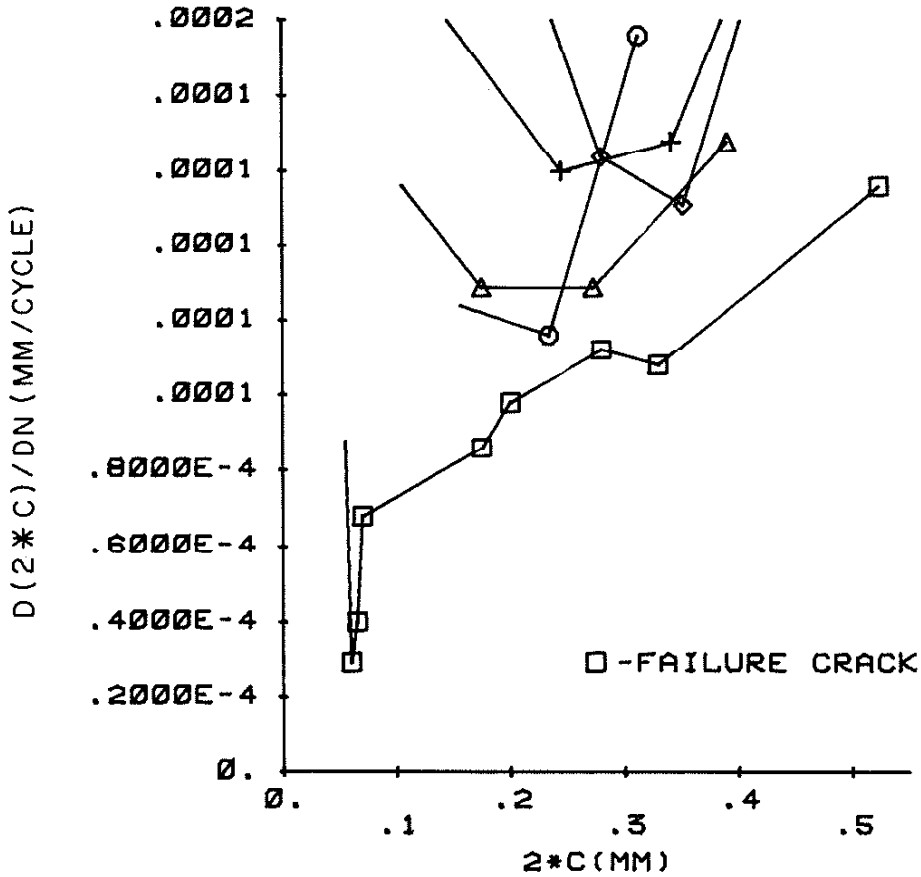

Figure A.14 Crack Growth Rate versus Crack Length
$\lambda = 0$, $\Delta\bar{\varepsilon}/2 = 0.5\%$, $R_\varepsilon = 0$

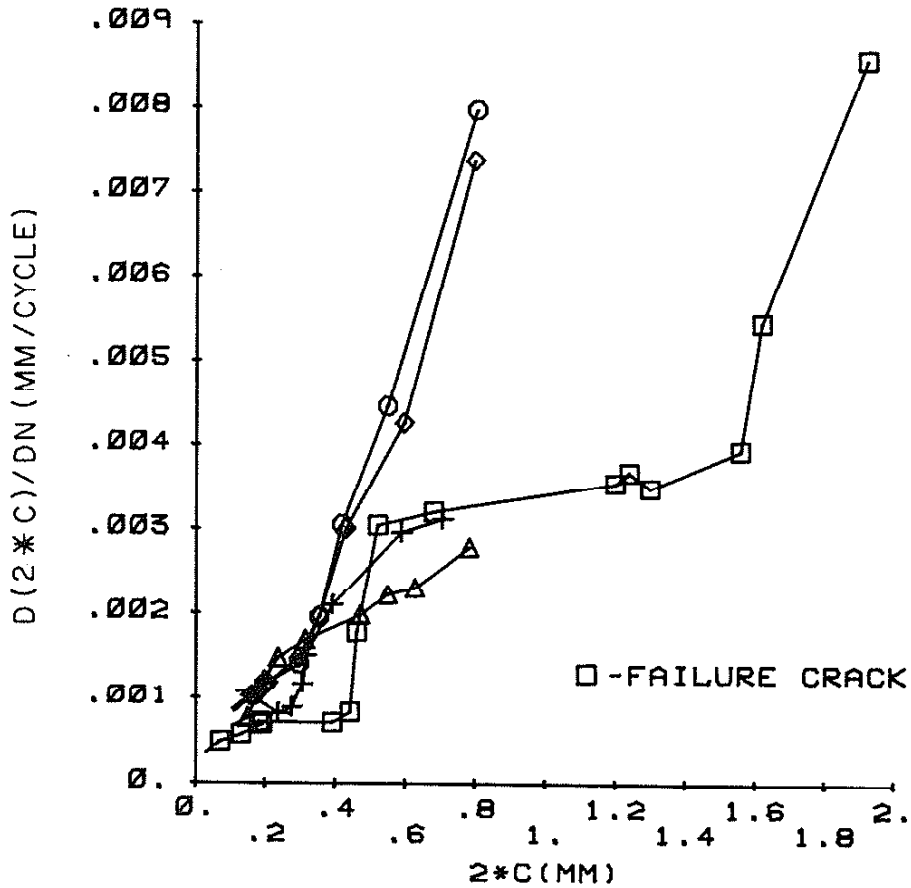

Figure A.15 Crack Growth Rate versus Crack Length
$\lambda = 0$, $\Delta\bar{\varepsilon}/2 = 1.0\%$, $R_\varepsilon = -1$

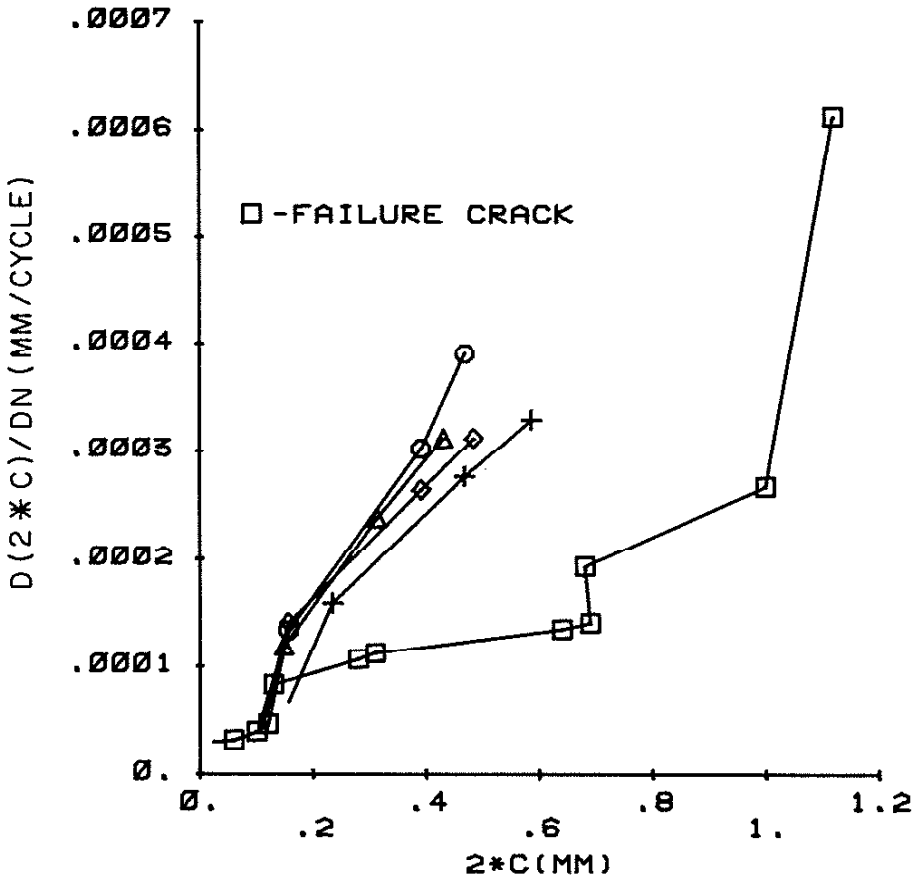

Figure A.16 Crack Growth Rate versus Crack Length
$\lambda = 0$, $\Delta\bar{\varepsilon}/2 = 0.5\%$, $R_\varepsilon = -1$

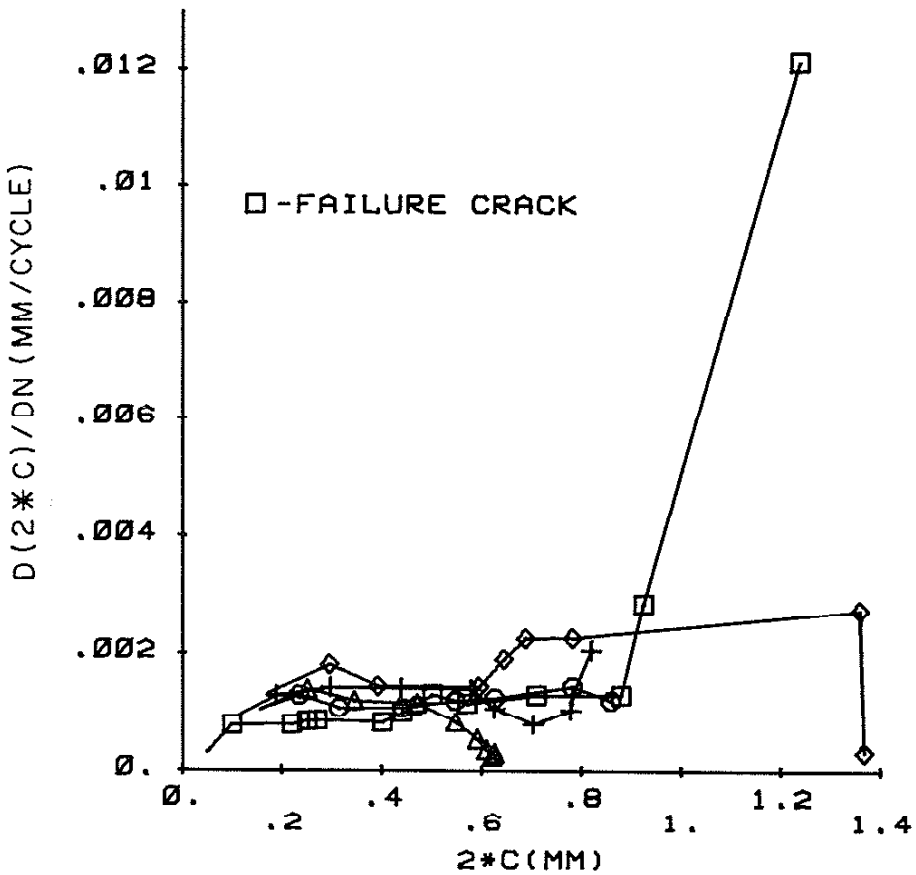

Figure A.17 Crack Growth Rate versus Crack Length $\lambda = \sqrt{3}$, $\Delta\bar{\varepsilon}/2 = 1.0\%$ $R_c = 0$

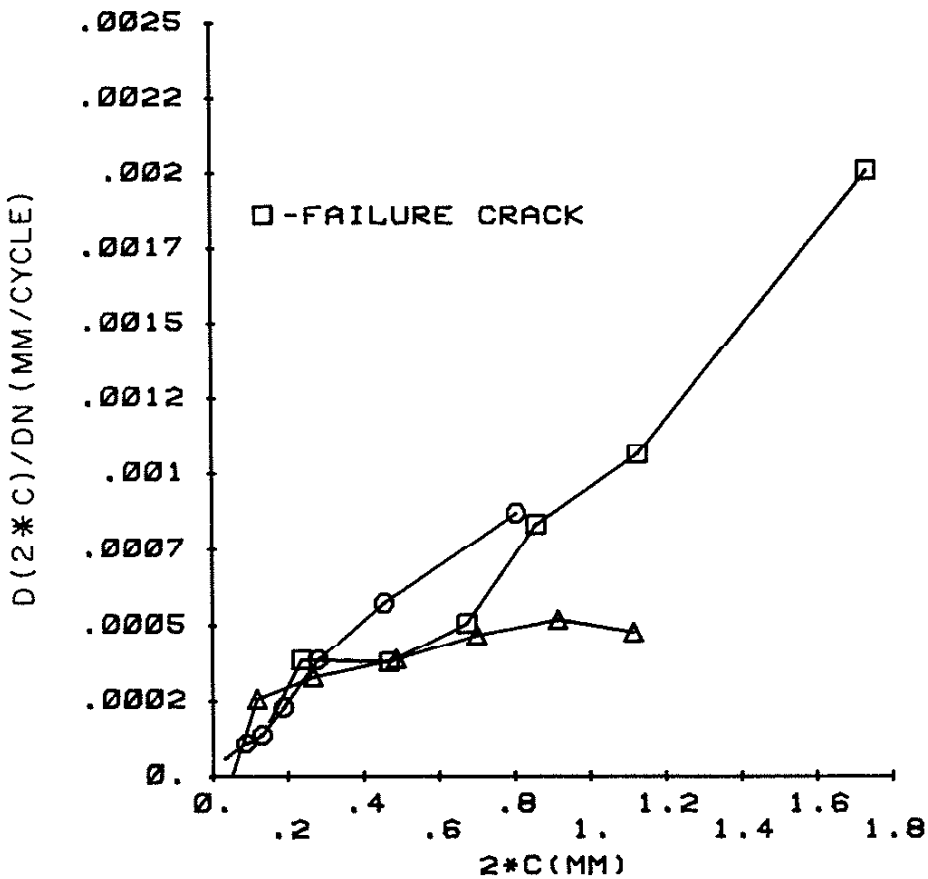

Figure A.18 Crack Growth Rate versus Crack Length
$\lambda = \sqrt{3}$, $\Delta\bar{\varepsilon}/2 = 0.5\%$, $R_\varepsilon = 0$

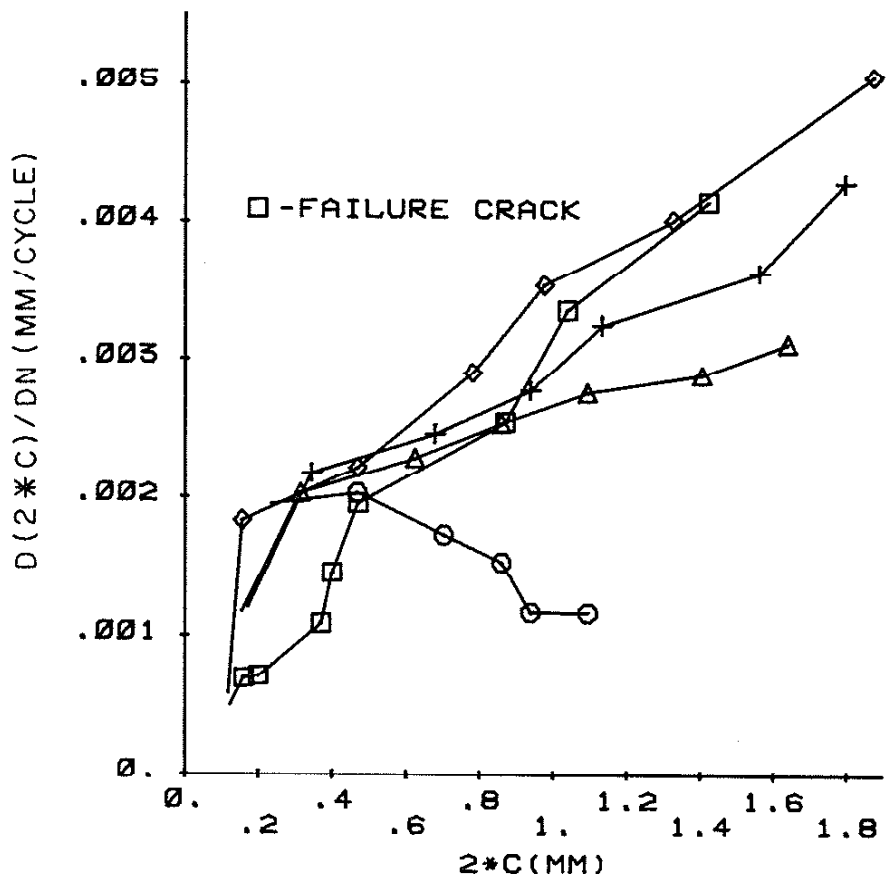

Figure A.19 Crack Growth Rate versus Crack Length
$\lambda = \sqrt{3}$, $\Delta\bar{\varepsilon}/2 = 1.0\%$, $R_\varepsilon = -1$

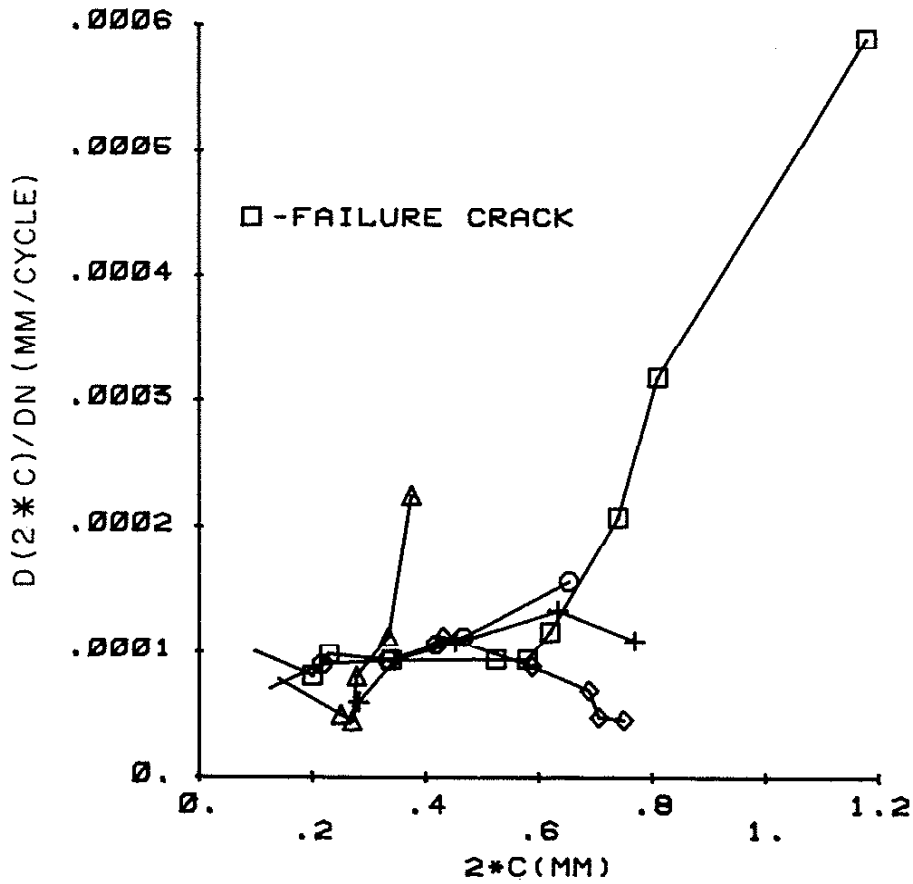

Figure A.20 Crack Growth Rate Versus Crack Length $\lambda = \sqrt{3}$, $\Delta\bar{\varepsilon}/2 = 0.5\%$, $R_{\varepsilon} = -1$

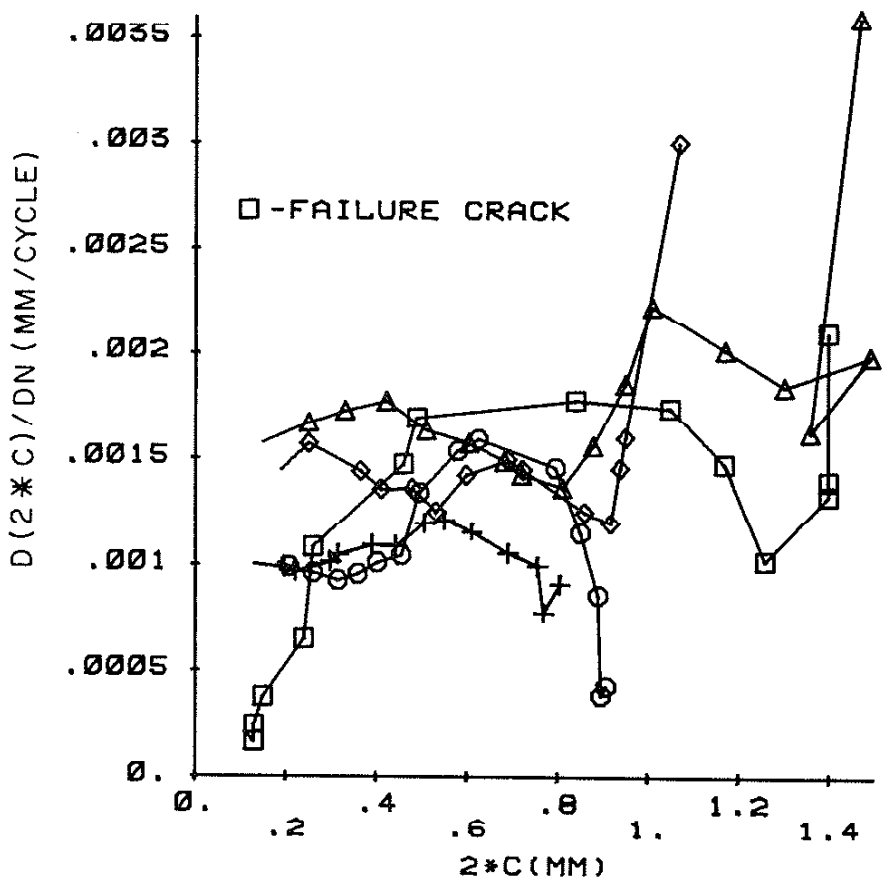

Figure A.21 Crack Growth Rate versus Crack Length
$\lambda = \infty$, $\Delta\bar{\varepsilon}/2 = 1.0\%$, $R_\varepsilon = 0$

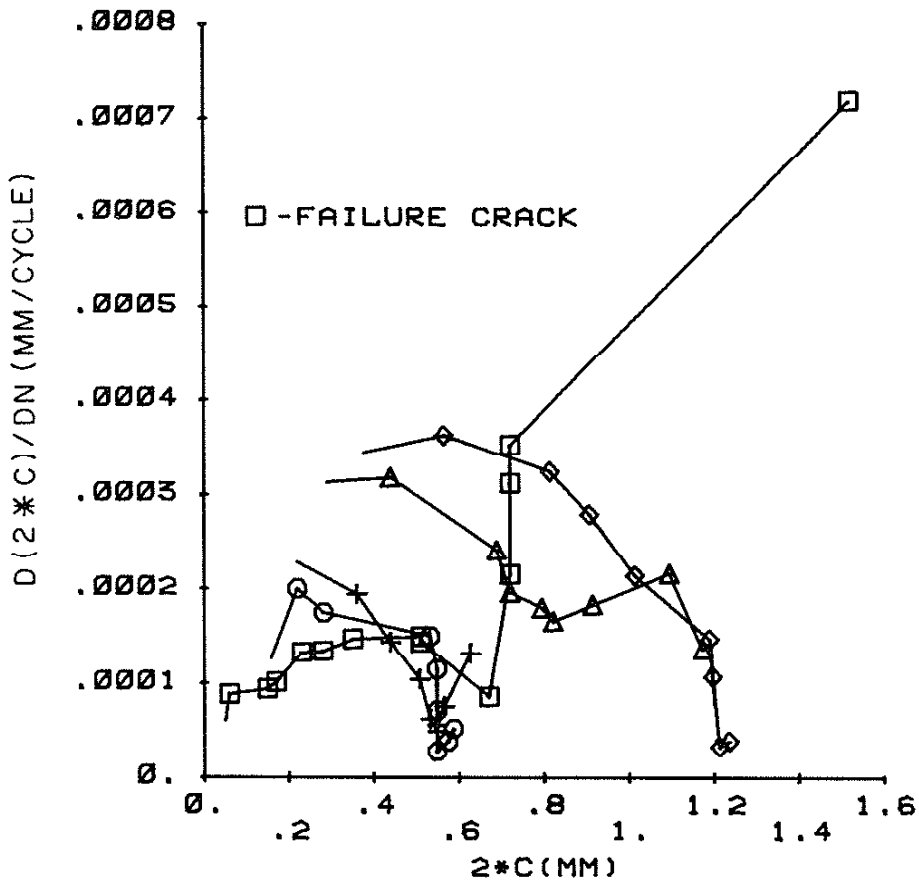

Figure A.22 Crack Growth Rate versus Crack Length
$\lambda = \infty$, $\Delta\bar{\varepsilon}/2 = 0.5\%$, $R_\varepsilon = 0$

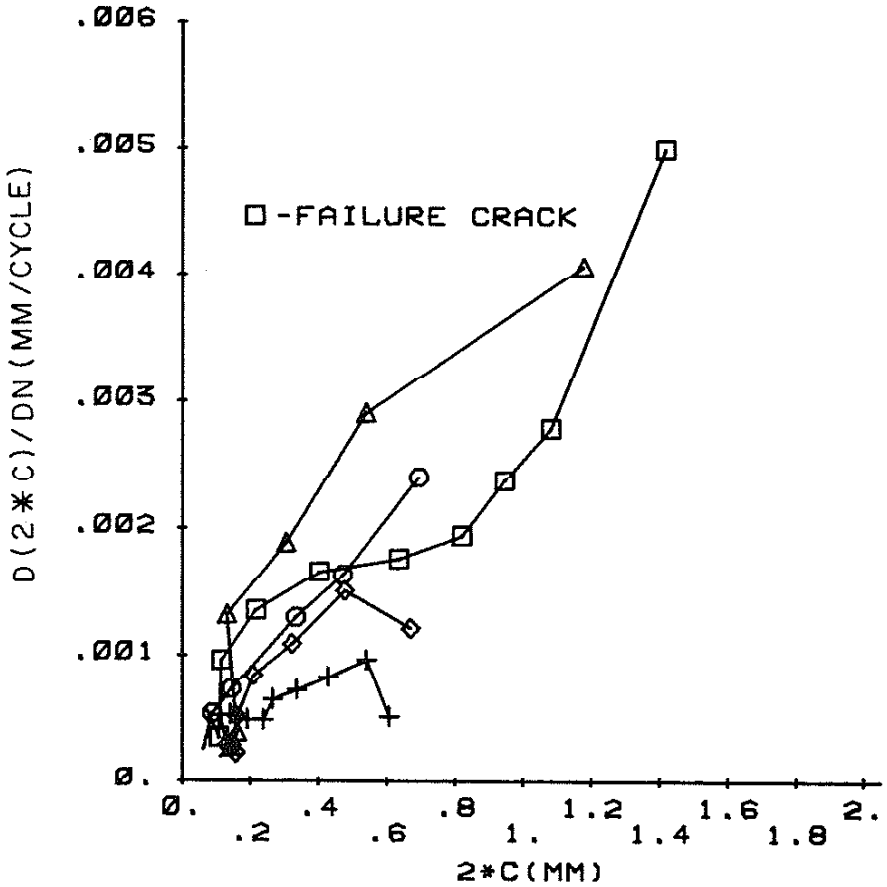

Figure A.23 Crack Growth Rate versus Crack Length
$\lambda = \infty$, $\Delta\bar{\varepsilon}/2 = 1.0\%$, $R_\varepsilon = -1$

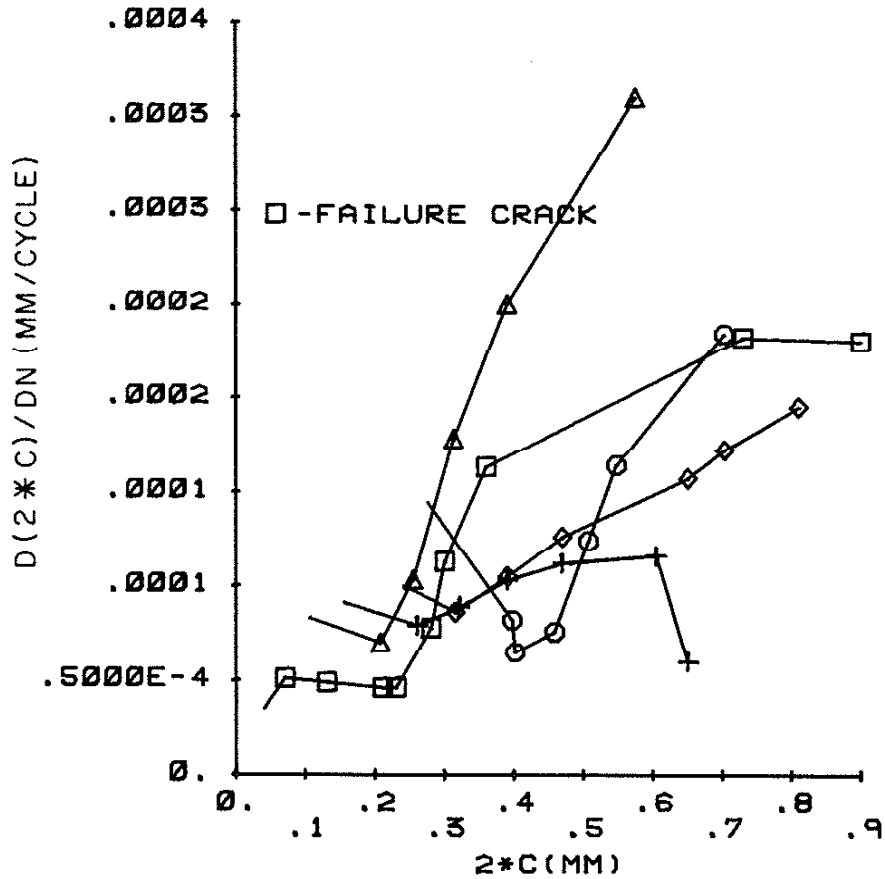

Figure A.24 Crack Growth Rate versus Crack Length
$\lambda = \infty$, $\Delta\bar{\varepsilon}/2 = 0.5\%$, $R_\varepsilon = -1$

REFERENCES

1. Krempl, E., The Influence of State of Stress on Low Cycle Fatigue of Structural Materials, ASTM 549, 1974.

2. Brown, M. W., and K. J. Miller, "A Theory for Fatigue under Multi-Axial Stress-Strain Conditions," Proc., Inst. Mech. Engrs., 187 (1973), pp. 745-755.

3. Garud, Y. S., "Multiaxial Fatigue: A Survey of the State-of-the-Art," JTEVA, Vol. 9, No. 3, 1981, pp. 165-178.

4. Socie, D. F., and T. W. Shield, "Mean Stress Effects in Biaxial Fatigue of Inconel 718," submitted to J. Eng. Mat. Tech., 1983.

5. Socie, D. F., L. E. Waill, and D. F. Dittmer, "Biaxial Fatigue of Inconel 718 including Mean Stress Effects," Biaxial/Multiaxial Fatigue, ASTM Special Technical Publication, to be published.

6. Leis, B. N., M. F. Kanninen, A. T. Hopper, J. Ahmad, and D. Broek, "A Critical Review of the Short Crack Problem in Fatigue," AFWAL-TR-83-4019, Battelle's Columbus Laboratories, Columbus, Ohio, January 1983.

7. Dowling, N. E., "Growth of Short Fatigue Cracks in an Alloy Steel," Scientific Paper 82-1D7-STINE-P1, Westinghouse R&D Center, November 22, 1982.

8. Ritchie, R. O., and S. Suresh, "Mechanics and Physics of the Growth of Small Cracks," Report No. UCB/RP/82/A1001, University of California, Berkeley, July 1982.

9. Lankford, J., "The Growth of Small Fatigue Cracks in 7075-T6 Aluminum," Fatigue Engr. Mat. Struct., Vol. 5, No. 3, 1982, pp. 233-248.

10. El Haddad, M. H., K. N. Smith, and T. H. Topper, "A Strain Based Intensity Factor Solution for Short Fatigue Cracks Initiating from Notches," ASTM STP 677, 1979, pp. 274-289.

11. Minakawa, K., and A. J. McEvily, "On Crack Closure in the Near-Threshold Region," Metallurgica, Vol. 15, 1981, pp. 633-636.

12. Tschegg, E. K., R. O. Ritchie, and F. A. McClintock, "On the Influence of Rubbing Fracture Surfaces on Fatigue Crack Propagation in Mode III," Int. J. Fatigue, Vol. 5, No. 1, 1983, pp. 29-35.

13. Waill, L. E., "Crack Observations in Biaxial Fatigue," Design and Materials Division Report No. 108, Department of Mechanical and Industrial Engineering, University of Illinois at Urbana-Champaign, 1983.

14. Beer, T. A., "Crack Shapes During Biaxial Fatigue," Design and Materials Division, Report 109, Department of Mechanical and Industrial Engineering, University of Illinois at Urbana-Champaign, 1983.

15. Irwin, G. R., "Fracture Mechanics Applied to Adhesive Systems," Treatise on Adhesion and Adhesives, Vol. 1, R. L. Patrik, ed., Marcel Dekker, New York, 1967, pp. 233-267.

16. Change, J. B., ed., Part-Through Crack Fatigue Life Prediction, ASTM STP 687, 1979.

17. Newman, J. C., Jr., "A Nonlinear Fracture Mechanics Approach to the Growth of Short Cracks," AGARD Specialists Meeting on Behavior of Short Cracks, Toronto, Canada, September 20-21, 1982.

18. Morris, W. L., M. R. James, and O. Buck, "Growth Rate Models for Short Surface Cracks in Al 2219-T851," Metallurgical Transactions, Vol. 12A, January 1981, pp. 57-64.

19. Hurd, N. J., and P. E. Irving, "Factors Influencing Propagation of Mode III Fatigue Cracks under Torsional Loading," ASTM STP 761, 1982, pp. 212-233.